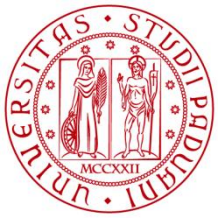

UNIVERSITÀ
DEGLI STUDI
DI PADOVA

UNIVERSITÀ DEGLI STUDI DI PADOVA

DIPARTIMENTO DI SCIENZE FARMACEUTICHE

SCUOLA DI DOTTORATO DI RICERCA IN
BIOLOGIA E MEDICINA DELLA RIGENERAZIONE
INDIRIZZO INGEGNERIA DEI TESSUTI E TRAPIANTI
XXIV CICLO

TESI DI DOTTORATO

AMNIOTIC FLUID STEM CELL THERAPY IN CHRONIC KIDNEY DISEASE PROGRESSION: THE CASE OF ALPORT SYNDROME

DIRETTORE DELLA SCUOLA : Ch.Mo Prof. Maria Teresa Conconi

COORDINATORE D'INDIRIZZO: Ch.Mo Prof. Maria Teresa Conconi

SUPERVISORE :Ch.Mo Prof. Pier Paolo Parnigotto

CORRELATORE: Dr. Laura Perin

DOTTORANDO : Sargis Sedrakyan

26 GENNAIO 2012

To My Family

CONTENTS

ABSTRACT

Chronic kidney Disease (CKD) is a global health problem. It is associated with gradual decline in renal function, which develops into end stage renal disease and culminates into renal failure. Many different etiological factors are involved in the initiation and progression of CKD. The two most prevailing medical reasons for the development of progressive kidney disease are diabetes and hypertension. Regardless of the site of the initial insult, which may either be the glomerulus or tubules, all forms of progressive kidney diseases follow a final common pathway that is interstitial and glomerular fibrosis together with loss of podocytes, therefore, loss of glomerular integrity and renal function. Current therapeutic options for CKD are few and limited to the administration of renin-angiotensin system blockers, dialysis and renal transplantation. Although, pharmacotherapies are effective in slowing down the rate of progression, they do not prevent end stage renal disease. On the other hand dialysis even though life sustaining does not solve the problem and is associated with very poor quality of life. Renal transplantation thus remains the most effective method to treat end stage renal disease, however, the shortage of donor organs and immune complications associated with it do not solve the problem either. Hence, development of novel therapies remains an urgent necessity.

Stem cell approach to Regenerative Medicine introduces vast possibilities for new therapies in acute as well as chronic diseases where current treatment options are either limited or inadequate. Stem cells derived from amniotic fluid (AFSC), which have emerged in recent years, represent a new source of stem cells with pluripotential properties, devoid of ethical issue associated with embryonic stem cells. Previous studies have proven the principle that AFSC can be used in regenerative medicine of the kidney due to their strong immunomodulatory properties and showed renoprotection when injected into an acute renal failure injury model in rodents.

The purpose of the current study was to investigate the role of stem cells derived from amniotic fluid in an animal model of chronic kidney disease. In particular, cells positively selected for CD117 (c-kit) were administered to mice with x-linked Alport Syndrome (XLAS), a well established genetic model to study chronic kidney disease. Alport disease is associated with mutations in the collagen type IV family of proteins, the α3, α4 and α5 chains, the absence of which alters the normal composition and function of the glomerular basement membrane leading to proteinuria, and ultimately loss of podocytes. We hypothesized that (AFSC) would be able slow down chronic progression in Alport kidneys by modulating key processes such as the immune response, pro-fibrotic events initiated by TGF-β signaling and cytokine/chemokine profile of the kidney via endocrine/paracrine mechanisms protecting the glomerular structure and preserving the filtration property of the organ.

Single dose of systemic injection of AFSC at an early stage of the disease, before the onset of proteinuria, prolonged the life-span of Alport mice by 20% on average. This also resulted into amelioration of the functional parameters of the kidney, lowered serum creatinine, BUN as well as proteinuria levels at 2.5 months post treatment. Treated kidneys demonstrated better morphology with less severe glomerulosclerosis, lesser deposition of collagen type I associated with interstitial fibrosis and reduced infiltration of macrophages and inflammatory cells compared to their non-treated siblings.

AFSC were detectable in glomeruli of injected mice but they did not differentiate into podocytes, and consequently, the α5(IV) chain of collagen missing in Alport mice was not replaced by AFSC treatment.

Our findings revealed significant downregulation of key regulatory cytokines, such as TNFα, CCL2, CXCL2 and M-CSF involved in pro-fibrotic M1 macrophage signaling pathway favoring tissue remodeling instead of tissue injury.

Finally, Alport mice receiving AFSC demonstrated preservation of podocyte numbers. In a closer look, glomerular cells stimulated with Angiotensin II showed increased Angiotensin II receptor type 1 (ANGTR1) expression, which was downregulated when treated with losartan (Angiotensin II antagonist). Similar to losartan AFSC decreased ANGTR1 expression, suggesting that AFSC may block the effects of Angiotensin II favoring glomerular survival.

In conclusion, AFSC slow down Alport progression via preservation of podocyte number, M2c activation of macrophages and modulation of kidney microenvironment through endocrine/paracrine mechanisms favoring tissue preservation and function, in particular preserving podocyte number and filtration property.

ABSTRACT IN LINGUA ITALIANA

Negli ultimi anni l'aumento nell'incidenza della Malattia Renale Cronica (Chronic Kidney Disease, CKD) è diventata un importante problema di salute pubblica. Principale manifestazione clinica della CKD è un graduale declino della capacità di filtrazione del rene che termina con lo sviluppo di insufficienza renale terminale (End Stage Renal Disease, ESRD). Infezioni, infiammazioni acute e croniche, malattie genetiche o la presenza di patologie a carico di altri organi, come per esempio il diabete, possono concorrere o essere causa diretta di danno renale. Questi insulti possono portare ad una progressiva perdita della funzione renale fino a raggiungere lo stadio finale di ESRD. Indipendentemente dalle origini eziologiche, la CKD evolve con la progressione di fibrosi glomerulare e interstiziale, apoptosi dei podociti con conseguente distruzione della struttura morfo-funzionale del rene e della sua capacità di filtrazione.

L'utilizzo di farmaci (come per esempio gli antiipertensivi ACE inibitori, o inibitori dell'anidrasi carbonica) spesso riesce a rallentare il progresso della malattia ma il trattamento farmacologico risulta essere meno efficace con il progredire dell'ESRD e può risultate nefrotossico con il passare del tempo. La dialisi, trattamento molto invasivo e costoso per la sanità, ed il trapianto con la scarsa disponibilità di organi e la crescente richiesta, hanno spinto alla ricerca di valide alternative con un minor costo sociale ed una maggior compliance da parte dei pazienti.

Molti studi si sono focalizzati nella scoperta di nuove fonti di cellule staminali per il trattamento di malattie renali acute e croniche dove le terapie correnti sono insufficienti ed inadeguate. Negli ultimi anni, il liquido amniotico è stato proposto come fonte alternativa per l'isolamento di cellule staminali da poter utilizzare in futuro per la terapia cellulare e, con particolare riguardo, per la rigenerazione del tessuto renale. In particolare, in studi recentemente pubblicati, le cellule staminali da liquido amniotico (AFSC) si sono distinte per la loro potente azione antiinfiammatoria e

renoprotettiva, con modulazione della risposta immunitaria in un modello murino di danno renale acuto.

Lo scopo di questo lavoro è quello di investigare il ruolo delle cellule staminali da liquido amniotico in un modello animale genetico di danno renale cronico (CKD). Nello specifico, cellule positive per il recettore di membrana CD117 (c-kit) sono state infuse in un modello murino di Sindrome di Alport, riconosciuto come uno dei più utili modelli più utili per lo studio di malattie renali croniche. La Sindrome di Alport è una grave malattia ereditaria e progressiva dovuta a mutazioni che coinvolgono le catene α3, α4 and α5 del collagene di tipo IV. L'assenza di tali catene altera la composizione fisiologica della matrice extracellulare renale (GBM, glomerular basement membrane) e provoca una marcata perdita di funzionalità che conduce a proteinuria e, con il tempo, a perdita dei podociti con conseguente blocco della filtrazione glomerulare.

Basandoci sui dati precedentemente ottenuti, in questo lavoro ipotizziamo che le cellule staminali da liquido amniotico abbiano la capacità di rallentare la progressione della CKD, tramite un'azione endocrina e paracrina su vari meccanismi patologici che includono la risposta immunitaria, la fibrosi indotta dall'attivazione di TGF-β . In aggiunta, ipotizziamo che l'azione positiva esercitata dalle cellule da liquido amniotico sia un effetto di mantenimento della struttura glomerulare con conseguente mantenimento della normale capacità di filtrazione. In particolare, una singola infusione di AFSC, amministrata nei primi stadi della malattia, è capace di prolungare la sopravvivenza nel modello murino di circa il 20% con un significativo miglioramento dei parametri fisiologici renali quali livelli di creatinina plasmatica, BUN e proteinuria, oltre due mesi dalla somministrazione. Inoltre, Il tessuto renale degli animali trattati presenta una morfologia normale con lieve sclerosi glomerulare ed una minore deposizione di collagene I, di solito associata a fibrosi interstiziale. A questo si accompagna una minore infiltrazione da parte di macrofagi e altre cellule del sistema immunitario rispetto agli animali non trattati. Una

vasta serie di esperimenti è stata quindi effettuata per investigare i meccanismi di azione tramite cui le cellule staminali da liquido amniotico esercitano il loro effetto positivo. Gli animali trattati presentano un maggior numero di podociti se comparati con i topi di controllo. La presenza di cellule infuse nei glomeruli nel tempo, non è stata però accompagnata da differenziazione in podociti e produzione di nuovo collagene, escludendo quindi che il maggiore numero di podociti sia dovuto a proliferazione e differenziazione delle cellule amniotiche. Dati ottenuti tramite esperimenti in vitro confermano l'effetto positivo delle AFSC nella risposta delle cellule del glomerulo all'Angiotensina II , tramite diminuzione nell'espressione del suo recettore di tipo 1 (ANGTR1), esercitando un effetto benefico di protezione delle cellule del golomerulo, in particolare dei podociti.

Contemporaneamente, una significativa variazione nel profilo immunostimolatorio è stata rilevata negli animali trattati, che presentavano una diminuzione significativa nell'espressione di molecole quali TNF-a, CCL, CXCL2 e M-CSF, coinvolte nella stimolazione di macrofagi di fenotipo M1, noti per la loro azione pro-fibrotica e pro-infiammatoria.
Per concludere, le cellule staminali da liquido amniotico sono capaci di rallentare la progressione della Sindrome di Alport tramite mantenimento del numero di podociti, attivazione di macrofagi M2c pro-rigenerativi a discapito dei pro-fibrotici M1 e modulazione endocrina/paracrina dei segnali cellulari all'interno del rene; favorendo il mantenimento strutturale e funzionale del tessuto renale.

INTRODUCTION

1. Chronic Kidney Disease

Chronic kidney disease (CKD) is a medical condition characterized by progressive and irreversible decline in renal excretory function as a result of renal tissue injury, reduced filtration rate and fibrosis. Persistent renal dysfunction leads to the accumulation of metabolic and waste products in the blood and organs, which can cause azotemia and multi-organ damage [1]. National Kidney Foundation defines CKD by the presence of kidney structural and functional abnormalities for 3 months or more [2]. Glomerular filtration rate (GFR) that represents the rate at which an ultrafiltrate of plasma is produced by glomeruli per unit of time is used as an estimate of the number of functioning nephrons or functional renal mass. Calculation of GFR is used in describing kidney disease severity that is classified into five stages according to the level of GFR [3], [Table 1]. It is an effective indicator of kidney function, and its evaluation is crucial for the diagnosis, staging and assessment of responses to treatment of CKD. Other physiological markers often tested to assess kidney function include serum creatinine levels and BUN, which become gradually elevated in blood as the disease gets worse. The loss of function usually takes months or years to occur. The final stage of CKD is called end stage renal disease (ESRD), at which point kidney function is defined below 15% of the normal. At this stage the kidneys cannot properly remove enough waste products and excess water from the body and symptoms associated with this condition may develop such as decreased urine output or no urine output, nausea, vomiting, loss of appetite, swelling of the feet and ankles. Regardless of initial cause CKD tends to progress to ESRD. Numerous epidemiological studies indicate that the prevalence of patients with ESRD is increasing worldwide [4-7]. As a result, CKD has become a major health problem on a global scale affecting 7.2% of the global adult population with the number dramatically increasing in the elderly. In addition, 2011 United States Renal Data System report

estimates the number of patients receiving dialysis treatment well over 570,000. Overall, these problems impose enormous socioeconomic burden on the affected individuals, families and societies.

GFR

Stage	Description	mL/min/1.73m^2	Relative terms
1	Kidney damage with normal or ↑ GFR	≥90	Albuminuria, proteinuria, hematuria
2	Kidney damage with mild ↓ GFR	60-89	Albuminuria, proteinuria, hematuria
3	Moderate ↓ GFR	30-59	Chronic renal insufficiency, early renal insufficiency
4	Severe ↓ GFR	15-29	Chronic renal insufficiency, late renal insufficiency, pre-ESRD
5	Kidney failure	<15 (or dialysis)	Renal failure, uremia, end-stage renal disease

TABLE 1: GFR and Renal Function.

1.1 Etiology of CKD

The etiology of CKD is complex and revolves around various factors which promote disease initiation and progression through either direct or indirect mechanisms. Primary diseases of the kidney causing initial insult to the organ include but are not limited to Fanconi Syndrome, hereditary nephritis (Alport Syndrome), Goodpasture Syndrome, Polycystic Kidney Disease, infections of the kidney and autoimmune diseases. Diabetes and hypertension are primary diseases of the pancreas and cardiovascular system, which are also leading causes for the development of glomerularonephritis and ESRD. The epidemiological landscape of CKD varies greatly in different regions of the world. In developing countries high prevalence of bacterial, viral, and parasitic infections are the principle causes for chronic glomerulonephritis and

interstitial nephritis. In more developed parts of the world, obesity, type II diabetes [4], and hypertension [8] remain the leading causes of CKD. According to the 2011 United States Renal Data System Report an estimated 13% of the adult population in the USA has some degree of CKD [4], and patients with diabetes and/or hypertensive kidney disease account for about 80% of all new cases of ESRD in the USA [9].

1.2 Characterization and progression of CKD

The common symptoms of kidney disease, characterized clinically by proteinuria, edema and uremia, were first described in 1827 by the English physician Richard Bright [10,11]. Bright's disease was used to describe kidney disease that is termed in modern medicine as acute or chronic nephritis. Current knowledge classifies and characterizes progressive renal disease in addition to the clinical signs and symptoms by expansion of the glomerulo-tubulo-interstitium and accumulation of extracellular matrix within this tissue compartments. However, depending on the type of etiology CKD can initiate in different compartments or structures of the kidney, such as in the glomeruli, in the tubules or in the renal vessels. It is well established now, that regardless of where injury begins, if it persists, the kidney will gradually self-destruct through a final common pathway that is glomerular and interstitial nephritis and fibrogenesis [12]. All these events eventually result into common renal structural and functional alterations affecting all renal structures. Accumulation of fibrotic scar tissue gradually replaces healthy functional nephrons. In the beginning, nephrons that are little damaged or non-affected adapt and functionally compensate the dysfunctional nephrons until over 60% of the nephrons become dysfunctional after which kidneys become incapable of cleaning the blood from waste products.

1.2.1 Mechanisms of CKD progression: inflammation

Many different cellular processes conspire in the progressive loss of kidney function. Generally, these events can be classified as either inflammatory or fibrotic. Inflammation plays a pivotal role in the progression of many, if not all, forms of CKD. Subsequent to kidney injury, inflammation is activated initially as a repair mechanism to eliminate the original insult by removing cell and matrix debris, and to repair the lost tissue components [13]. However, when an inflammatory process proceeds in an uncontrolled manner, it results into progressive fibrosis, which in turn causes distortion of the intricate cellular architecture of the nephron initiating a vicious cycle that eventually leads to loss of renal function.

The pathogenesis of inflammation is complex and multifactorial, involving the interaction of cytokines, chemokines and adhesion molecules. Renal inflammation is characterized by glomerular and tubulointerstitial infiltration by inflammatory cells, such as neutrophils, lymphocytes and macrophages, dendritic cells and mast cells. They release inflammatory and pro-fibrotic cytokines, such as IL-1, IL-6 and tumor necrosis factor-α (TNF-α) further stimulating renal inflammation, which causes more damage to kidney structures.

1.2.2 Mechanisms of CKD progression: fibrosis

Renal fibrogenesis is considered to be a failed wound healing process that occurs after an episode of very severe renal injury or as a result of chronic repetitive insults. It is a complex multistage dynamic process involving inflammatory cell infiltration, mesangial and fibroblast activation, epithelial to mesenchymal transition, endothelial to mesenchymal transition, cell apoptosis and extracellular matrix synthesis and deposition orchestrated by a network of enzymes, cytokines/chemokines, growth factors adhesion molecules and signaling processes. The dynamic process of fibrogenesis

can be simplified by characterizing the complex cellular and molecular events associated with disease initiation and progression into sequential steps or categories. These events consist of: (1) Injury to the tissue, (2) recruitment of inflammatory cells, (3) release of fibrogenic cytokines, and (4) activation of collagen producing cells.

1.2.3 Role of macrophages in renal inflammation and fibrosis

Macrophages play an important role in the dynamic process of renal fibrogenesis. Macrophages are white blood cells within tissues, produced by the division of their circulating progenitors, monocytes. They have heterogeneous phenotypes and demonstrate an incredible functional plasticity [14,15]. During enhanced disease states, inflammatory monocytes from circulating blood are recruited to the injured site in response to cytokine cues and undergo differentiation into two broad but distinct subsets of macrophages that are categorized as either classically activated (M1) or alternatively activated (M2). In general, M1 macrophages have an inflammatory profile, which promotes renal pathogenesis leading to tissue damage and fibrosis. Alternatively, M2 macrophages have been evidenced to promote tissue remodeling and angiogenesis through increased endocytic capabilities, reduced proinflammatory cytokine secretion and production of various trophic factors [16-18].

1.2.4 Role of extracellular matrix in CKD

Under normal physiological conditions kidney cells continuously synthesize and deposit new extracellular matrix (ECM) in the basement membranes of tubules, glomeruli and blood vessels. This, however, does not result into a cumulative accumulation of ECM in these tissues, because the exact same amount of ECM gets degraded in a reverse process. This balance is maintained by proteins called matrix metalloproteinases (MMPs) that degrade ECM, and their inhibitors called tissue inhibitors of metalloproteinases (TIMPs) [19,20]. In CKD, the

balance between ECM synthesis and degradation is disrupted in favor of more ECM accumulation, a process defined as fibrosis. Activated fibroblasts are the principle ECM producing cells that generate a large amount of ECM components including fibronectin and type I and type III collagens. Gomerular basement membrane (GBM) is a special kind of an ECM in the kidney contiguous with glomerular capillaries, which provides structural integrity to the glomerulus and functions as a filtration barrier between blood and an ultrafiltrate of plasma that will become urine. Any alterations in GBM composition might result in weakened structural integrity of the GBM and loss of function.

1.2.5 TGF-β and renin-angiotensin-system drive fibrogenesis

The cellular machinery that is responsible for activation and synthesis of ECM components during CKD, such as fibronectin, laminin, collagens type I, III, IV and VI is regulated by TGF-β1 signaling, a member of the TGF-β superfamily of growth factors, which also includes activins and bone morphogenetic proteins (BMP). TGF-β was discovered more than 30 years ago as a factor produced by transformed cells that induced the anchorage-independent growth of normal rat kidney cells [21]. They are pleiotropic molecules that regulate cell proliferation, differentiation, apoptosis, migration and adhesion of many different cells types [22]. TGF-β is also critical for normal kidney development and function. It is expressed by most mammalian cells and by all the cells of kidney. Under pathologic conditions during CKD TGF-β1 is highly elevated further enhancing fibrogenesis by inducing the transformation of renal tubular epithelial cells to matrix producing myofibroblasts via epithelial to mesenchymal transition [23].

The renin-angiotensin-system (RAS) is also known to play in important role in the development of renal fibrosis [24]. RAS is well recognized as a dual vasoactive system acting as both a circulating endocrine system and a local tissue paracrine system [25]. Angiotensin II is the most important

effector molecule of the RAS . It plays an important role in CKD acting as a pro-fibrotic cytokine stimulating the synthesis of pro-inflammatory and chemotactic factors such as MCP-1 and TGF-β. Angiotensin II induced TGF-β activity results in hypertrophy in tubular epithelial cells and matrix synthesis in mesangial cells [26,27]. It promotes fibrogenesis through enhancement of TGF-β signaling by increasing Smad2 levels (a downstream mediator of TGF-β signal) and by augmenting the nuclear translocation of phosphorilated Smad3. Angiotensin II is also shown to regulate matrix degradation by blocking protease activity through PAI-1 induction [28].

1.3 Treatment options for CKD

Current practice paradigms for the treatment of CKD have been historically centered on slowing its progression and reducing the co-morbidities associated with this condition. Because the symptoms associated with chronic renal failure develop gradually at a slow pace, therapy of CKD is usually directed at an asymptomatic condition detected only by laboratory testing. The development of end stage renal disease is highly correlated with cardiovascular disease and diabetes [4,8], and the efficiency of fighting CKD relies on the effectiveness of therapy across a range of primary diseases. Hence, preventive measures aimed at treating hypertension and diabetes can mitigate forthcoming renal complications.

Angiotensin converting enzyme inhibitors (ACEi) and angiotensin II receptor blockers (ARBs) are standard drugs for primary hypertension. Besides their antihypertensive role, these pharmacotherapies have significant renoprotective properties and are each especially effective in slowing the progressive decline of GFR in CKD [29-32]. According to a recent meta-analysis the benefits of RAS inhibition for non-diabetic renal diseases are strongest in those patients with proteinuria of more than 1000mg/day [30]. In contrast, clinical trials among diabetic nephropathy patients indicate that ACEi and ARB therapies are more effective when

applied in the early microalbuminuric phase of diabetes [33-35,32]. A very recent clinical follow up study of Alport patients, reported that early therapy with ACEi significantly improves patient survival, and the quality of life by delaying dialysis treatment for years [36]. Hence, the capacity of RAS inhibitors to delay progression of diabetic and non-diabetic nephropathy crucially depends on the time at which therapy is started. Despite the controversy regarding the nature of relationship between proteinuria and progressive renal injury, by which ACEi and ARBs are thought to benefit in certain diseases, there is general consensus on two other mechanisms: that being hemodynamic /antihypertensive actions and anti-inflammatory/anti-fibrotic actions.

Overall, early therapy with pharmaceuticals can be a good starting point to treat CKD but at long term these therapies are not effective and do not prevent end stage renal failure because they interfere with very specific pathways. Mechanisms that lead to ESRD are multiple and very complex and the administration of one or more medicines is not enough to treat and cure CKD. Hence, even if on pharmacological therapy many patients eventually require renal replacement therapy, or dialysis.

Hemodialysis or peritoneal dialyses are both clinical procedures that utilize a man-made dialyzer to substitute kidney function by removing wastes such as creatinine and urea, as well as eliminating extra water and restoring the proper balance of electrolytes in the body. Renal dialysis is usually initiated when the renal function drops below 15% and symptoms or complications of kidney failure become apparent including but not limited to nausea, vomiting, loss of appetite and fatigue. Dialysis performs roughly about 10% of the total kidney function and does not reverse chronic kidney disease or kidney failure; thus it is not a complete replacement therapy. In addition to its major role in maintaining extracellular homeostasis, the kidney performs many other functions. It is regarded as an endocrine organ, responsible for the secretion of hormones that are critical in maintaining hemodynamics (renin, angiotensin II, prostaglandins, nitric oxide, endothelin, and bradykinin), red

blood cell production (erythropoietin), bone metabolism (1,25-dihydroxyvitamin D 3 or calcitriol) [37], as well as gluconeogenesis [38]. The conventional renal replacement therapies, based on diffusion, convection, or absorption, provide only filtration; they do not replace these lost homeostatic, regulatory, metabolic, and endocrine functions of the kidney [37].

Chronic hemodialysis is an ongoing, expensive and life-altering treatment. Although life-sustaining, it does not provide a high quality of life to most patients. There are certain risks and complications associated with dialysis treatment, which include hypotension, arrhythmia, infection, thrombus formation, possible headaches, nausea or confusion.

Today, kidney transplantation is the treatment of choice for patients with ESRD, because kidney transplantation has lifestyle advantages and is cheaper than dialysis. However, because the number of patients in need for renal replacement therapy is growing and the availability of donor kidneys for transplantation is very limited, many adults on the donor waiting list undergo dialysis or die on dialysis before they receive an organ [39]. In addition, about 2.5% of transplant patients develop anti-GBM glomerulonephritis leading to rapid graft rejection [40]. Despite all these, kidney transplantation is generally the only satisfactory treatment. In the US, more than 50,000 people are diagnosed with ESRD every year, yet only 20,000 receive a kidney transplant. Moreover, current immunosuppressive drugs such as, tacrolimus, mycophenolate and sirolimus needed to prevent organ rejection, have significant side effects. In the short term, infection is a particular concern, especially with viruses such as cytomegalovirus [41], and/or fungi such as candida albicans, C. glabrata, C. guilliermondii, C. krusei and Saccharomyces cerevisiae [42]. However, in the long term, the incidence of most cancers is increased in patients who are immunosuppressed. The risk of cancer incidence in patients now under the novel, more aggressive immunosuppressive therapies, may be higher than expected [43]. For these reasons alternative strategies to treat CKD are needed. Stem cell therapy is a promising new

area of investigation not only for kidney [44], but for treatment of many other organs and diseases [45]. Hence, if successful cell based therapy may be the future alternative.

1.4 Alternative therapy for CKD: stem cells

Within the past decade stem cells have emerged as a potential therapeutic tool by virtue of the unique stem cell tropism and pro-regenerative capacity. Recent advancements in stem cell biology introduce the possibility of regenerative approach to treat renal disease. The kidney is a complex organ and has a very limited regenerative potential of its own. Nevertheless, many studies collectively suggest that stem cells of both endogenous and exogenous origin play a beneficial role and have the potential to rescue acute and chronic renal phenotypes. The feasibility of stem cell therapy to treat renal disease has been extensively studied in models of Acute Kidney Injury (AKI) [46- 49], but only a few investigations have addressed the use of stem cells in models of CKD. Most reports have so far been concentrated on transplantation of whole bone marrow (BM) or fractions thereof, such as bone marrow derived mesenchymal stem cells (BMSC). Similar to cell therapy in AKI models, in most of these studies only little integration of exogenously administered cells has been observed, suggesting that integration and differentiation of donor cells might be of minor importance and that instead cell therapy may involve mechanisms that interfere with the inflammatory and fibrotic pathways activated during chronic progression [44]. When injected into mouse models of chronic kidney failure, BMSC appear to contribute to kidney repair. However, the beneficial effects of BMSC transplantation, although statistically significant, have been modest in scope and BMSC have not been shown to improve survival in these animals. These findings highlight the need to improve the efficacy of the specific stem cell therapies used and possibly to look at new sources of stem cells that might be more suitable for treating chronic kidney diseases. Therefore, our current knowledge of potential beneficial outcomes of stem cell treatments of CKD

and the underlying mechanisms of interaction between stem cells and chronically damaged renal tissue is still a very new area of investigation with many open questions.

1.4.1 Stem cells and their properties

The idea and the term “stem cell” was first introduced by Russian histologist Alexander Maximov in 1906 as part of his theory of hematopoiesis, according to which hematopoietic precursors descend from the stem cells due to local impacts generated by marrow stroma creating conditions for hematopoietic cell differentiation [50]. Since then, novel discoveries have emerged describing and characterizing stem cells of various origins, including evidence of adult neurogenesis by Joseph Altman et al. in 1960 [51], self-renewing cells in mouse bone marrow in 1963 by McCulloch et al. [52], followed by the derivation and introduction of the term “mouse embryonic stem cells” from the inner cell mass by Gail Martin in 1981 [53]. 17 years later in 1998 first human embryonic stem cells were derived by James Thomson and his co-workers at University of Wisconsin-Madison [54]. In 2006 first induced pluripotent stem cells were created in Yamanaka’s lab [55]. Shortly after stem cells lines derived from mouse and human amniotic fluid were reported in 2007 by Dr. Anthony Atala at Wake Forest University [56]. For over a century the initial concept of stem cells later substantiated by hard evidence has evolved into a solid scientific discipline called Regenerative Medicine. The 21st century has begun with great excitement and expectations in regenerative medicine. There is new hope that by means of stem cells and innovative technologies challenging problems in medicine, in particular end stage organ failure, may be overcome.

Stem cells are distinguished from all other cells by the two essential properties that they have (1) the capacity of self-renewal which allows cells to go through numerous cycles of cell division while maintaining the undifferentiated state [57], and (2) the capacity to differentiate into various

cell lineages giving rise to more specialized cell types under appropriate conditions [58]. Based on their differentiation potential stem cell are categorized as totipotent if they can differentiate into embryonic and extra-embryonic cell types [59], pluripotent if they can differentiation into representative cells of all the three embryonic germ layers, multipotent, if they can produce cells of a closely related family [60], and unipotent if they can produce only one cell without losing the self-renewal capabilities [61]. Multipotent and unipotent cells are commonly referred also as progenitors.

1.5 Our model of CKD: Alport Syndrome

Alport Syndrome (AS) is a genetic disorder caused by structural defects in type IV collagen, which is an integral component of the glomerular basement membrane (GBM). AS was first described by Dr. Cecile Alport in 1927 as a progressive familial nephropathy that disproportionately affected males and was associated with hearing loss [62]. The incidence of AS is estimated to be approximately 1 in 50,000 live births, but because of the familial nature of the disease, regional differences in disease frequency are common. AS is most commonly transmitted in an X-linked manner accounting 80 to 85% of all cases, but shows autosomal recessive inheritance in about 15% of cases and autosomal dominant inheritance in about 5% of cases. X-lined dominant trait inheritance is characterized by greater disease severity in hemizygous males than in females [40]. In heterozygous female patients the disease is much milder, manifested only by intermittent hematuria [63].

The entire surface of each individual nephron and collecting duct is coated by a basement membrane [9]. Basement membranes are of clear importance to the function of the kidney. The GBM is distinctive because of its great thickness (300-350nm) and its position between two cell layers, podocytes (the visceral epithelium) and endothelial cells (glomerular endothelium) [64]. Type IV collagen is the primary structural component of all basement membranes, including the kidney GBM. It consists of six

genetically distinct α-chains (α1 through α6) each encoded by a separate gene. Genes for COL4A1 and COL4A2 are on chromosome 13, COL4A3 and COL4A4 are on chromosome 2, and COL4A5 and COL4A6 are on the X chromosome. These six α-chains assemble into triple helical protomers that in turn form hexamers that are found in basement membranes. Combinations of only three triple helical protomers are naturally found in basement membrane: α1α1α2(IV), α3α4α5(IV), and α5α5α6(IV). Furthermore, these protomers are known to pair up in only three combinations to form hexamers: α1α1α2(IV)-α1α1α2(IV), α3α4α5(IV)-α3α4α5(IV) and α1α1α2(IV)-α5α5α6(IV). The α3α4α5(IV)-α3α4α5(IV) network is the main form of type IV collagen in the normal mature GBM. In glomerular development α1α1α2(IV)-α1α1α2(IV) network predominates in the immature GBM and must undergo a developmental switch with replacement by the α3α4α5(IV)-α3α4α5(IV) network [Figure 1]. All known mutations that cause AS are found in COL4A3, COL4A4, or COL4A5. Mutations in any of the genes can lead to a failure of this normal process, leading to persistence of the immature α1α1α2(IV)-α1α1α2(IV) network in the GBM. As a result, the GBM of patients with AS contains predominantly α1α1α2(IV)-α1α1α2(IV) network rather than α3α4α5(IV)-α3α4α5(IV) [65-72]. This immature basement membrane appears normal early in life but becomes damaged over time resulting into the clinical manifestations of AS.

The first subtle manifestations of classical AS (X-Linked) usually appear early in life with an onset symptom of microscopic hematuria usually detectable in the first year of life [73]. Proteinuria is usually absent at this time but develops and increases progressively with age leading to hypertension, ESRD and renal failure. AS inevitably leads to ESRD during adolescence or early adulthood, and about 50% of patients develop ESRD by the age of 20 years [40]. Most males with X-linked disease develop ESRD, often by age 30. The female carrier of X-linked mutations also develop progressive renal disease.

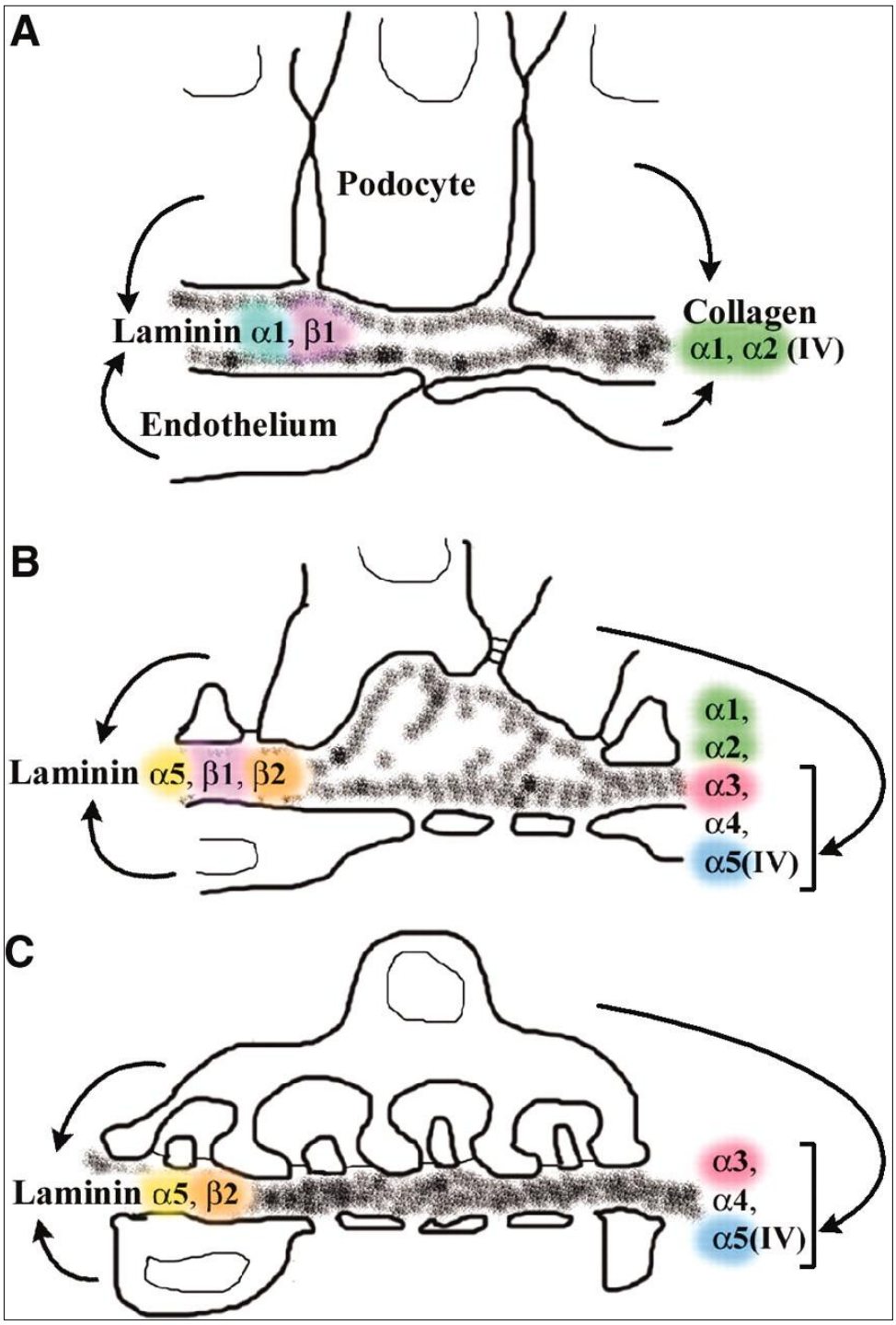

FIGURE 1. Diagram showing development of the glomerular capillary wall, stages of GBM assembly, and cellular origins of different collagen (IV) isoforms. The composition of both laminins and collagens changes as the glomeruli matures (A-C). Both endothelial cells and podocytes produce the collagen α1α1α2(IV) network. By contrast, the collagen α3α4α5(IV) network originates solely from podocytes. (This diagram is adapted from Abrahamson DR et al. 2009)

Microscopically, Alport syndrome is characterized by alternating zones of thinning and thickening of the GBM, splitting and lamellation of the GBM with loss of the normal lamina densa, accumulation of ECM in other interstitial regions of the kidney accompanied by increased expression of standard markers of fibrosis [74]. Podocytes which are the principle cells that synthesize the GBM, display variable foot process effacement seen under electron microscopy.

Diagnosing AS maybe somewhat challenging due to the heterogeneous nature of the disease, involving mutations in different α-chains of type IV collagen. Skin biopsy may be successfully used to diagnose patients with X-linked AS [75]. However, in most instances using a combination of electron micrography and immunohistology on kidney biopsy samples for collagen (IV) α-chains is required for more accurate diagnosis. Genetic testing is yet another diagnostic tool that is gradually becoming more available in routine medical practice. This and recent advances in our understanding of the structure of type IV collagen have led to dramatic progress in unraveling the pathogenesis of AS.

AS serves as a model of understanding progression of chronic renal fibrosis in mice [76,77], and humans [78]. Two mouse models are now commercially available for research to study CKD in hereditary nephritis that differ with respect to disease progression due to differences in compensatory mechanisms: (1) COL4A3 autosomal knockout model (129-*Col4a3*^{tm1Dec}/J) raised against 129x1/SvJ, and (2) COL4A5 X-liked knock-in model (B6.Cg-*Col4a5*^{tm1Yseg}/J) raised against c57BL/6J [79-82]. These animal models represent the human equivalent of AS, and thus represent a valuable model to study CKD. For the purpose of our study we chose the X-linked alport mouse model to investigate the role of AFSC therapy in CKD for two reasons: (1) X-linked AS is the most common form of the disease in humans accounting for about 80% of all cases, and (2) the life-span of this strain which is roughly about 6 month, provides enough time to evaluate possible effects attributable to stem cell therapy.

1.5.1 Stem cell therapy for Alport Syndrome

Handful of studies have been published in recent years investigating the role of stem cell therapy in CKD, using the mouse models of AS, as described earlier. In 2006 two independent studies by Sugimoto et al. and Prodromidi et al., using bone marrow transplantation into COL4A3$^{-/-}$ alport mice on C57BL/6J background claimed improved renal morphology and function post stem cell delivery [83,84]. Both studies reported differentiation of bone marrow cells to express mesangial and podocyte markers, without ruling out the possibility of cell fusion, and partial restoration of α3(IV) expression in GBM. Attenuation of renal fibrosis was also reported, accompanied with improvement in physiologic markers such as serum creatinine, BUN and proteinuria. However, because of the small number of integrated cells, Prodromidi et al. also speculated that paracrine actions could contribute to the beneficial effects of whole BM [85]. In a later study Katayama and coworkers reported that irradiation alone can prolong the life-span and improve physiologic parameters of COL4A3$^{-/-}$ Alport mice on 129x1/SvJ background without the need for BM transplantation [86]. These drastic differences in results could be explained by differences in the mouse background (C57BL/6J vs 129x1/SvJ) and the timing and dose of irradiation. Studies in non-irradiated COL4A3$^{-/-}$ mice on C57BL/6J background were later conducted to validate the therapeutic potential of BM-derived stem cells in treatment of Alport [87]. Multiple injections of wild-type BM cells was reported to improve renal histology and function correlating with de novo expression of the missing α3(IV) chain in the GBM. Unfortunately, no data on cell integration and animal survival was reported. On the other hand blood transfusion from wild-type mice was shown to improve Alport survival, with integration of the donor cells into the host glomeruli. Positive results were also obtained by treatment with undifferentiated mouse embryonic stem cells (mESC), suggesting that plasticity could be an important property of the so far unidentified therapeutic cell type in BM and blood. [87]. According to one study the beneficial effects of BM transplantation

observed in Alport mice is attributed to the hematopoietic stem cell (HSC) fraction, rather than the mesenchymal stem cells (MSC) within bone marrow [85]. Furthermore, multiple injections of BMSC in COL4A3-/- mice on 129x1/Svj background ameliorated interstitial fibrosis but did improve neither kidney function nor animal survival [88].

Given the confounding results obtained using different animal models and timing and dosing of injections, it is not clear at this point whether MSC from bone marrow could account for the therapeutic effects of BM transplantation in Alport disease.

OBJECTIVES

CKD is a serious medical problem associated with high rates of morbidity and mortality. Especially, the growing prevalence of diabetes and hypertension as well as the aging population are the major factors causing the observed rise of ESRD in recent years. Treatment options are few and limited mainly to the RAS inhibitors, conventional renal dialysis and kidney transplantation, the latter being the most effective treatment option of all. However, the shortage of donors and risks associate with these therapies suggest the investigation of alternative strategies for organ regeneration.

With the emergence of stem cells as potential therapeutic agents the putative usage of stem cells in the repair of kidney injury came into focus. In a novel effort to understand the mechanistic complexity of chronic kidney disease progression, and to explore the possibilities of stem cell therapy as an alternative to the current modalities we have investigated the role of stem cells derived from amniotic fluid in a mouse model of chronic kidney disease, Alport Syndrome.

Our study was designed to investigate whether amniotic fluid derived stem cells (AFSC) were capable of slowing down or possibly reversing chronic

kidney disease progression in Alport mice. Stem cell infusions were performed at an early stage of the disease, before the onset of proteinuria. Assessment of animal survival post AFSC treatment was conducted to evaluate the effectiveness of the therapy. In our earlier studies using AFSC, we were able to demonstrate that when injected into an embryonic kidney these cells did not only survive but also incorporated into primordial kidney structures in an *ex vivo* co-culture system [89]. Based on these findings, we were also interested to determine whether AFSC derived from wild-type mice could synthesize and deposit the missing α3/α4/α5 chains of collagen type IV once delivered into the glomeruli of collagen α5 (IV) deficient knock-in model of Alport mice.

Using AFSC therapy in a well established CKD model of Alport mice we aimed to uncover the essential regulatory mechanisms by which stem cells communicate anti-fibrotic signals. Experiments designed at histologic, cellular and molecular level were performed to understand the dynamic and complex role of AFSC in modulating host immune responses, myofibroblast differentiation and activation, and the synthesis and remodeling of the extracellular matrix. If new targets of therapy are identified the whole paradigm of chronic kidney disease treatment will shift from current efforts of slowing down disease progression to one of reversal.

MATERIALS AND METHODS

1. Derivation and Preparation of Amniotic Fluid Stem Cells (AFSC)

1.1 Extraction of mouse amniotic fluid and cell culture

Samples of mouse amniotic fluid from pregnant C57BL/6J females (12-15 days of gestation) were extracted from each embryo using a 29.5 gauge needle, and cultured separately in 35mm Petri Dishes [BD Biosciences] on a glass surface with Chang's media (α MEM, 20% Chang B and 2% Chang C) [Irvine Scientific], 1% L-Glutamine [Gibco/Invitrogen], 20% of ES-FBS [Gibco/Invitrogen] and 1% antibiotic [Pen/Strep, Gibco/Invitrogen]. Cells were cultured in humidified incubator at 37^{o} Celsius and 5% CO_2.

1.2 Selection of AFSC

Total cells extracted from mouse amniotic fluid were expanded for several passages but were not allowed to become over confluent. Then, cells with c-kit^{+} expression were selected out of the total population using standard Magnetic Sorting (MACS) techniques [Miltenyi Biotech]. Cells positively selected for c-kit were cultured onto 35-60mm Petri Dishes [BD Biosciences] at 70% confluence with Chang's media as described above. Samples from each embryo were processed and cultured separately to avoid mixing. Clonal cells were derived and characterized for differentiation capability and expression of pluripotent markers according to protocols outlined by Perin et al. [56].

1.3 Labeling of AFSC with CM-DiI and Qdot

AFSC were labeled with either a surface marker CM-DiI [Invitrogen], or a cytoplasmic marker Qdot [Qtracker 800, Invitrogen] for easy identification and tracking of cells when injected in mice *in vivo*. All the labeling steps were performed according to the manufacturer's instructions. Briefly, the

cells were incubated with a working solution of CM-DiI of 1mg/mL for 5 minutes at 37°C followed by an incubation of 15 minutes at 4°C and 3 washed with PBS. For the Qdot method, cells were incubated with the working solution of Qtracker800 (Qdot) for up to 1 hour at 37°C followed by 3 washes in PBS.

2. Mouse Model of CKD: Alport Syndrome

2.1 Animal model

Transgenic Alport mice [B6.Cg-Col4α5^{tm1Yseg}/J, stock #006283] on C57BL/6J background were purchased from The Jackson Laboratory. Detailed information of the mouse strain development is provided in Table 2. Alport colonies were maintained using a homozygous/hemizygous breeding scheme. In our laboratory mice homozygous for the Col4α5 (IV) allele begin to succumb to the disease at 11 weeks of age with a mean survival of 23.5 weeks.

Allele Symbol	Col4a5tm1Yseg
Allele Name	targeted mutation 1,
Allele Type	Targeted (knock-in)
Common Name(s)	COL4A5^{-};
Mutation Made By	Yoav Segal, University of Minnesota
Strain of Origin	129X1/SvJ
ES Cell Line Name	ESVJ-1182
ES Cell Line Strain	129X1/SvJ
Gene Symbol and Name	Col4a5, collagen, type IV, alpha 5
Chromosome	X
Gene Common	ASLN; ATS; CA54;

A targeting construct was designed to insert a G213T transversion into exon 1. This mutation was predicted to convert codon 5 from a glycine to a stop codon. Expression of the alpha5(IV) chain was lost in mutant kidneys from males. Basement membrane expression of the alpha 3(IV) chain was lost as well as that of the alpha6(IV) chain. Expression of alpha1(IV) and alpha2(IV) was conserved. Expression of the alpha5(IV) and alpha3(IV) chains in kidneys from females was mosaic, reflecting X-inactivation.

TABLE 2: General Information on The Mouse Strain Derivation

2.2 Mouse genotyping

All experimental and control Alport mice were genotyped to confirm the mutation of the collagen α5(IV) gene. Tail tissue samples were obtained from day 12-16 postnatal mice and processed for PCR analysis. Briefly, tissue samples were lysed in DirectPCR lysis reagent [Viagen] for 45 minutes at 85°C. 2μL of the lysate was then applied to run a PCR reaction following the reaction conditions outlined in Table 3.

Reaction Component	Volume (μl)
ddH2O	4.56
10 X AB PCR BufferII	1.2
25 mM MgCl2	0.96
2.5 mM dNTP	0.96
20 uM oIMR5290	0.3
20 uM oIMR5291	0.3
5 mM DNA Loading Dye	1.66
5 U/ul Taq DNA Polymerase	0.06
DNA	2
Total Volume	12

Primers Name	Sequence
oIMR5290	accacactgaccacagttcaa
oIMR5291	ccacccagggtagctgtcta

PCR Conditions

Temp.	Cycling
94°C	3.0 min
94°C	30 sec
61°C	1 min
72°C	1 min
72°C	2 min
10°C	hold
repeat 35 times	

TABLE 3: PCR Reaction Conditions For Alport Genotyping

(Invitrogen PCR reagents were used in all experiments)

Agarose gel electrophoresis was performed on PCR products, and the genotype was determined based on DNA size as follows: wild-type 124 base pairs and mutant 158 base pairs.

2.3 Experimental design

The mice were divided into 3 groups based on their treatment status: (A) Wild-type C57BL/6J mice; (B) Col4α5$^{-/-}$ mice; and (C) Col4α5$^{-/-}$ mice injected with AFSC at 1.5 months of age. Mice of the same age were used in all experiments, and littermate controls were used to minimize individual variability. Three experiments were designed independent of each other to address the following:

Experiment #1: 11 group (A) mice and 15 group (B) mice were left to reach the humane endpoint in order to evaluate the life-span of treated and non-treated groups.

Experiment #2: 4 group (B) [*one control per each time point*] and 12 group (C) mice were sacrificed at 24 hours (n=3), 5 days (n=3), 1 month (n=3) and 2.5 months (n=3) post treatment to evaluate cell fate in different organs.

Experiment #3: 15 group (A) mice, 25 group (B) mice and 25 group (C) mice were sacrificed at 5 days, 1 month and 2.5 months after injection to evaluate treatment outcomes.

2.4 Injection of AFSC

AFSC labeled with a tracking dye were prepared for injection into mice. Briefly, the cells were counted and the viability was determined by using a hemocytometer and trypan blue staining method. The cells were then passed through a 100μm cell strainer to obtain a single cell suspension. We administered about 1 million of the labeled AFSC by intra-arterial (intracardiac) injection through the chest wall into the left ventricle using a

29.5-gauge needle with careful monitoring under isofluorane inhalation anesthesia.

All animal experiments were performed in adherence to the National Institute of Health Guidelines for the Care and Use of Laboratory Animals, and with local Institutional Animal Care and Use Committee (IACUC) approval. IACUC is the Institutional Animal Care and Use Committee, on charge of overseeing CHLA's animal use programs, animal facilities, and policies ensuring appropriate care, ethical use and human treatment of animals.

2.5 Blood collection, creatinine and BUN measurements

Blood samples were collected before the start of treatment and at each of the time points (experiment #3 above) from all experimental groups (A, B and C) to evaluate renal performance by measuring creatinine and BUN levels. Blood was collected through a puncture in the facial vein with 4mm point length animal lancet [Braintree Scientific] following standard operating procedures approved by IACUC at Children's Hospital Los Angeles.

Blood samples (50μL per mouse) were collected into plasma separation tubes with lithium heparin. They were centrifuged at 13,000 RPM for 3 minutes, and the plasma (upper layer) was removed and stored at -80^{o}C until further use. A maximum of 15% of circulating blood volume was sampled in a given 14 day period. For creatinine analysis 30μL serum samples in duplicates were loaded into 96-well microplates including the standards. Working solution prepared by mixing 100μL reagent A and 100μL reagent B per well was quickly added to all wells and optical density was read at 1 min (OD_1) and 5 min (OD_5) at 490nm absorbance [BioAssay Systems]. The collected data was processed according to the instructions in the kit to obtain creatinine concentration in mg/dL. A similar kit [BioAssay Systems] was used to measure BUN following manufacturer's instructions.

2.6 Urine collection, proteinuria analysis

Urine samples were collected simultaneously with blood by placing the mice in metabolic cages for 18 hours overnight stay, one mouse per cage [Harvard Apparatus]. Mice were given free access to water, but food was restricted for the duration of their stay in the metabolic cages to avoid contamination of urine with food particles. Collected urine samples were transferred into eppendorf tubes and stored at -80^{o}C until further use.

Proteinuria was assessed by determining the albumin-to-cratinine ratio using an enzyme-linked immunoassay (ELISA) for albuminuria [Immunology Consultants Laboratory], and quantitative colorimetric assay kit for urine creatinine [BioAssay Systems] following manufacturers' protocols. Briefly, for albumin ELISA 100μL of urine samples and standards were loaded into 96-well microplate previously coated with anti-albumin antibody in duplicates, followed by 30 minutes incubation at room temperature. All wells were then washed and incubated with 100μL of Enzyme-Antibody Conjugate in dark for 30 minutes. The wells were washed again and treated with 100μL of TMB Substrate Solution for 10 minutes, after which the reaction was stopped with Stop Solution and the absorbance of the contents was determined at 450nm. Final albumin concentrations (ng/mL) were interpolated from the albumin standard curve. Urine creatinine concentration was determined by the same method that was described for blood (section 2.5).

3. Tissue Processing

Experiment #2 and #3: Mice were tranquilized with intraperitonial injection of 100mg/10Kg Ketamine/Xylazine and strained onto a surgical board. The heart was exposed through a ventral incision extending from the lower abdomen to the chest cavity. All mice were exsanguinated with PBS through the left ventricle until all organs were either pale or white. Kidneys were harvested and processed as outlined in section 3.1 for Experiment #2 and section 3.2 for Experiment #3.

3.1 AFSC fate determination and organ processing

Experiment #2: In order to evaluate the fate of AFSC in Alport mice after intracardiac infusion, the mice were sacrificed at the designated time points (see secton 2.3 Experimental Design) and four major organs including the heart, kidney, liver and lung were processed for flow cytometric analysis by fluorescent automated cell sorting (FACS). A non-injected littermate served as a negative control for each time point. Also, in a separate experiment Qdot labeled AFSC were serially diluted and FACS analyzed to establish the minimum detectable signal (1:100,000 is the minimum detectable threshold).

Heart: Heart tissue was minced and digested for 2 hours at 37^{o}C with 0.5mg/mL Collagenase Type II [Worthingto] and 1.2mg/mL bovine serum albumin (BSA) prepared in ADS buffer (116 mM NaCl, 20 mM Hepes, 1.0 mM NaH_2PO_4, 5 mM KCl, 0.8mM Mg_2SO_4, 5.5 mM glucose, pH 7.4). The tissue lysate was centrifuged for 5 minutes at 400g and the pellet was resuspended in PBS and subsequently filtered through 70μm and 40μm nylon mesh filters [BD Biosciences] to obtain single cell suspension.

Kidney: Kidneys were minced and digested with 4mg/mL solution of dispase II [Worthington] for 1 hour at 37^{o}C with constant gentle stirring (350 mg tissue per 10mL solution) prepared in DMEM [Invitrogen]. Following the digestion, the tissue was filtered through a 70μm nylon cell strainer [BD Biosciences] and washed twice in PBS.

Lung: In order to isolate the lung cells, chest cavity was opened and the lungs were exposed. 20U/mL dispase [Worthington] was infused into the lungs with a 21 gauge angiocatheter inserted into the trachea. The lungs were then placed in a 50mL tube containing 1mL of the dispase solution and incubated at room temperature for 45 minutes with gentle shaking. After the incubation, the lungs were transferred onto a clean petri dish containing 0.2mL DNAse I [Invitrogen] and incubated again for 10 minutes. The final lysate was filtered through a series of filters (100μm to 40μm) and washed twice in PBS.

Liver: Liver tissue was similarly minced and digested for 2 hours at 37^{o}C in 10mL enzymatic solution prepared in PBS containing 5mg collagenase [Worthingto], 5mg pronase [Worthington] and 1mg DNase I [Sigma-Aldrich]. After the incubation, the tissue was passed through 70μm nylon cell strainers and washed twice in PBS.

Prior to organ harvest all mice were exsanguinated with PBS through the left ventricle until all organs were either pale or white. All single cell suspensions were fixed in 1% paraformaldehyde [Polysciences] prior to FACS processing. Data acquisition and analysis of all organs by flow cytometry was performed with Vantage BD FACSDiva 5.0.1 flow cytometry system and BD FACSDiva5.1.3 software

3.2 Histology and immunohistochemistry

Immediately after kidneys were harvested renal capsule was removed to allow easy penetration of the fixative and processing solutions. At this point, the two kidneys from each mouse were each cut in half and each half kidney was processed differently based on the experimental needs.

For histology kidneys were processed by two methods to obtain frozen and paraffin embedded sections. A one-half kidney was prepared with O.C.T, snap frozen in liquid nitrogen and stored at -80^{o}C. For paraffin processing the tissues were first washed in PBS for 5 minutes then fixed in 10% formalin [Polysciences] for 2 hours at room temperature. Post fixation the kidneys were washed in 70% ethanol for 2 hours, followed by two washed in 100% ethanol for two hours and placed in toluene, twice for 40 minutes, then one hour in a solution of toluene/paraffin and paraffin overnight. The following morning the kidneys were entirely embedded in paraffin and prepared for sectioning. 5μm paraffin sections were stained with PAS (Periodic Acid Schiff) [Sigma-Aldrich] using standard histological protocols to study kidney morphology of all experimental groups for assessment of tissue damage and fibrosis. Jones silver stain was performed on Ventana NexES automated special stainer using Jones H&E

staining Kit from Ventana to evaluate basement membrane deposition (Pathology Laboratory, Children's Hospital Los Angeles).

For immunohistochemistry, thin deparaffinized kidney sections (5μm) were blocked in 3% BSA and immunostained against Macrophage/L1 Protein/Calprotectin Ab-1 [Thermo Scientific] at 1:50 dilution, S100A4 [FSP-1 Abcam] at 1:100 dilution with an overnight incubation at 4^{o}C, WT-1 [Santa Cruz Biotechnology] at 1:50 dilution and with an incubation time of 1 hour at 37^{o}C. Biotinylated secondary antibodies [Vector Laboratories] were used at 1:100 dilution. Slides were developed with DAB substrate [Vector Laboratories], followed by Hematoxylin and Eosin stains and mounted with Aqua Mount [Lerner Laboratories]. A Leica DM100 Microscope was used for imaging.

Paraffin embedded sections were also immunostained for fluorescence microscopy with antibody against α1 chain of Collagen type IV [Life Span Bioscience] at 1:50 dilution for 1 hour at room temperature, Collagen I [Abcam] at 1:250 dilution, CD80 [Abcam] at 1:50 dilution, Macrophage/L1 Protein/Calprotectin Ab-1 [Thermo Scientific] at 1:50 dilution at 4^{o}C over night, VEGF [Abcam] at 1:200 dilution for 1 hour at room temperature, followed by FITC-conjugated secondary antibody at 1:100 dilution. Sections were counterstained with 4',6-diamidino-2-phenylindole (DAPI) [Vector Laboratories].

In addition, frozen sections were stained with immunofluorescence CD150 [Abcam] at 1:25 dilution at 37^{o}C for 1 hour, PECAM-1 (CD31) [BD Biosciences] at 1: 200 dilution for 1 hour at room temperature and WT1 [Santa Cruz Biotechnology] at 1:50 dilution and with an incubation time of 1 hour at 37^{o}C. All Collagen IV α-chains [H12 (α1), H22 (α2), H31 (α3), RH42 (α4), H53 (α5), B66 (α6) Shingei Medical Research, Japan] were incubated at room temperature for 1 hour at 1:50 dilution. A Leica DM RA fluorescent microscope was used in conjunction with Open Lab 3.1.5 software to image the staining.

3.3 Evaluation of glomerular sclerosis

The degree of glomerular sclerosis was determined in histology sections stained with PAS reagent. All experimental groups, (A,B,C) were analyzed using 10 mice per group. The sclerotic index was examined in 50 randomly selected glomeruli. Glomerulosclerosis was assessed using a three level scale: normal-mild (for none to minimally sclerotic glomeruli with less than 33% fibrosis), moderate (for intermediate glomeruli with 33-66% fibrosis) and severe (for glomeruli with over 66% fibrosis) [90]. All assessment and analysis were performed in a blinded manner.

3.4 Evaluation of interstitial fibrosis

Interstitial fibrosis was determined by quantification of collagen type I deposition in the interstitial space of wild-type, non-injected and injected kidneys using immunofluorescently stained histology sections and TissueQuest 3.0.1.0131 software [Tissue Gnostics]. Four different interstitial areas were evaluated per cross section per mouse (n=10 per experimental group). All counts were performed in a blinded fashion.

3.5 Count of podocytes and S100A4 positive cells

In order to determine whether AFSC resulted into a preservation of podocyte numbers $WT1^+$ cells were counted in wild-type, non-injected and injected mice by evaluating 50 randomly selected glomeruli per mouse (n=10 in each experimental group). The fraction of $S100A4^+$ cells was evaluated in 4 different interstitial areas per cross section per mouse (n=10 per experimental group). All counts and analysis were performed in a blinded manner.

3.6 Gene Expression Analysis by Real Time PCR

One-half kidneys from treated and control groups were minced in small pieces and total RNA extracted using RNeasy kit [Qiagen] according to the manufacturer's instructions. Quantitative Real Time PCR for TNFα, CCL2, CXCL2, M-CSF, IL1R-I, IL1R-II was performed at 5 days and 1 month time points using a Roche Light Cycler 480 and Light Cycler TaqMan Master Mix. Real Time PCR conditions were as follows: 90^{o}C for 10 minutes, 60^{o}C for 10 seconds, 72^{o}C for 1 second with the analysis of the fluorescent emission at 72^{o}C. 35 cycles were carried out for each experiment. We also performed Real Time PCR for all the α chains of type IV collagen (α1, α2, α3, α4, α5 and α6) at 5 days, 1 month and 2.5 months to determine whether the rare presence of AFSC in the glomeruli were able to produce the missing collagen(IV) α5 chain. The sequence of all the primers and their corresponding probes are provided in Table 4.

3.7 TGFβ/BMP and EMT PCR arrays

RNA from wild-type (n=3), non-injected (n=3) and injected (n=3) mice were obtained as previously described for the Real Time PCR. Briefly, RT^2 First Strand Kit [SABiosciences] was used to convert mRNA to cDNA. This cDNA was then added to the SABiosciences RT^2 SYBR Green qPCR Master Mix. Each sample was used to perform quantitative gene expression analysis on specific arrays, c# PAMM-035F and c# PAMM090F. All steps were done according to the manufacturer's protocol for the Roche Light Cycler 480. The online tool http://www.sabiosciences .com/ pcrarraydataanalysis.php) offered by the manufacturer was used to analyze the data, including significant values and fold changes. Fold changes for the gene expression were investigated between injected mice and their non-injected siblings.

TABLE 4: RT-PCR Primer Sequences and Corresponding Probes

Gene Name	Probe	Primer Sequences
Angiotensin II receptor type 1	32	cgccagcagcactgtaga
		ggaggggtgaattcaaaa
Interleukin 1 receptor, type II	67	gtgccctgacctgaaagaat
		tccttattgcctttatccaagagt
Interleukin 1 receptor, type I	45	cgaaccgtgaacaacacaaa
		cagaggcaccatgagacaaa
CD80	91	tcgtctttcacaagtgtcttcag
		ttgccagtagattcggtcttc
CD86	107	gaagccgaatcagcctagc
		cagcgttactatcccgctct
M-CSF	68	cagctgcttcaccaaggact
		tcatggaaagttcggacaca
TNF-alpha	49	tcttctcattcctgcttgtgg
		ggtctgggccatagaactga
CCL2	62	ggctggagagctacaagagg
		ctcttgagcttggtgacaaaaa
CXCL2	49	ccagccacacttcagccta
		cagttcactggccacaacag
Ym1	68	tcttcagtgttctggtgaagga
		gatcttgtacccagacttgattacg
Col4a1	60	ctcctggcaagaatggagat
		aatccacgagcaccctga
Col4a2	3	cagcctctggatcggatact
		actagggactggcctccac
Col4a3	9	tgaagggagacctgggaga
		cacccttctggaagtgactg
Col4a4	51	gcgcacaaccaggaccta
		tacaggaaaggcatggtgct
Col4a5	72	gaatgaaaggagaccctgga
		ttgcctggtttacctcttgg
Col4a6	51	cacctggacctttgggaat
		ttgcatgccatcatcacc

3.8 Western Blot analysis

Total protein from kidneys was extracted and stored at -80^{o}C in a RIPA buffer supplemented with protease and phosphatase inhibitors [Santa Cruz Biotechnology] until use. SDS-PAGE was performed using Novex 4-20% Tris-glycine gels and standard protocols. Proteins were transferred onto a 0.45μm PVDF membrane [Millipore] and probed with antibodies to ID2 at 1:1000 dilution [Abcam], BMP-7 at 1:500 dilution [Abcam], pSMAD2 at 1:1000 dilution [Cell Signaling], pSMAD1/5 at 1:500 dilution [Cell Singaling]. Horseradish Peroxidase (HRP)-conjugated secondary antibodies [Simga-Aldrich] were applied in concentrations as follows: 1:10,000 for anit-mouse, 1:20,000 for anti-rabbit. Detection of antigens was performed using ECL Western Blotting detection Reagents [Amersham Biosciences/GE Healthcare], impressed on Biomax Light Film [GE Healthcare]. Data from four independent experiments were quantified by densitometry, and all measurements were normalized against their corresponding housekeeping gene, β-actin. Protein extraction and Western Blotting for collagen (IV) α2, α3, and α5 chains was performed following the protocols described in Sugimoto H et al. [83]. Briefly, kidneys were minced and homogenized in PBS with complete protease inhibitors, centrifuged and resuspended in PBS with protease inhibitors and homogenized for the second time. Tissue homogenates were centrifuged and pellets were re-suspended in 1M NaCl containing DNAse I [25mg/mL, Invitrogen]. The samples were vortexed and incubated at room temperature for 10 minutes. After centrifugation pellets were re-suspended in 2% sodium deoxycholate with protease inhibitors, vortexed and centrifuged again. Pellets were digested in collagenase type I (1unit/mL, Worthington] overnight to solubilize the NC1 domains of type IV collagen. Under reducing conditions protein extracts were separated and transferred onto a PVDF membrane as described above. Blotted membranes were blocked with 3% BSA containing 50mM Tris-HCl buffer (pH 7.5) and 150mM NaCl for over eight hours, washed three times with 0.1% Tween-Tris buffer, then treated with primary collagen type IV antibodies (H22

(α2), H31 (α3), M54 (α5)) [Shigei Medical Research Institute, Japan], for two hours diluted 1:100 in 1% BSA containing 50mM Tris-HCl buffer (pH 7.5) and 150mM NaCl. HRP-conjugated anti-rat secondary antibody [Santa Cruz Biotechnology] was applied thereafter and the blots were developed as described above.

3.9 Transmission Electron Microscopy (TEM)

Fresh half kidneys (n=3 per each experimental group) underwent primary fixation with 2% glutaraldehyde in sodium phosphate buffer then were post-fixed in 1% osmium tetroxide for 1 hour and dehydrated in 50%, 70%, 90%, 95%, 100% ethanol and propylene oxide 10 minutes each. Samples were further infiltrated with Epoxy resin mixture (Eponate 12 resin). Ultra-thin sections were collected on copper grids and stained with 10% uranyl acetate in 50% methanol and modified Sato lead stain. Morgagni 268 Electron Microscope was employed to picture acquisition (Pathology laboratory, Children's Hospital Los Angeles).

4. In Vitro Experiments

4.1 AFSC co-culture with stimulated macrophages

C57BL/6J wild type mice (n=5) were injected with 1mL of a 4% sterile thioglycollate solution [Brewer Thioglycollate Medium, DIFCO] into the peritoneal cavity under isofluorane anesthesia to stimulate macrophages *in vivo*. These mice were sacrificed with CO_2 administration after 4 days and macrophages were harvested by lavage of the peritoneal cavity [91]. Cellular culture was established for 24 hours for the following groups: 1. Non-activated macrophages 2. LPS [30ng/mL, Sigma-Aldrich] activated macrophages 3. Activated macrophages plus AFSC in 10:1 ratio 4. AFSC alone and 5. AFSC stimulated with lipopolysaccharide (LPS). Supernatant was collected and analyzed for multiple cytokine array using Proteome

Profiler Array Kit c# ARY006 and following the protocols suggested by the manufacturer [R&D Systems]. In addition, RNA was extracted and Real Time PCR for CD80, CD86, MCR1, IL1-RI, IL1-RII and YM1 was performed as previously described [see section 3.6].

4.2 AFSC co-culture with stimulated glomerular cells

C57BL/6J wild type mice (n=5) were infused with 15mL of 90% DMEM and 10% ES-FBS under pentobarbital anesthesia. Kidneys were extracted, minced, and digested with 1mg/mL collagenase I [Worthington], 100U/mL deoxyribonuclease I [Sigma-Aldrich] prepared in PBS at 37^{o}C for 30 minutes. After incubation the tissues were filtered twice through a 100μm nylon cell strainer and once more through a 70μm cell strainer, centrifuged at 1500 RPM for 5 minutes and the glomeruli were cultured in DMEM media containing 10% FBS, 1% antibiotics [Pen/Strep Gibco], and 0.2% Puromycin [Gibco] [92,93]. Three days after the primary culture cells began to migrate out from the glomeruli. These cells were grown and expanded for 4-5 passages and evaluated for WT1 expression to identify podocytes, PECAM-1 for endothelial cells and α-smooth muscle actin (α-SMA at 1:25 dilution at 37^{o}C for 1 hour, [Abcam]) for mesangial cells using immunofluorescence as previously described [see section 3.2]. Also, cellular culture was established for 4 hours for the following groups: 1. Glomerular cells 2. Glomerular cells in the presence of Ang II [Sigma-Aldrich] at concentration of 10^{-5}M twice at 2 hours interval 3. Glomerular cells in the presence of Ang II at concentration of 10^{-5}M twice at 2 hours interval plus 100μM of losartan [Sigma-Aldrich] 4. Glomerular cells in the presence of Ang II at concentration of 10^{-5}M twice at 2 hours interval plus AFSC in 10:1 ratio 5. AFSC alone, and 6. AFSC cells in the presence of Ang II at concentration of 10^{-5}M twice at 2 hours interval. RNA was harvested from all experiments (1 through 6) and Real Time PCR for Angiotensin receptor 1 (ANGTR1) was performed as previously described [see section 3.6].

5. Statistical Analysis

Statistical analysis was performed using SigmaPlot 11 data analysis software [Systat Software Inc]. Statistical differences between groups were determined using ANOVA and an unpaired *t*-test for data sets that passed the Shapiro-Wilk normality test or Mann-Whitney Rank Sum test for those data that failed the Shapiro-Wilk normality test. Kaplan-Meier curves were used for the survival study, and the log-rank (Mantel-Cox) test was used to determine statistical significance. A value of $p<0.05$ was considered statistically significant. All data are presented as mean±SEM.

RESULTS

1. AFSC Characterization

AFSC derived from c57BL/6J mouse present a fibroblastic shape on a petri dish culture plate [Figure 5A]. A clonal population of AFSC positively selected for the c-kit marker differentiated into adipocyte like cells staining positive for oil-red-O [Figure 5C], into osteoblast like cells expressing alkaline phosphatase [Figure 5E], and into skeletal muscle like cells expressing tropomyosin [Figure 5G]. Furthermore, undifferentiated AFSC express embryonic and mesenchymal stem cell markers such as OCT-4 [Figure 5H], alkaline phosphotase [Figure 5I] and Thy-1 [Figure 5J] as determined by FACS analysis. This expression profile indicates that our clonal population indeed has a wide differentiation potential.

2. Effects of AFSC on Alport Syndrome Mice

2.1 Alport animal model: effect of AFSC therapy on renal physiological markers

Col4a5$^{-/-}$ Alport mice raised on c57BL/6J genetic background develop CKD and succumb to renal failure at about 6 months of age. Histological evaluation of diseased kidneys using PAS staining showed abnormal glomerular morphology and abundant fibrotic lesions within the interstitial spaces [Figure 6A], whereas wild type kidneys presented with normal histology [Figure 6B]. Infusion of AFSC into Alport mice at 1.5 months of age improved average survival by 20% [Figure 6C]. Physiological parameters defining kidney function such as serum creatinine, BUN and proteinuria showed singnificant improvement and stayed closer to the reference normal at 2.5 months post AFSC treatment when compared to alport mice that were not treated [Figure 6D-F].

2.2 In vivo tracking of AFSC

AFSC labeled with a fluorescent marker (Qdot) presented strong detectable signal under fluorescent microscopy before injection [Figure 7B] and were also detected in kidney section 5 days post injection [Figure 7C]. Majority of them were localized within glomerular structures, with modest presence detected in the interstitial space [Figure 7D]. Distribution of AFSC in different organs such as in kidney, lung, liver and heart were further analyzed by FACS screening at the following time points: 24 hours, 5 days, 1 month and 2.5 months. At 24 hours time point, cells were detected in all of the 4 organs, but twice as many cells were present in the kidney as in the lung or liver or heart taken individually, accounting for an average of 0.10% of the total kidney cells [Figure 7E-H]. At 5 days cells were detectable in all the tested organs but the heart. They accounted for an average of 0.13% in the kidney, 0.01% in the lung, and 0.04% in the liver. At 1month and 2.5 months much fewer cells were detected in the kidney, constituting about 0.03% and 0.01% respectively [Figure 7E]. The AFSC numbers in the lung remained relatively constant for the last two time points detectable at 0.04% and 0.01% levels respectively [Figure 7F].

2.3 Assessment of renal morphology with and without AFSC injection

Experimental mice and their corresponding controls were evaluated histologically with PAS staining for the extent of glomerular and interstitial scarring at 1month and 2.5 months to determine the effects of AFSC therapy on renal morphology [Figure 8A-E]. Alport mice both with and without AFSC injection demonstrated similar level of glomerular sclerosis in all 3 categories at 1month as follows: normal < 2%, moderate > 60% and severe >30% [Figure 8D]. In contrast, there existed significant differences between littermate Alport untreated and treated mice in the fraction of glomeruli with moderate and severe fibrosis at 2.5 months. In particular, untreated Alport mice demonstrated a progressive increase in

the number of severely sclerotic glomeruli reaching well over 80%, whereas in the treated animals this number remained at 40% on average [Figure 8E].

In wild-type mice, COL4α1 is expressed in Bowman's capsule (BC), and in the basement membrane of tubules (TBM), while it is absent from the GBM [Figure 8F]. On the contrary, Alport mice at 4 month of age (corresponding to 2.5 month time point after AFSC injection) demonstrate increased accumulation of COL4α1 in the GBM as well as in BC [Figure 8G]. Alport mice receiving AFSC injections on the other hand appeared more normal at 2.5 months, with significantly less accumulation of COL4α1 in both GBM and BC. In addition, CM-DiI labeled AFSC were detectable in small numbers in the glomeruli of treated mice [Figure 8H].

In order to determine whether the deposition of new extracellular matrix is driven by fibrogenesis we performed histologic and quantitative analysis on the presence of type I collagen and myofibroblasts within the kidneys of the experimental groups. Wild-type kidneys had minimal to none presence of type I collagen, and no myofibroblasts in the renal interstitium as detected by a S100A4 (FSP-1) staining [Figure 9A-F]. Between the treated and non-treated Alport mice, treated animals demonstrated only mild deposition of collagen I after 2.5 months [Figure 9C], while non-treated mice showed abundant accumulation of collagen I throughout renal interstitium [Figure 9B]. These observations were confirmed by quantification of staining by measuring the surface area of positively stained areas [Figure 9G]. Similarly, injection of AFSC also reduced the number of S100A4 positive cells in the interstitial space when compared to their non-treated littermates [Figure 9D-F]. Statistical evaluation using positive S100A4 cell counts per cross sectional area revealed significant difference between injected and non-injected Alport mice at 1 month post therapy. No significant differences were detected in this same data between experimental groups at 2.5 month (4 month of age) [Figure 9H].

2.4 Gene and protein analysis of TGF-β and EMT pathways

In other to determine the mechanism behind the anti-fibrotic effects of AFSC demonstrated in the injected mice at 1month and 2.5 months, we looked at renal gene expression profiles for markers involved in TGF-β signaling pathway and the epithelial to mesenchymal transition (EMT) process by Real Time PCR. We detected significant downregulation of important transcription factors of TGF-β pathway such as Twist1, Snail2, Wnt11, Wnt5a, Zeb1, Zeb2 and Sparc, accompanied with upregulation of TGF-β pathway antagonist markers including Smad1, Smad5, Id2 at 5 days after AFSC injection [Figure 10]. Genes involved in matrix deposition were also down in expression in the treated mice versus untreated controls such as Fn1, Vcan, Collα1, Itgβ5, Coll3α1, Coll5α2, MMP-2, MMP-9 and fibronectin [Figure 10].

On the protein level we detected significant upregulation of pSMAD1/5 and ID2 at 5 days, confirming similar results from Real Time PCR. No change in BMP-7 and pSMAD-2 expression was detected [Figure 11]. Taken together these findings support the antifibrotic effects of AFSC detected in kidneys of Alport mice.

2.5 Effects of AFSC on macrophage recruitment and phenotype activation

The interstitial fibrosis detected in non-treated Alport mice at 2.5 months time point is also associated with large influx of macrophages [Figure 12B], meanwhile, as shown in Figure 12C mice that received AFSC infusions showed less macrophage infiltration in the renal interstitium. A spectrum of genes important for macrophage recruitment and activation were analyzed to determine the phenotypic identity of these macrophages. Real Time PCR analysis of AFSC treated kidneys at 5 days detected significant downregulation of genes involved in signaling pathway of M1 macrophages, such as TNFα, CCL2, CXCL2 and MCS-F together with an

upsurge in M2 specific expression of IL1-RII gene [Figure 12D]. At 1 month treated animals still showed significant downregulation of CXCL2, as well as IL1-RI, while IL1-RII was still upregulated when compared to their non treated siblings indicating macrophage activation more in favor of the M2 phenotype [Figure 12E]. In order to confirm these data we looked at additional markers that further characterize M1 and M2 marophages. The presence of M2 macrophages was increased in the interstitial space of treated mice at 2.5 months as demonstrated by CD150 immunofluoresence staining [Figure 13A-C]. Moreover, double immunostaining for CD80 and macrophage/L1 protein characterizing M1 macrophages was more prominent in the non-treated kidneys [Figure 13D-F]. Quantitative analysis of the immunostaining demonstrated significant statistical difference in M1 macrophage presence between treated and non-treated mice at 2.5 months [Figure 13G].

In order to confirm AFSC involvement in the observed differences in the recruitment and activation of macrophages we performed an *in vitro* co-culture assay of AFSC with macrophages activated with lipopolysaccharide (LPS). A protein array of the co-culture supernatant at 24 hours, in the presence of AFSC, showed significant decrease in the markers associated with macrophage recruitment such as IL-6, CCL5, RANTES and TNFα, which are highly elevated during CKD. In addition, IL1-RA, which antagonizes pro-inflammatory effects of IL-1 and prevents macrophage infiltration and inflammation was significantly elevated with AFSC exposure [Figure 14A]. Furthermore, markers specific for M1 macrophages such as CD80, CD86 and IL1-RI were decreased as shown by Real Time PCR analysis [Figure 14B]. Taken together these data indicate decreased signaling for recruitment of macrophages to the kidney and suggesting a phenotype switch of macrophages towards a more regenerative M2 activated state when in presence of AFSC.

2.6 Effects of AFSC on glomerular cells

Since Alport syndrome is associated with loss of podocytes as the diseases progresses we wanted to determine whether the functional and morphological benefits resulting from AFSC injection might be attributed to preservation of podocyte number. To this purpose we evaluated WT1 positive cells within glomeruli of treated and untreated kidneys. Mice injected with AFSC had more podocytes relative to non-injected mice, and about the same as the wild-type. The podocyte loss in the non-treated mice was significantly more compared to the other two groups at 2.5 months post injection [Figure 15A-D]. Next, we were interested to see whether AFSC differentiation into podocyte-like cells was the reason for their preservation in treated animals. Double staining for WT1 and AFSC tracking dye (Qdot) revealed no podocyte differentiation at 2.5 months after injection [Figure 15E]. On the other hand AFSC signal was co-localized with PECAM-1 and VEGF indicating that AFSC may undergo endothelial-like differentiation expressing VEGF [Figure 15F-G].

In order to confirm our observation that AFSC do not differentiate into podocytes we investigated all the α-chains of type IV collagen at mRNA [Figure 16] and protein [Figure 17] levels as well as histologically [Figure 18]. Consistent with lack of differentiation of AFSC into podocytes, we did not detect any new production of COL4α5 [Figure 16E, 17A and 18Q]. mRNA expression for COL4α1, COL4α2 and COL4α3 demonstrated gradual increase over time as detected at 5 days, 1 month and 2.5 months in both treated and non treated groups compared to wild-type [Figure 16 A-C]. Increase in COL4α4 gene activity was relatively modest [Figure 16D], whereas COL4α5 and COL4α6 activity was downregulated [Figure 16E,F]. These results are further supported by histology at 2.5 months, where treated and non-treated mice show increased expression for COL4α1 and COL4α2, decreased and irregular expression for COL4α3 and COL4α4 and no expression for COL4α5 and COL4α6 as compared to wild type [Figure 18]. Protein western blot analysis was the final

confirmation showing no difference in the ECM collagen deposition except the COL4α2, which is much lower in treated mice suggesting a possible difference in regulation of α-chain expression in the GBM of treated mice [Figure 17].

2.7 Effects of AFSC on GBM splitting

GBM splitting (thinning/thickening) is one of the typical characteristics of Alport syndrome, hence we investigated whether or not the GBM of injected mice was protected from this phenomenon. As shown in [Figure 19A-C], non-treated Alport mice have a glomerular structure that is far more damaged, and the GBM architecture severely destroyed versus treated mice and wild-type. Ultrastructural analysis demonstrated structural preservation of GBM and less splitting in the treated kidneys when compared to non-treated ones [Figure 19E,F]. Wild-type mice had normal GBM architecture without any signs of splitting [Figure 19D].

2.8 AFSC modulate Angiotensin II signaling

In order to find a mechanistic link that supports the beneficial outcomes, such as reduction in proteinuria, attenuated fibrosis and preservation of podocyte number attributed to AFSC injections in Alport mice, we investigated for possible modulation of Angiotensin II (Ang II) signaling in a co-culture system using glomerular cells isolated from kidneys of Alport mice. The isolated cells representing the early outgrowth cells from cultured glomeruli, were mostly podocytes as shown by a positive staining for WT1 [Figure 20A], with a small number representing mesengial cells (α-SMA^{+}) [Figure 20C]; no endothelial cells appeared to be present [Figure 20B]. These glomerular cells were stimulated with Ang II either, with and without the presence of AFSC or losartan. The following results were obtained: Ang II receptor (ANGTR1) was highly elevated with Ang II stimulation, while it was significantly downregulated in the presence of

losartan, an Ang II receptor antagonist as shown by Real Time PCR [Figure 20D]. When AFSC were added to the co-culture, the expression of the ANGTR1 was again significantly downregulated, similar to that of losartan. This data suggest that AFSC can antagonize Ang II signaling by dropping the ANGTR1 expression, which ultimately favors podocyte survival [Figure 20D].

DISCUSSION

As part of the urinary system, the kidneys perform several important physiological functions vital to the organism. They are responsible for the regulation of the body fluid volume and composition acting as natural filters of the blood. Primarily, they play a central role in regulating the volume of the internal environment, electrolyte balance and water concentration in the body. They do so by excreting just enough water and inorganic ions to keep the amounts of these substances in the body relatively constant. In addition, kidneys remove metabolic waste products, such as urea and creatinine into the urine, which can be toxic from accumulating in the body. Besides the main filtration functions, kidneys can also synthesize glucose from amino acids and other precursors during prolonged fasting and release it into the blood, and can also act as endocrine glands secreting hormones. The kidney is a highly vascular organ and receives approximately 20% of the cardiac output from the renal arteries. The two kidneys together filter on average about 200 liters of fluid from the bloodstream, and 2% of this filtrate leaves the body in the form of urine every day [94]. Thus, kidneys play an important homeostatic role in maintaining normal physiological balance of body fluids and by doing so they also have a critical role in regulating blood pressure through the renin-angiotensin-system, functioning as an endocrine organ. Alterations in the structure or function of any of the renal filtration components can shift the homeostatic balance of body metabolites, which can easily be detected by clinical assays.

The functional unit of the kidney is the nephron. Each nephron consists of an initial filtering component called the renal corpuscle and a tubule that extends out from the renal corpuscle. Each renal corpuscle contains a glomerulus and a Bowman's capsule. The renal tubule is continuous with a Bowman's capsule. It is a very narrow hollow cylinder made up of a single layer of epithelial cells. The epithelial cells differ in structure and function along the tubules length and are divided into segments according to their

specific roles. The tubular segments are the proximal tubule, loop of Henle and a distal tubule [Figure 2].

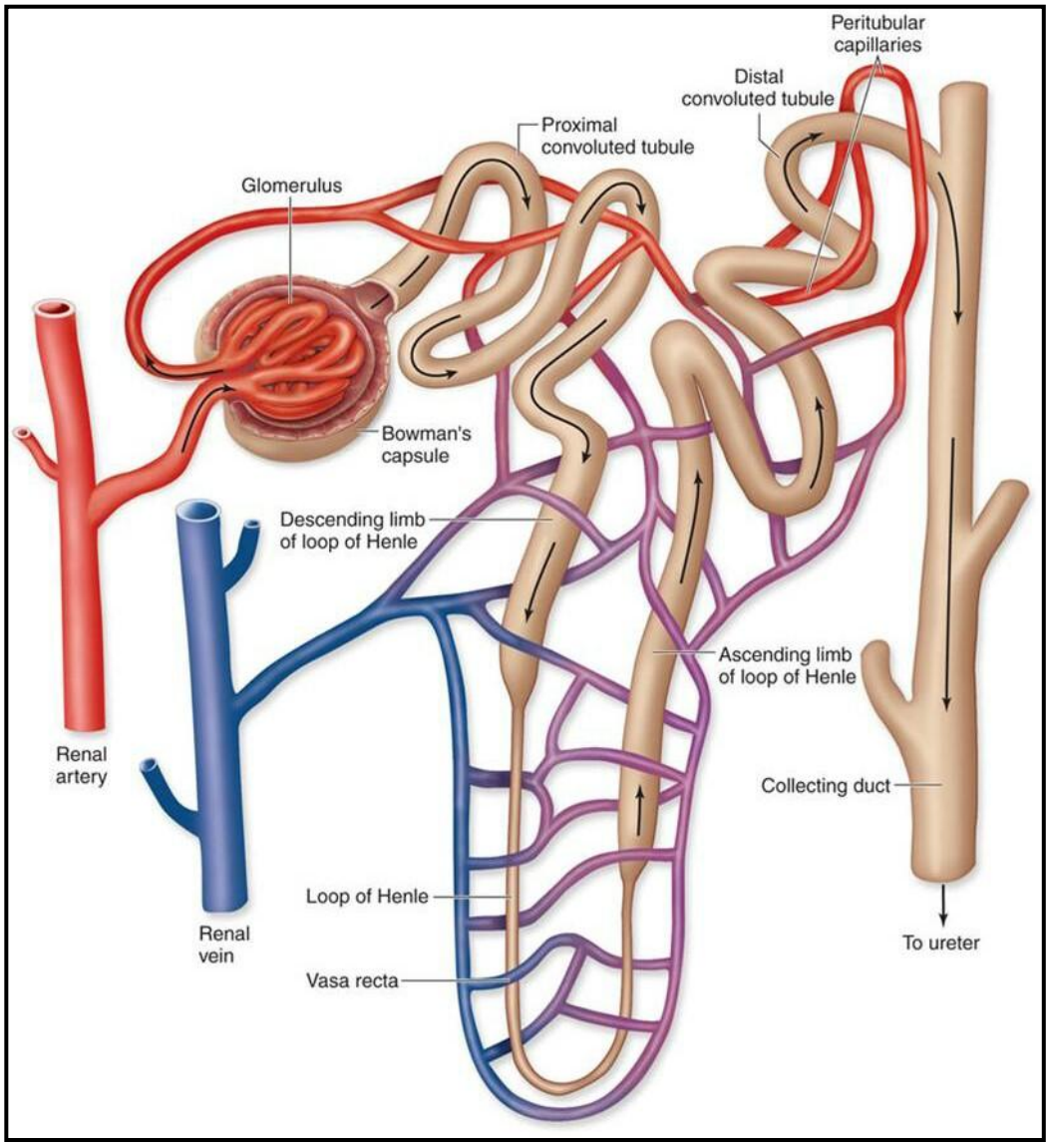

FIGURE 2. Schematic illustration of a nephron. Ultrafiltrate is produced across the glomerular filtrate membrane and travels through the renal tubules in the direction indicated by the black arrow. A complex process of reabsorption and secretion occurs across the tubular epithelial cells as the filtrate passes from the proximal to distal end of the tubules. Concentrated urine leaves the nephron via a ureter. (This diagram is adapted from www.Baileybio.com)

The fluid flows from the distal tubule into the collecting duct system, collects in the renal pelvis and leaves the kidney via the ureter. The primary role of the tubules is to reabsorb water and the essential non waste solutes (electrolytes) found in the filtrate and return it into the bloodstream. This whole process is orchestrated in a very complex reabsorptive and secretary mechanisms. Proximal tubule and Henle's loop ensure most of the reabsorption, whereas the distal tubule does the fine tuning for most of the substances, determining the final amounts excreted in the urine by adjusting their rates of reabsorption.

The role of the glomerulus is critical to the normal function of the tubules, because the ultrafiltrate that travels through the tubules is generated across the glomerular filtration membrane. So, the principle function of the glomerulus is the generation of an ultrafiltrate of plasma. The structural features of the glomerulus determine the composition of the ultrafiltrate, by allowing the passage of some substances, such as electrolytes and waste molecules, while blocking others, such as proteins. Architecturally, the glomerulus consists of a dense capillary network known as the glomerular tuft enclosed by the Bowman's capsule [Figure 3]. The Bowman's capsule is made up of the outer parietal, and inner visceral epithelial layers (podocytes). The space between the two cell layers is referred to as Bowman's space. Glomerular filtration occurs through the capillary wall into the Bowman's space from where the filtrate is directed toward the proximal tubule. The filtration barrier consists of three layers: 1) an innermost endothelium of the capillary, 2) the glomerular basement membrane (GBM), and 3) a layer of podocytes with interdigitating foot processes connected by slit diaphragms, which is also the inner layer of the Bowman's capsule. The endothelial cells of the capillaries are highly fenestrated and allow the passage of plasma proteins and other substances out of the capillary lumen into the GBM. The GBM is an extracellular matrix composed of type IV collagen, laminin, proteoglycans and nidogen which forms the structural foundation of the glomerular capillary to which endothelial and podocyte cells are anchored on both

sides. In addition, GBM is an important component of the filtration barrier, as the anionic charges of its macromolecules play an important role in the charge-selectivity during filtration, disallowing the passage of proteins and large molecules into the urinary space [95].

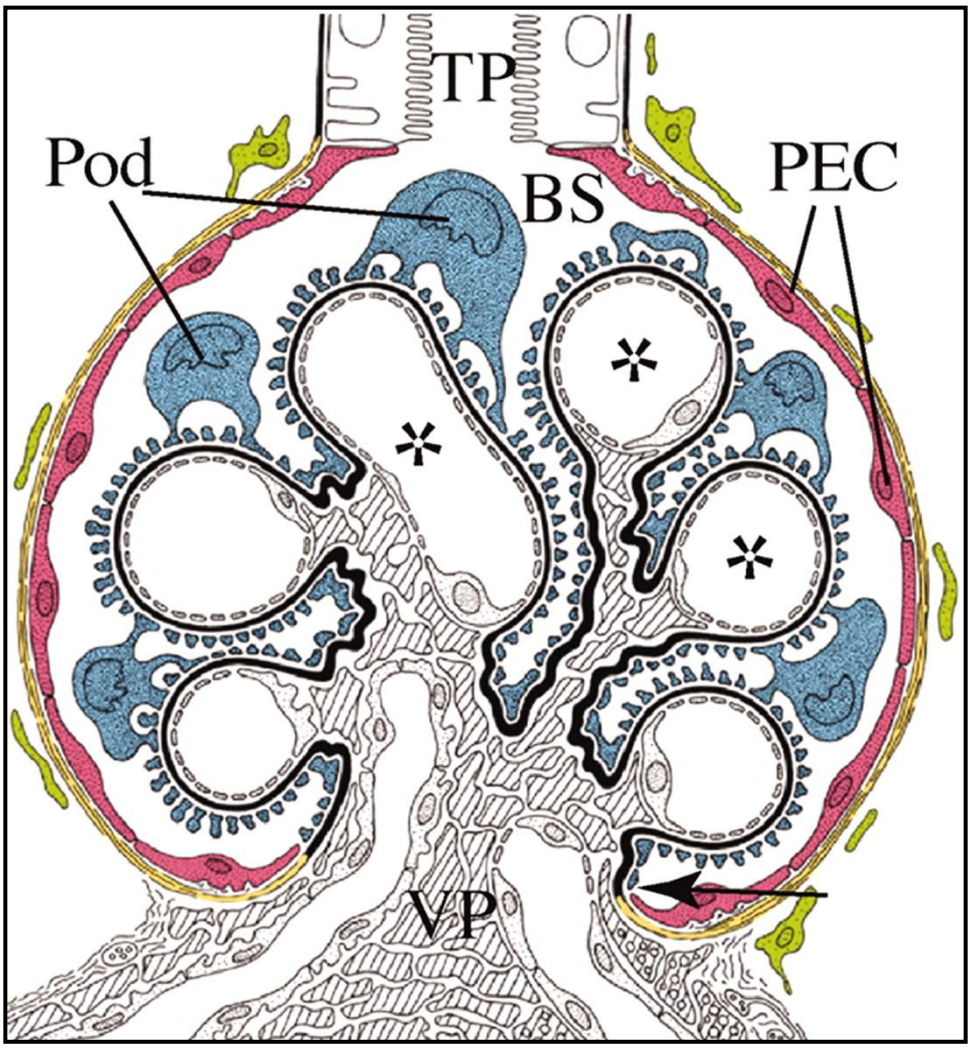

FIGURE 3. Renal glomerulus. The glomerular basement membrane (black) forms a continuous barrier between the glomerular epithelium and the endocapillary compartment that contains mesangial cells (shaded) and endothelial cells of the glomerular capillaries (*). Primary urine is filtered across the three-layered filtration barrier (endothelial cells, glomerular basement membrane, and Pod) into Bowman's space (BS). (This picture was adapted from Appel D. et al. 2009)

The podocyte that is covering the outside of the glomerular capillary is a highly specialized epithelial cell with a prominent cell body and large cytoplasmic projections (major processes) that divide into long thin processes (foot processes). The slit diaphragm is a highly specialized cell-cell junction that connects adjacent foot processes [Figure 4]. The protein complexes that make up the slit diaphragm have essential roles in the maintenance of the glomerular filtration barrier. Any alteration in their composition can result into the retraction of foot processes, a phenomenon that is well known to be associated with proteinuria. Taken together, all the three layers of the glomerular capillary wall need to be intact in order to maintain normal filtration function.

CKD is the manifestation of the changes in kidney structure and function that develops over many months or years variably depending on etiological factors. Most renal pathologies that lead to ESRD originate within the glomerulus and it is established that the dysfunction of podocytes is fundamental in this process. Therefore, dysfunction of the glomerulus is the hallmark of all major types of progressive kidney disease such as focal segmental glomerulosclerosis, membranous glomerulopathy, diabetic nephropathy, lupus nephritis, Alport Syndrome (AS), and others.

Our investigation on the possible therapeutic role of AFSC in CKD is based on the AS model. AS is a genetic form of kidney disease, affecting the normal development and composition of the GBM. As explained in the introduction, GBM undergoes structural remodeling during kidney development. The type IV collagen network of GBM in the embryonic kidney is comprised entirely of α1 and α2 chains. With the maturation of the glomeruli, the collagen type IV α1 and α2 chains are eliminated progressively from the GBM, and the α3(IV)-α5(IV) chains become the only collagen type IV chains available. In AS, mutations in any of the α3(IV)-α5(IV) chains prevent this modification in the GBM composition, leaving the kidneys with embryonic-like basement membrane. As a result of the missing collagen (IV) α-chains (α3, α4 or α5) in the GBM, glomerular structure and function become compromised

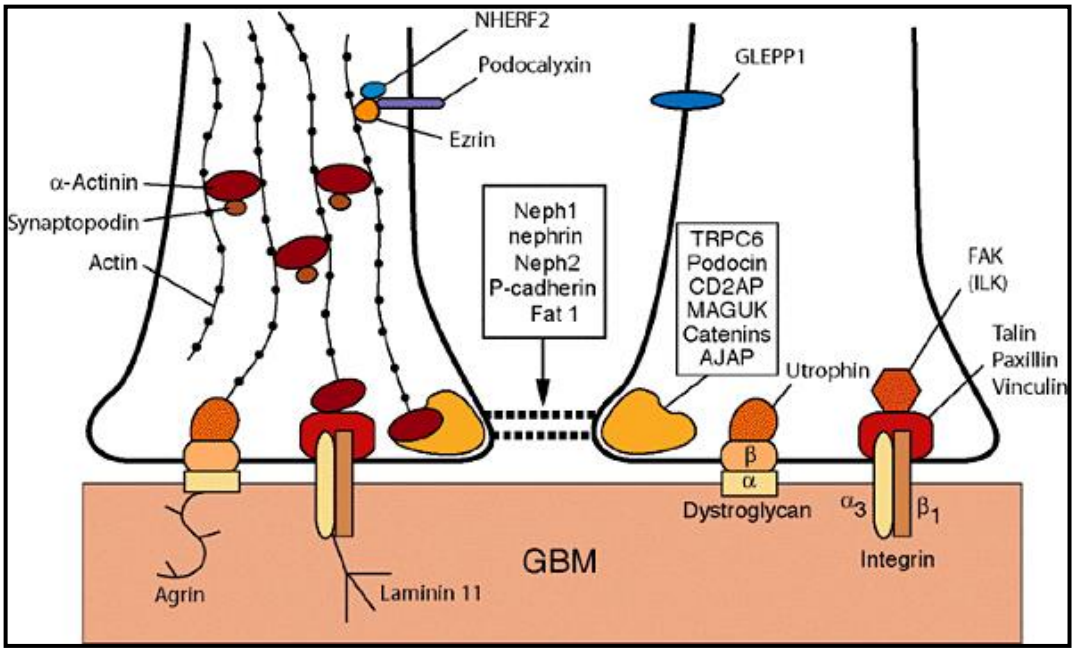

FIGURE 4. Schematic drawing of the membrane domains of the podocyte: the filtration slit diaphragm, basal membrane, and apical membrane domains. Molecular interactions within these domains of the podocyte foot processes are represented. (This picture is adapted from: William L. Clapp and Byron P. Croker; "Genitourinary tract – Kidney". Ed. Stacey E. Mills. Histology for Pathologies, 3rd Edition. Lippincott Williams & Wilkins, 2006. 874)

---

over time leading to progressive kidney disease and renal failure. The molecular mechanisms by which the altered GBM composition precipitates into structural and functional deterioration in AS is yet not clear. Nevertheless, few possible general mechanisms have been proposed suggesting that 1) defective composition of Alport GBM eventually succumbs to the physiological pressures and stress of normal glomerular function [96], 2) changes in GBM composition may alter the homeostasis of GBM remodeling by distorting the communication signals between cells and the extracellular matrix of GBM [79], or alternatively, 3) both of the above principles may be equally involved in contributing to Alport glomerular disease [97]. Accumulation of new data will eventually reshape our current understanding of mechanisms causing Alport disease, facilitating the discovery of more effective diagnostic and treatment methods for patients. Regardless of how much we now understand Alport disease on the mechanistic level, intense efforts are underway to find

novel therapies that will effectively treat progressive loss of renal function associated with AS, as well as other forms of CKD.

Stem cells possess tremendous amount of therapeutic potential due to their unique multifactorial properties, and thus have been under intense investigation being studied as prospective therapeutic agents that may serve as treatments for many acute and chronic diseases, including CKD. In particular, bone marrow derived mesenchymal stem cells have been extensively studied in mouse models of AS. Previously reported results obtained with injection of MSC as well as with whole bone marrow transplantation have shown some degree of protection against progression of AS. Differentiation of donor stem cells into renal cell phenotypes has been reported in several studies [83,87], while immune modulation is suggested to be the principle mechanism of stem cell protectionism in few other studies of mouse models of AS [85,88]. It has, however, been difficult to compare these studies because of diverse backgrounds in the mice investigated and experimental designs. The importance of the genetic background is explained by the observations that C57BL/6J Alport mice exhibit increased life-span compared to their 129x1/SvJ counterparts. This phenomenon is explained by the alternative collagen switch that involves the incorporation of α5 and α6 (IV) collagen chains, resulting in more stabilized GBM structure in C57BL/6J Alport mice. As a result of this and such other complications the particular mechanism by which stem cells protect kidneys from progressive damage in the case of Alport disease is not yet clearly understood [98,83,87].

We chose to study the ColIVα5 mutant strain of AS, as it represents the most common form of Alport disease in humans. This mouse model was derived from C57BL/6J background and unlike some reports [99] no backcrossing with other mouse strains such as 129x1/SvJ, were performed [81]. We used homozygous female and hemizygous male mutant mice in all our experiments. Based on our experience these mice develop progressive kidney disease with an onset hematuria and proteinuria at 3 months of age with a mean survival age of 25 weeks (~5.8

months). We used clonal population of AFSC in all injection experiments to minimize outcome variability. In addition, no irradiation of recipient mice was performed, since Katayama et al. demonstrated that irradiation by itself is renoprotective and prolongs animal survival in Alport mice by yet unknown mechanism [86]. In order to further optimize our results, we performed all experiments using only mice with similar body weight and renal physiological parameters. Injections of AFSC were performed in the early phase of disease (6 weeks of age or ~1.5 months) before the onset proteinuria when structure and function of the kidney would be least compromised and more amenable to repair. It is important to note, that proteinuria is one of the most important predictors of progression of CKD, and also assumes increased risk for cardiovascular disease. The passage of excess plasma proteins across the glomerular capillary wall may accelerate kidney disease progression to end stage renal failure by various pathways; one such example would be induction of tubular chemokine expression and complement activation that lead to inflammatory cell infiltration in the interstitium and sustained fibrogenesis [100-102]. Hence, early intervention may be directed at preventing the onset of proteinuria, subsequently blocking distractive pathways leading to end stage kidney failure, rather than challenged by complications that emanate from it at much later time. Importantly, we present the first ever study investigating stem cell therapy in ColIVα5 AS mice, as previous studies were all conducted using ColIVα3 AS mice raised against either C57BL/6J or 129x1/SvJ backgrounds, in which the rate of disease progression greatly vary from our model. Taking into full consideration all known information from previous experiments and based on our experience with AFSC we hypothesized that a single early injection of AFSC would be beneficial in prolonging the life-span of AS mice.

AFSC possess pluripotential capabilities both in vitro and in vivo [103,89], can easily be expanded in culture and are devoid of the ethical issues concerning the use of embryonic stem cells. Previously, we have demonstrated the successful participation of AFSC in the development of

nephron units. [89]. AFSC injected into embryonic kidneys integrated into the renal vesicle and C- and S-shaped bodies that constitute the primordial structures of the kidney. In addition renal differentiation of AFSC was demonstrated by expression of GDNF and other developmental kidney markers, indicating that AFSC have the potential to differentiate into renal cell types and express kidney specific markers. Contrary to this, however, AFSC demonstrate only minimal integration and differentiation into tubular epithelial cells when injected directly into the kidney in a mouse model of acute tubular necrosis [103]. Instead, AFSC demonstrate strong renoprotective properties *in vivo*. They have the ability to secrete cytokines that can modulate the local immunoinflammatory response and support recovery of damaged tubular epithelial cells. Such marked differences in AFSC behavior give us some ground to speculate that probably the microenvironment in embryonic kidney stimulates AFSC differently from that in adult kidney injury models. It is very likely that embryonic kidney driven by developmental signals promotes recruitment of AFSC and their differentiation whereas, under pathological conditions in vivo such stimuli may not be present, resulting in a totally different response.

After systemic injection of cells in Alport mice AFSC localization into kidney structures was minimal, constituting only about 0.1% of total cells at 24 hours, which dropped tenfold to 0.01% by 2.5 months after injection [Figure 7]. Localization of AFSC into other organs like the lung, liver and heart were minimal to none compared to the kidney indicating that they were either destroyed or ended up deviating from these organs owing to the luck of homing signals [104].

Alport mice treated with AFSC acquired survival benefit and lived 20% longer on average relative to the non-treated mice. Prolonged survival corresponded with renal functional improvements as reflected in the serum creatinine, BUN and proteinuria measurements, as well as general amelioration of renal morphology, manifested in preservation of glomerular and interstitial structures [Figure 6]. In particular, injected mice presented less glomerular and interstitial deposition of extracellular matrix in the form

of COL4α1 and Collagen Type I respectively [Figure 8,9]. Based on these findings we were interested in elucidating the mechanistic pathways by which AFSC could modulate fibrotic processes in the kidney. Renal fibrogenesis is a dynamic and complex process that involves many different cell types and molecular signaling mechanisms. Recent findings in this regard indicate that activated macrophages that are derived from their circulating precursor monocytes play an important role in promoting renal fibrogenesis [105,106]. Consistent with findings that partial or complete depletion of macrophages using various toxins or sub lethal radiation can significantly ameliorate tissue fibrosis in rodent models of CKD [107-113], our mice treated with AFSC demonstrated less infiltration of macrophages into renal interstitium at 2.5 months post treatment [Figure 12A-C]. Simultaneously, decreased number of myofibroblasts in the interstitial space was detected [Figure 9D-F], the cell type largely responsible for deposition of new extracellular matrix [114]. Hence, the correlation that we found between morphological outcomes associated with AFSC injection and limited presence of macrophages and myofibroblasts hinted the possibility that AFSC might be involved in modulating the signals involved in recruitment and activation of these cell types. Furthermore, there is a general recognition that in the kidney, macrophage derived TGF-β may potentiate fibrosis by paracrine activation of collagen producing myofibroblasts and promotion of tubular epithelial cell transdifferentiation into myofibroblasts [115,116]. This in part explains the beneficial effects observed in kidney after complete or partial depletion of macrophages, which is also in accordance with our observations in Alport mice. Myofibroblasts can derive from various sources by transdifferentiation or through activation of local interstitial fibroblasts but specific markers are lacking that will distinguish them from other cell types [117]. Nevertheless, we evaluated the change in expression of key regulators of EMT (epithelial to mesenchymal transition) and TGFβ/BMP signaling pathways in an effort to find target genes that may either directly or indirectly be activated or suppressed in AFSC injected kidneys. The dramatic changes in gene expression involved in the deposition of

extracellular matrix and development of fibrosis as illustrated in Figure 10 five days after AFSC infusion indicate that perhaps AFSC modulate the microenvironment in the damaged kidney, possibly through activation of BMP-like pathway. Downregulation of TGF-β1 and associated downstream mediators accompanied by upregulation in anti-Mullerian hormone (AMH) and Smad1/5 indicate the possibility of such a mechanism, as it has been demonstrated that AMH acting through ALK6 (BMP type I receptor) can activate Smad1 pathway [118], and Smad1 dependent transcription, as well as Smad6 expression mediated by ALK2 (BMP type I receptor) receptor complexes [119]. In addition, we detected significant increase in the protein levels of ID2 in injected kidneys at day 5 [Figure 11G,H]. ID2 (inhibition of differentiation 2) is HLH (helix-loop-helix) protein that binds to basic HLH family of transcription factors and dominantly antagonizes their transcriptional activity [120]. In a mouse model of pulmonary fibrosis it has been shown that ID2 or ID3 overexpression decreases the COL1A2 promoter activity in myofibroblasts [121]. Thus, upregulation of ID2 in our model may be similarly involved in decreasing the TGFβ induced promoter activity of type I collagen, resulting into attenuation of extracellular matrix deposition in the renal interstitium.

Mouse and canine models of AS have elevated expression of MMP-2 and MMP-9 in the renal cortex [122,123], suggesting that MMPs may play an important role in matrix accumulation associated with progressive renal scaring in these models. Zeisberg et al. [124] demonstrated that in AS, inhibition of matrix metalloproteinases critical in remodeling of extracellular matrix, such as MMP-2 and MMP-9, before the onset of proteinuria provides substantial disease protection through preservation of GBM and extracellular matrix integrity. Similarly, our findings demonstrate that with injection of AFSC before the onset of proteinuria, transcription activity of these two MMPs were significantly decreased at 5 days after injection [Figure 10], resulting in a preservation of glomerular and interstitial structures, possibly including amelioration of the GBM in treated mice, as confirmed by transmission electron microscopy analysis. This whole

evidence of changes in gene expression profile along the TGFβ superfamily of important transcription factors as well as in genes critically involved during EMT after AFSC injection suggests that AFSC can modulate TGFβ/BMP signaling by yet unidentified mechanism that favors renal protection and slows down the progression of AS.

Macrophages are the oldest cell type in the hematopoietic system and have largely remained unchanged throughout evolution over millions of years [125]. As briefly described earlier macrophages originate from their circulating precursor monocytes that are in turn derived from common bone marrow myeloid progenitors [126]. In different physiological conditions monocytes, guided by specific cytokine cues, are recruited and undergo activation process to become macrophages in tissue compartments or interstitial space that sends out the signals. Tissue macrophages are critically important cells. During development macrophages not only clear of dying cells, but also play a trophic role in promoting organ growth and nephrogenesis in the developing kidney [127]. They are also critically involved in all forms of acute [128] and chronic renal injury [129], including transplantation [130], as well as repair [131]. Macrophages, together with the cytokine environment, play a critical role in determining the balance between progressive fibrosis and resolution of inflammatory injury. Macrophages exhibit a range of phenotypes, a phenomenon that has been described as macrophage polarization or heterogeneity [132,14]. Upon recruitment they can undergo either classical activation generating M1 phenotype, or alternative activation, which produces M2 phenotype macrophages. Elevated expression of INF-γ, TNFα, and M-CSF induce pro-inflamamtory M1 polarization characterized by the production of IL-1, IL-12, IL-15, IL-18, IL-23, MCP-1 as well as ROS, NO, iNOS and NOS2 which in turn strongly influence the outcome of Th1, Th17 and $CD4^+$ T cell responses promoting tissue damage and fibrosis. M1 polarized macrophages are characterized by unique surface markers such as CD86, CD80, MHC class II^{hi}, IL-1R, $IL12^{hi}$, $IL\text{-}23^{hi}$ and $IL10^{lo}$.

High levels of IL-4 or IL-13, which induce M2a and IL-10 and TGF-β which induce M2c polarization are thought to suppress immune responses and promote tissue remodeling through increased endocytic capabilities, reduced proinflammatory cytokine secretion and production of various trophic factors [16-18]. Because macrophages are plastic cells they can also change between activation states in response to the ever-changing microenvironment and alter their effect from pro-inflammatory to anti-inflammatory, by switching from M1 to M2 or vise versa.

In our model of AS we knew from gross histologic evaluation that injection of AFSC significantly ameliorated infiltration of macrophages into interstitial space. Furthermore, we detected strong modulation of cytokine and chemokine cues that determine the activation status of macrophages. In particular, mice that were treated with AFSC demonstrated a significant decrease in levels of TNFα, CCL2 and CXCL2 at 5 days post injection [Figure 12]. These markers are highly expressed during chronic inflammation and in the presence of M1-type microphages [14]. Consistent with this expression profile we also detected significant reduction of M1 polarized microphages in injected kidneys as shown by double immunostainings with CD80 and L1 protein [Figure 13D-F]. In addition, IL1-R type II which acts as a decoy receptor and inhibits the activity of its ligands (isotypes of IL-1) was significantly downregulated in treated kidneys, suggesting that AFSC probably modulate macrophage activation by promoting M2 polarization 5 days after injection of AFSC in treated mice. A month after injection, macrophages were limited in the interstitial space and expression of IL-1R type I, typical of M1 and CXCL2 were decreased in our treated mice whereas expression of IL-1R type II was still upregulated as detected by Real Time PCR [Figure 12D,E]. In order to investigate whether the detected changes in cytokine and chemokine expression could be directly attributed to AFSC, we performed in vitro co-culture assays between AFSC and lipopolysaccharide-stimulated macrophages. The results from this assay strongly indicate that our *in vivo* results were a direct effect of AFSC because molecules such as TNFα, IL-

6 and CCL5 (RANTES) which is shown to be essential in macrophage recruitment in Alport syndrome [133] were all downregulated in the presence of AFSC [Figure 14A]. In addition, AFSC were able to deactivate macrophages by blocking the expression of receptors such as CD80 and CD86 [Figure 14B], which promote a strong Th1 response and exert antiproliferative and cytotoxic activities [134].

The positive effects of AFSC were not limited to the renal interstitium, where inflammation and fibrosis were reduced and the integrity of tissue structures were preserved but also in the glomeruli, where less accumulation of the pathologic collagen and preservation of podocyte numbers were observed in mice that were treated with AFSC compared to their non-treated controls. Because AS is first of all a disease of the collagens, it was important to determine whether AFSC were capable of treating the collagen α5(IV) mutation in our mice; in other words we wanted to find out whether AFSC could differentiate into podocytes and ultimately produce the missing chain of collagen IV, the cause of AS in our model. As it can be interpreted from our results (Figures 16E,17A,1Q) no *de novo* production and deposition of the α5(IV) collagen was detected in treated animals, neither at gene transcription level nor at the level of protein, shown by histology and further confirmed by western blotting at 2.5 months. However, slight downregulation in Col4α1 and Col4α2 were detected at 5 days post treatment in treated mice, when compared to their untreated siblings; and this observation is thought to have influenced their decreased observance in the GMB of treated mice 2.5 months after injection, as detected by immunohistochemistry [Figure 18]. In the absence of collagen α5(IV) chain α3 and α4 chains which along with α5 form a trimer and are localized in the GBM were also mostly absent in both treated and untreated mice similar to other reports in autosomal recessive mouse models (Col4α3) of AS. [135,87].

Contrary to findings reported by Kalluri and colleagues [87], we did not observe injected AFSC differentiating into podocyte like cells [Figure 15E]. This is consistent with recent studies in both acute kidney disease

[136,137], and CKD models other than Alport syndrome [138] and in Alport mice treated with MSC [88]. Nevertheless, the injected cells present within the glomeruli seem to express VEGF, probably indicating their ability to commit to endothelial-like cells [Figure 15F,G]. VEGF is an important signaling pathway during kidney disease progression, because its inactivation [139,140] as well as overexpression [141] results in proteinuria. In our model of AS progression of CKD is associated with loss of podocyte numbers in the glomerulus as was determined by quantification of WT1 positive cells in AS compared with wild type kidneys at 4 months of age. Interestingly, mice treated with AFSC demonstrated significant preservation of podocyte numbers as compared to their untreated controls [Figure 15A-D]. Based on these observations we can possibly speculate that the VEGF expression by AFSC may be involved in this phenomenon of podocyte preservation.

Podocytes play a key role in the progression of AS because they are the cell type responsible for synthesizing the GBM [142] and podocyte loss is shown to be associated with the development of glomerular sclerosis in human studies of type I and II diabetic nephropathy [143,144] in IgA nephropathy [145], in the chronic puromycin model of glomerulosclerosis [146] and in TGF-β transgenic mice [147]. The role of the podocyte is shown to be critical in the filtration process. Because podocytes cover the outer aspect of the GBM, they are the final barrier to protein loss. Hence, it is not surprising that podocyte effacement is associated with proteinuria. Several important factors have been identified that lead to the effacement of podocyte foot processes: 1) interference with the slit diaphragm complex, 2) direct interference with the actin cytoskeleton, 3) interference with the GBM, or with podocyte GBM interaction, and 4) interference with the negative surface charge of podocytes or with the activity of a membrane-bound tyrosin phosphatase, known as GLEPP1. In AS it is believed that podocyte GBM interaction may be the mechanism behind the podocyte loss in this model. Cosgrove and colleagues [148] have demonstrated that integrin $\alpha 1\beta 1$ plays an important role in the dynamic

remodeling of the GBM during AS, by promoting the deposition of pathologic laminins ($\alpha2\beta1\gamma1$ $\alpha2\beta2\gamma1$) in the GBM, which interfere with the binding of podocyte foot processes with laminin $\alpha5\beta2\gamma1$ via integrin $\alpha3\beta1$ (highly expressed on podocytes), and this results into podocyte effacement. Similarly, Gross et al. [149] have shown that collagen-receptor DDR1 that is localized at the lateral base of podocytes plays an important role in matrix-cell interaction between GBM and podocyte. It is believed that collagen mutations in AS might result in different binding affinity to their receptors such as DDR1, resulting into podocyte injury.

Podocytes also express Angiotensin II (Ang II) receptors and have been shown to be target cells for its action [150]. Ang II is a renal growth factor and a true cytokine with an active role in renal pathology. It is one of the major effector molecules of the renin-angiotensin system (RAS). Ang II plays an important role in podocyte apoptosis and initiation of albumiuria. Overexpression of Ang II receptor type I (ANGRT1) has been shown to cause substantial structural changes and nephron loss in transgenic rats, resulting in the development of proteinuria and progressive glomerulosclerosis [151].

In treating CKD, inhibitors of the RAS have been shown to be effective in ameliorating proteinuria and progressive fibrosis in a variety of human renal diseases [152-154,31]. However, the timing of the pharmacological intervention is critical for the outcome of such therapies, as it has been shown that the efficacy of angiotensin converting enzyme (ACE) inhibitors in non-diabetic renal disease is not significant in patients with proteinuria below 0.5g/day [152]. Contrary to this, studies in animal models have demonstrated that early but not late intervention with RAS inhibitors improves proteinuria in diabetic nephropathy rats [29]. Therefore, whether such therapies are effective in delaying CKD progression largely depends on the etiology and the stage of the disease. Interesting data from Gross O. and colleagues demonstrated that early angiotensin-converting enzyme inhibitor (ACEi) therapy can delay ESRD and improve the life expectancy of patients with AS. According to their retrospective analysis of over 250

patients the authors concluded that antihypertensive and antiproteinuric properties of ACEi are more beneficial with early therapy, and the earlier the therapy the better is the outcome [36]. Although, many different factors synergistically influence disease progression and manipulation of one of them might not be enough in producing desirable outcomes, the measurable benefits of RAS inhibitors cannot be underestimated. As a matter of fact, ACEi and angiotensin receptor blockers are the mainstays of therapy utilized to slow down the progression of CKD in humans [155-157]. Because of the major importance of the RAS in renal pathology and the role of ANG II in particular, we were interested to find out whether AFSC could modulate this important molecular pathway in our Alport mice, and also whether the beneficial outcomes from AFSC injections could be attributed to this modulation, if any.

Our *in vitro* co-culture experiments demonstrated that glomerular cells, predominantly podocytes, activated by Ang II, expressed high levels of angiotensin receptor type I (ANGTR1), which is an important component of angiotensin signaling. This observation is consistent with previous reports showing that podocytes express Ang II receptors and has been shown to be a target cell for Ang II action. Excessive Ang II signaling induces podocyte damage and consequent detachment from the GBM by downregulating the expression of nephrin, an important adhesion molecule of the slit diaphragm [158,151]. With the addition of AFSC to the co-culture system we observed decreased ANGTR1 expression, similar to that induced by losartan, an Ang II antagonist [Figure 20]. We speculate, on the basis of these experiments, that AFSC have the ability to interfere with Ang II signaling in podocytes through the downregulation of ANGTR1, thus protecting these cells from Ang II-induced damage, resulting in a delay of podocyte effacement or detachment from the GBM. Furthermore, we believe that a single injection of AFSC transiently interferes with Ang II signaling, leading to renoprotection over the intermediate term, in addition to effects on cytokine modulation and amelioration of fibrosis.

Taken together, our results indicate that a single injection of AFSC into a mouse model of X-linked Alport Syndrome provides significant protection from progressive kidney disease resulting into prolonged survival of treated mice. It is important to emphasize that CKD is not reversed by a single injection of AFSC and that treated animals do eventually succumb to ESRD, albeit later than untreated mice. Increased survival of injected mice corresponded with significant improvement in renal morphology, demonstrated by less infiltration of inflammatory and fibrotic cells, improved glomerular and interstitial fibrosis, and preservation of podocyte numbers. Renal functional measurements were also better in treated mice.

Analysis of important cellular and molecular markers involved in regulating key inflammatory and fibrotic processes along with evidence that AFSC do not differentiate into podocyte-like cells we speculate that the effect of AFSC in promoting these changes is all driven by immunomodulatory paracrine/endocrine mechanisms. As a matter of fact, our finding that AFSC can interfere with angiotensin II signaling by blocking angiotensin type I receptor, with the same exactly effect of losartan, has never been shown previously in any stem cell therapy chronic renal model.

CONCLUSION

In a pursuit of finding novel therapies to treat kidney diseases, in particular CKD and to better understand the cellular and molecular events that participate in the disease progression we applied AFSC to Alport mice. AFSC are established to have multipotential properties. We established that one single injection of AFSC can significantly increase the life-span of treated animals, along with morphological and functional improvements. We also discovered that although AFSC home to the kidneys after injection, they do not differentiate into podocyte-like cells, and therefore no production of the missing α5(IV) collagen was detected, as podocytes are the only cells in the glomerulus that synthesize this particular chain of type IV collagen. Despite the lack of differentiation treated kidneys were significantly protected from progressive damage, probably through mechanisms favoring preservation of podocyte numbers. We found substantial differences in the molecular profile of treated kidneys, when compared to untreated controls, indicating that AFSC are likely involved in modulating the immune and fibrotic processes slowing down the sharp decline in renal function of Alport mice. Finally, we found evidence that AFSC can interfere with Ang II signaling, via its receptor and produce the same effect as an Ang II receptor blocker (ARB), losartan. In conclusion, we can state that one single injection of AFSC in the early stage of Alport disease, before the onset of proteinuria can be beneficial in slowing down the progression to end stage renal failure, and hence might be potential tool for development of new therapies to treat chronic kidney disease and other diseases of similar nature.

FUTURE DIRECTIONS

Throughout our study of AFSC therapy in Alport mice, we documented several important findings: 1) preservation of podocyte numbers, 2) downregulation of Ang II signaling, and 3) alteration of macrophage recruitment and activation signaling in favor of M2 phenotype. On the basis of these findings the future aims of this project are the following:

1) Investigate whether AFSC interfere with podocyte-GBM interactions, that may lead to preservation of podocyte integrity by focusing on integrin signaling pathways.

2) Determine whether the *in vitro* effect of AFSC on Angiotensin II signaling via its receptor (ANGTR1) is true also *in vivo* in Alport mice.

3) Perform multiple AFSC injections in Alport mice and determine whether increased intervention may prove more beneficial.

FIGURES AND LEGENDS

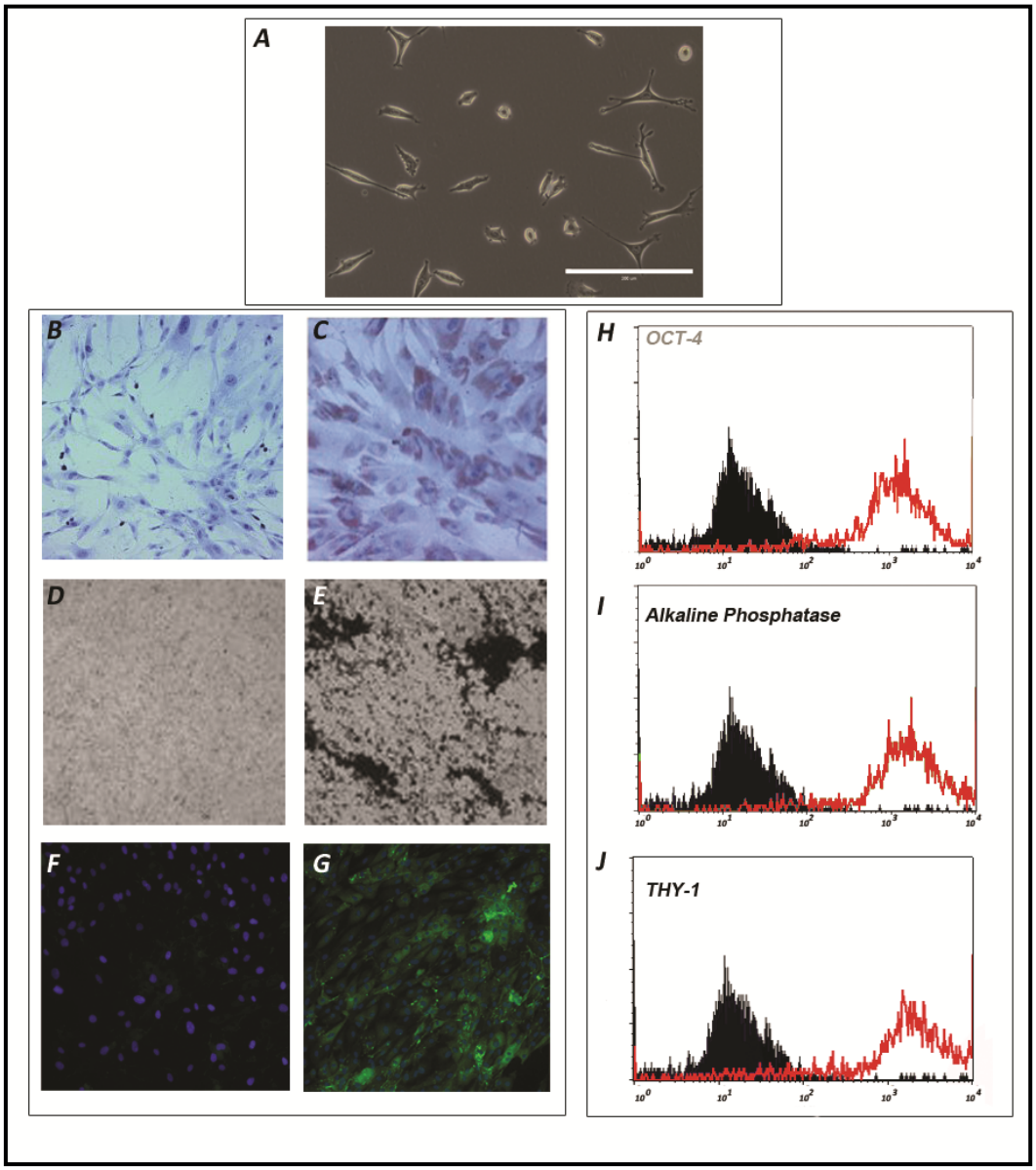

FIGURE 5. AFSC characterization and pluripotential capacity. After 19 passages, AFSC present a fibroblastoid appearance under bright field microscopy (A, X20). AFSC, under appropriate stimuli, are able to differentiate into adipocyte-like cells, as shown by oil-red-O staining (C, X10); into osteoblast-like cells, as indicated by alkaline phosphatase activity (E, X10); and into myocyte-like cells, as shown by expression of tropomyosin (G, X10), compared with controls (B, D, and F, X10). In addition, AFSC express mesenchymal and embryonic stem cell markers such as OCT-4 (H), alkaline phosphatase (I), and THY-1 (J), as shown by FACS analysis of undifferentiated cells.

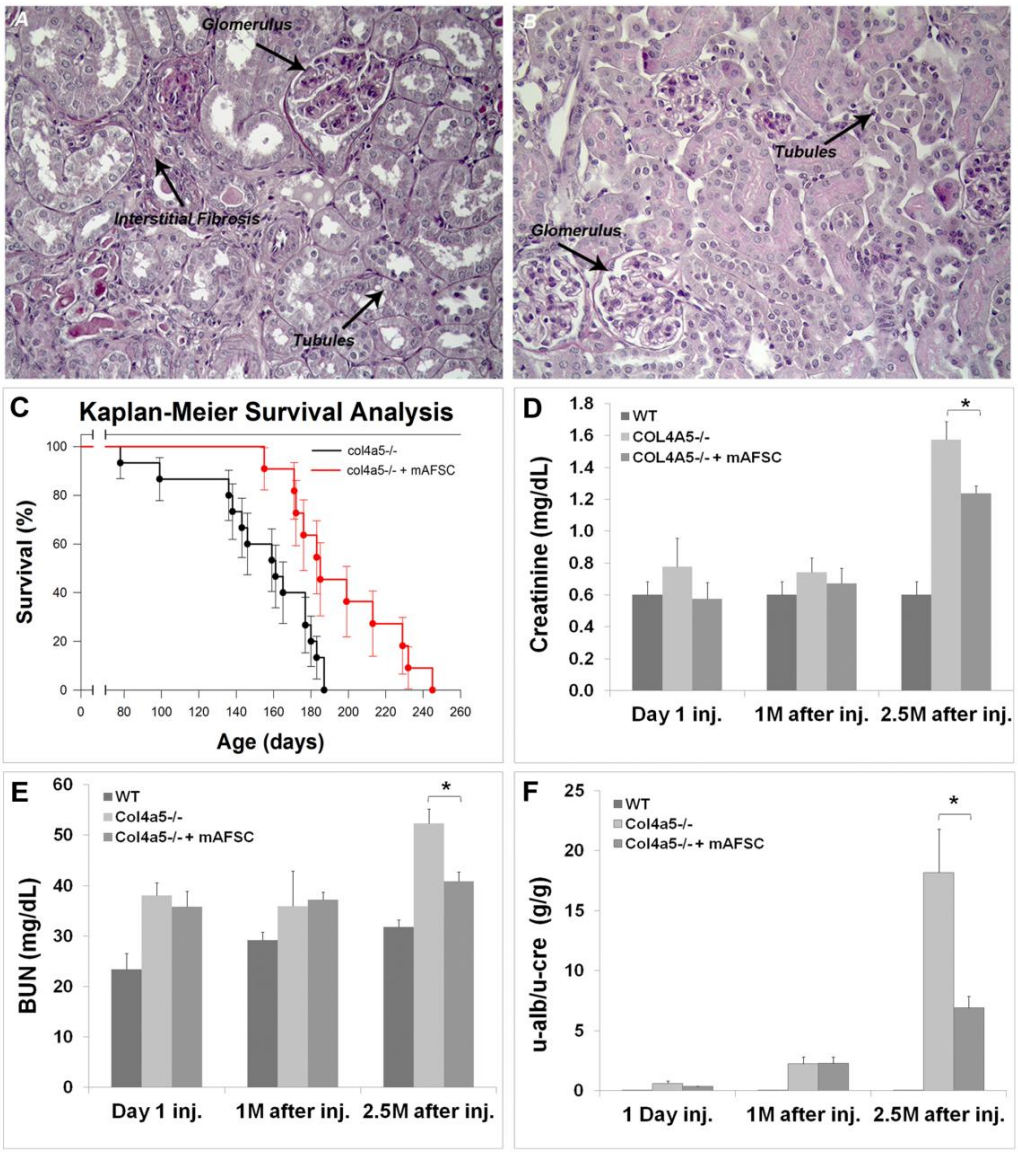

FIGURE 6. AFSC injections prolong animal survival and improve renal function. The progression of Alport syndrome leads to expanded fibrosis both in glomerular and interstitial spaces (A and B). Wild-type mice present normal renal morphology without any abnormalities (A, X20) compared with Col4a5$^{-/-}$ mice that exhibit progressive kidney disease (B, X20), as shown in representative periodic acid-Schiff staining pictures of kidney sections from mice killed at 5 months of age. Black arrows point to globally sclerotic glomeruli, widespread tubular cast formation, diffused interstitial fibrosis, and abundant infiltration of inflammatory cells. Injection of AFSC increased the lifespan of treated mice and ameliorated serum creatinine, BUN and proteinuria when compared with controls (C-F). Survival analysis of Col4a5$^{-/-}$ injected with AFSC at 1.5 months after birth (black, n=11) versus non-injected Col4a5$^{-/-}$ mice (red, n=15) demonstrated that injected mice had a mean increase in lifespan of 20% (C). Comparison of serum creatinine levels in Col4a5$^{-/-}$ mice injected with AFSC (n=15), non-injected Col4a5$^{-/-}$ (n=15), and wild-type (WT) controls show significantly lower serum creatinine levels at 2.5 months after AFSC injection in treated mice compared with their non-treated controls. (D). Furthermore, significant amelioration in BUN (E) and proteinuria (F) was also detected in mice at 2.5 months after injection.

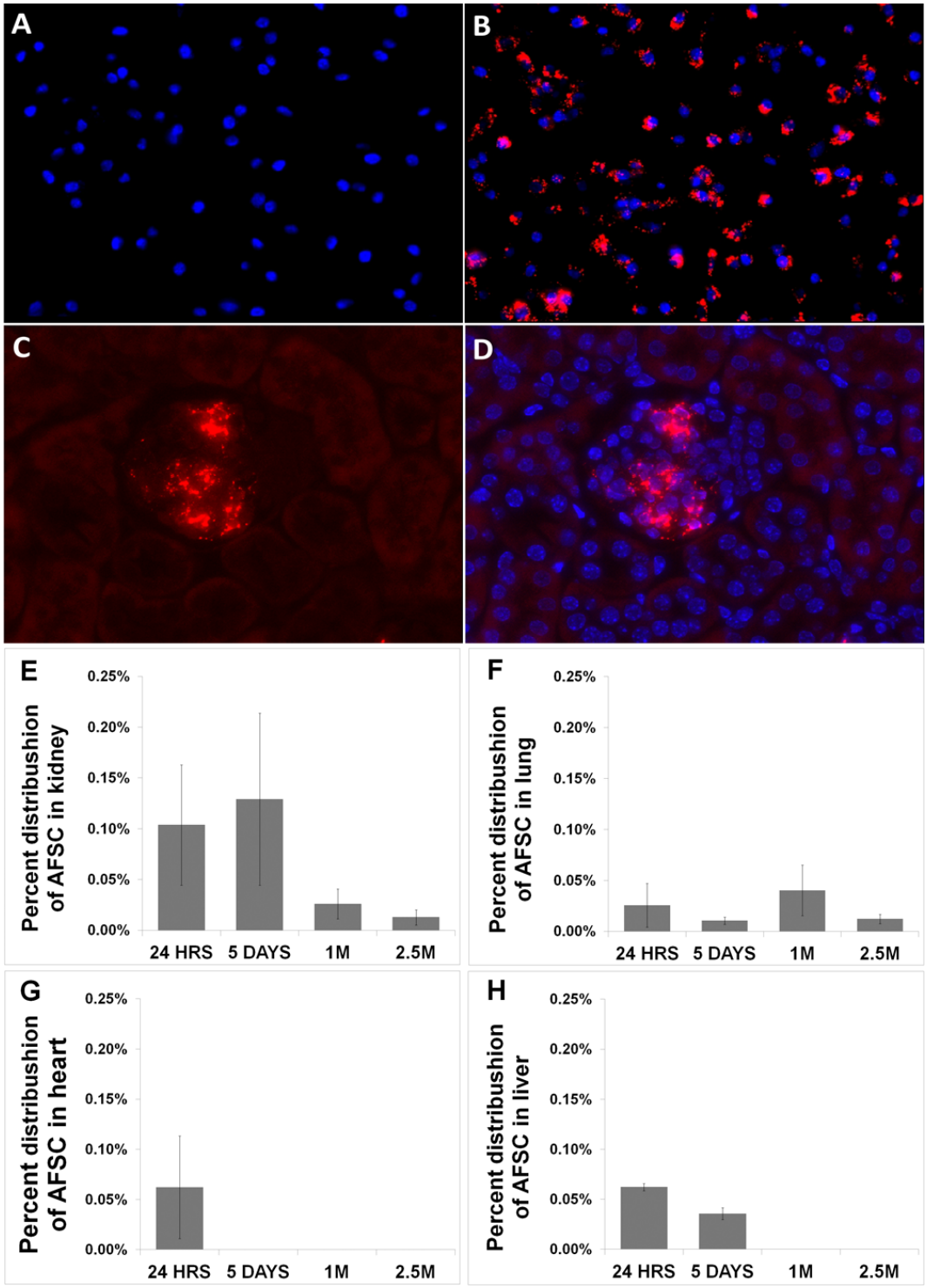

FIGURE 7. In vivo tracking of AFSC. AFSC before (A) and after (B) Qdot labeling. Injected cells were traceable after 5 days and could be detected by fluorescence (red, Qdot label) within glomeruli (C) and (D). Presence of these cells in kidney, lung, liver and heart, as detected by FACS, was demonstrated at 24 hours, 5 days, 1 month, and 2.5 months after injection (E-H). At 24 hours AFSC were present in all four organs, with the majority being localized in the kidney, accounting for an average of 0.1% of the cells (E). At the later time points, no cells were present in the heart (G) and liver (H). After 2.5 months, 0.01% AFSC were detected in the kidney as well as in the lung. All values are presented as mean ± SEM (*P<0.05).

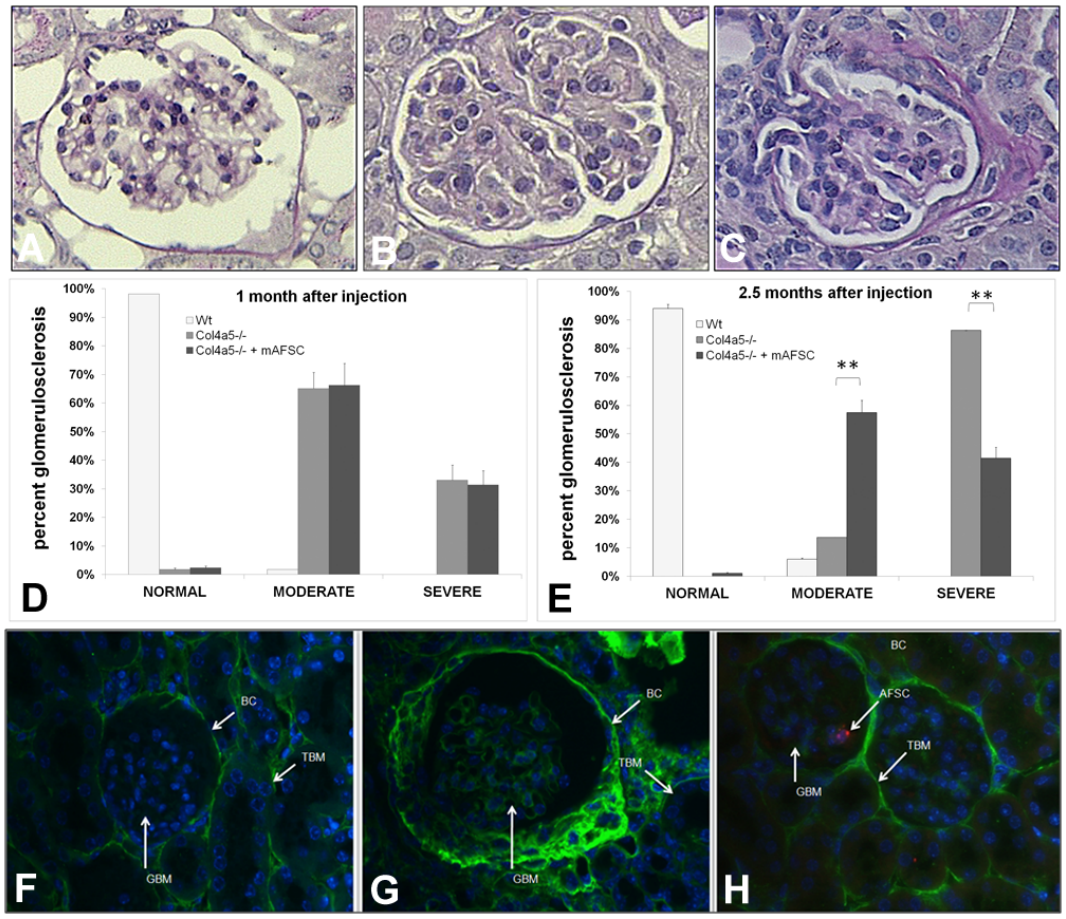

FIGURE 8. AFSC injection ameliorated glomerular fibrosis in AS mice. Using periodic acid-Schiff staining, glomeruli of Col4a5$^{-/-}$ mice injected with AFSC, Col4a5$^{-/-}$ non-treated mice and wild-type mice were scored according to the severity of fibrosis and the representative images are shown as follows: normal-mild (0%-33%) (A, X40), moderate (33%-66%) (B, X40) and severe (66%-100%) (C, X40). As shown by graphs, the injected mice present less sclerotic glomeruli than their non-injected siblings at 2.5 months after injection (D-E). AFSC reduced COL4α1 deposition within the glomeruli (F-H). Injected mice showed less glomerular deposition of COL4α1 compared with non-injected mice. Representative pictures show COL4α distribution (green) in wild-type mouse (F, X40), non-injected Col4a5$^{-/-}$ mouse killed at 4 months after birth (G, X40), and Col4a5$^{-/-}$ mouse injected with AFSC at 1.5 months after birth and sacrificed at 2.5 months after injection (H, X40). Rare AFSC labeled in red with CM-DiI were seen inside the glomeruli of injected mice (arrow, H) (BC, Bowman's capsule; TBM, tubular basement membrane; GBM, glomerular basement membrane).

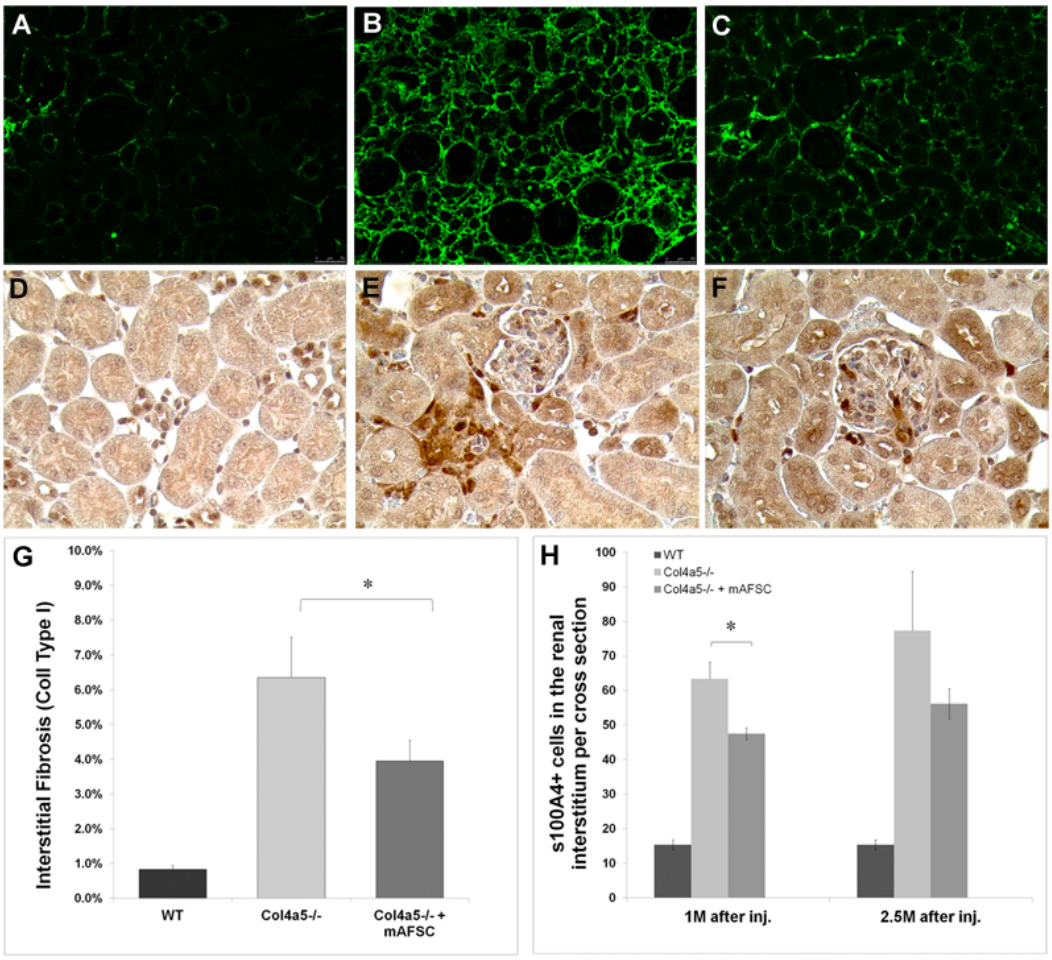

FIGURE 9. AFSC injection ameliorates interstitial fibrosis. Injection of AFSC diminished the deposition of extracellular matrix in the interstitium, as shown by quantification of collagen I (A-C and G). In the representative picture of injected mice (C, X20; n=10) the presence of collagen I is clearly less than in the non-injected mice (B, X20; n=10) and is much more similar to that of the wild-type (A, X20). These data were confirmed by quantification of staining. Graph in G compares collagen I accumulation per cross-section in all experimental groups analyzed morphometrically using HistoQuest software, revealing a statistically significant difference at 2.5 months after injection. Injection of AFSC also reduced the number of S100A4-positive cells (D-F and H). This marker is mostly expressed by cells undergoing myofibroblast transformation and by cells actively producing collagen during the progression of fibrosis, including endothelial cells and macrophages. In treated mice (F, X20), the number of S100A4-positive cells in the interstitial space is reduced compared with their untreated siblings (E, X20). The graph in H represents the change in number of S100A4-positive cells per cross-section in mice injected (n=10) at 1.5 months after birth and killed at 2.5 and 4 months of age versus non-injected (n=10) mice of the same age. All values are presented as mean ±SEM (*P<0.05). (WT, wild-type).

TGFβ/BMP Pathway Gene Expression of Col4a5-/- + AFSC compared to Col4a5-/- 5 days after injection					
Name	Gene Symbol	Fold Regulation	Name	Gene Symbol	Fold Regulation
Anti-Mullerian hormone	Amh	3.3066	Inhibitor of DNA Binding 2	Id2	4.2047
Bone gamma carboxyglutamate protein 2	Bglap2	4.9314	Nuclear receptor subfamily 0, group B, member 1	Nr0b1	1.9661
Distal-less homeobox 2	Dlx2	3.8781	MAD Homolog 1 (Drosophila)	Smad1	2.443
Growth differentiation factor 3	Gdf3	3.1719	MAD Homolog 5 (Drosophila)	Smad5	3.5851
Growth Differentiation Factor 6	Gdf6	3.2161			
Caldesmon 1	Cald1	-3.7029	Nodal Homolog (Mouse)	Nodal	-3.15
Chordin	Chrd	-7.593	Platelet derived growth factor, B polypeptide	Pdgfb	-4.6525
Collagen, type I, alpha 1	Col1a1	-94.6589	Platelet derived growth factor receptor, B polypeptide	Pdgfrb	-6.3879
Collagen, type III, alpha 1	Col3a1	-14.812	Serpin peptidase inhibitor, clade E	Serpine1	-6.2709
Collagen, type V, alpha 2	Col5a2	-3.0356	Snail homolog 2 (Drosophila)	Snai2	-3.3839
Endoglin	Eng	-9.1981	Secreted protein, acidic, cysteine-rich (osteonectin)	Sparc	-3.8691
Estrogen receptor 1	Esr1	-5.5098	Transforming Growth factor, beta I	Tgfb1	-3.5768
Fibronectin 1	Fn1	-10.893	Transforming Growth factor, beta receptor II	Tgfbr2	-14.3668
Growth Differentiation Factor 1	Gdf1	-9.6109	Twist homolog 1 (Drosophila)	Twist1	-3.6435
Integrin Beta 5	Itgb5	-28.5351	Versican	Vcan	-4.7634
Jun oncogene	Jun	-17.2437	Wingless-type MMTV integration site family, member 11	Wnt11	-19.726
Keratin 19	Krt19	-24.062	Wingless-type MMTV integration site family, member 5a	Wnt5a	-3.447
Matrix metallopeptidase 2	Mmp2	-4.2242	Zinc finger E-box binding homeobox 1	Zeb1	-2.7107
Matrix metallopeptidase 9	Mmp9	-11.2772	Zinc finger E-box binding homeobox 1	Zeb2	-2.9187

FIGURE 10. AFSC can modulate important genes of fibrosis progression and matrix deposition, including MMPs. Real Time PCR Analysis of renal gene expression for markers involved in cellular activation, proliferation and differentiation pathways including TGFβ/BMP signaling demonstrated that AFSC promoted the downregulation of genes involved in fibrosis after 5 days of injections. Important transcription factors of TGFβ pathway such as Twist1, Snai2, Wnt11, Wnt5a, Zeb1, Zeb2 and Sparc as well as genes involved in matrix deposition including Fn1, Vcan, Coll1α1, Itgβ5, Coll3α1, Coll5α2, Mmp-2, Mmp-9 and fibronectin were significantly downregulated in the AFSC treated Col4a5$^{-/-}$ (n=3) mice versus untreated controls (n=3). Values are presented as mean ± SEM ($p < 0.05$).

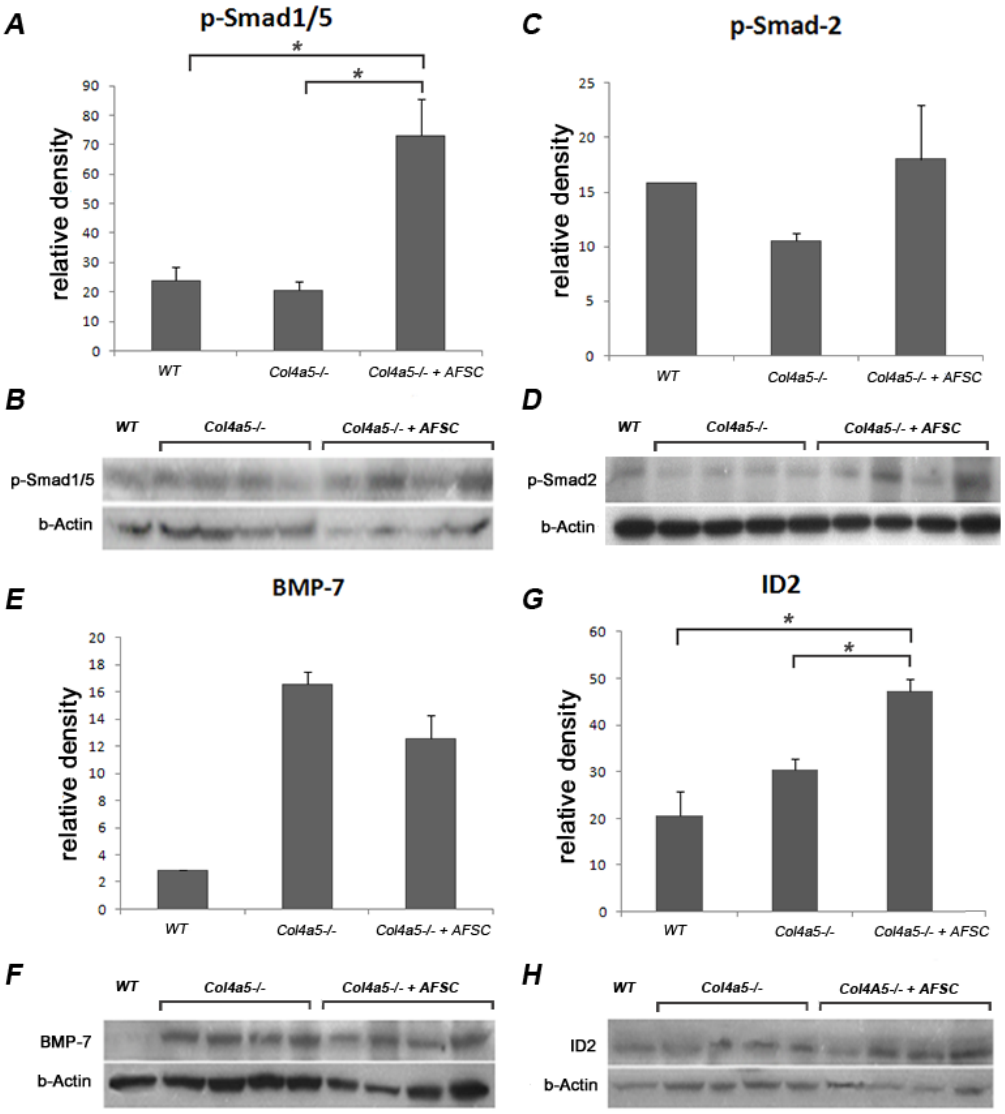

FIGURE 11. AFSC modulated the expression of SMADs signaling. Representative immunoblots of pSMAD1/5 (A), pSMAD2 (C), BMP-7 (E) and ID2 (G). Total renal protein isolated from WT (n=4), treated mice (n=4) and non-treated mice at (n=4) indicated that AFSC upregulated pSMAD1/5 and ID2 with no modification in BMP-7 or pSMAD2 expression after 5 days of injection possibly suggesting and alternative activation of the pSMADs. Data from four independent experiments were quantified by densitometry (all measurements were normalized against their corresponding housekeeping gene, β-actin) comparing expression of pSMAD1/5 [60kDa] (B), pSMAD2 [60kDa] (D) BMP-7 [49kDa] (F), ID2 [29kDa] (H) and between WT, treated and non-treated mice. Values are presented as mean ± SEM (*$p < 0.05$). (WT, wild-type)

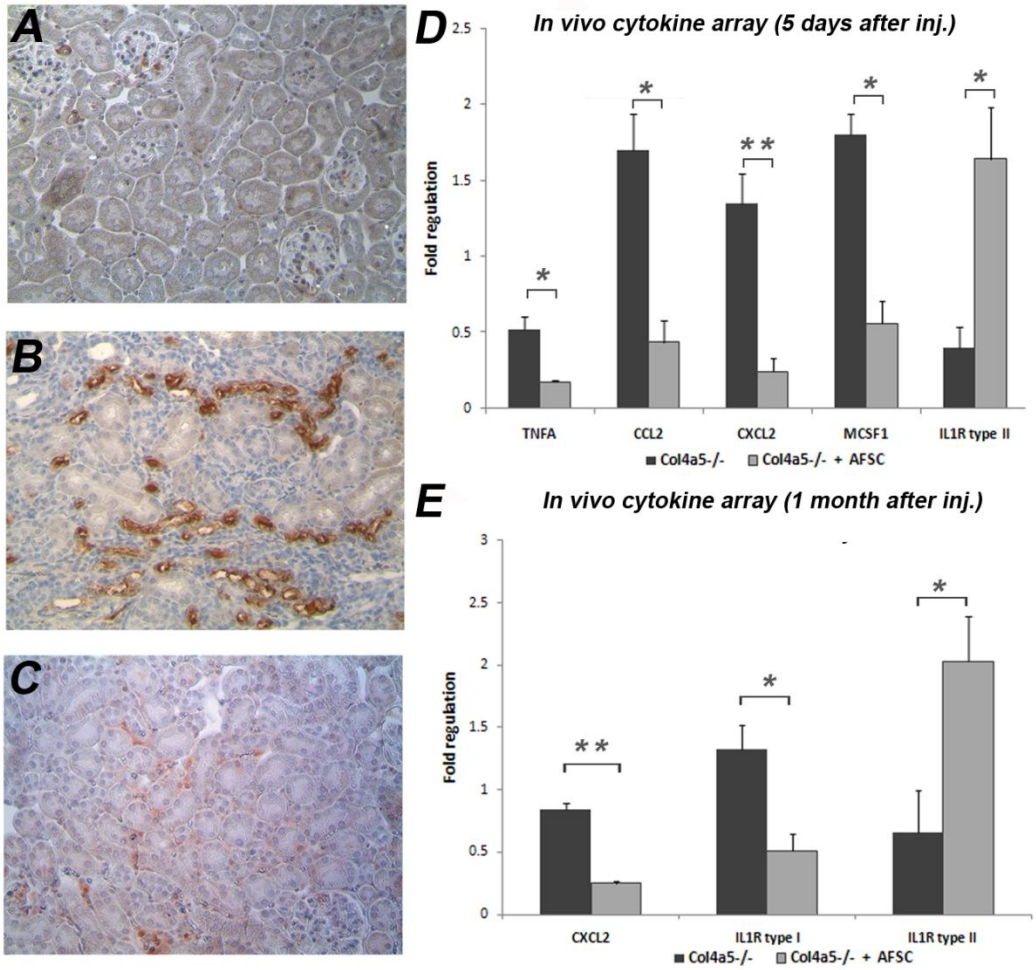

FIGURE 12. Injected mice present less macrophages recruitment and relative increase in M2 macrophages. The representative distribution of macrophages by immunohistochemistry between wild-type (A, X10) and non-injected (B, X10) and injected Alport syndrome mice (C, X10) at 2.5 months after AFSC administration demonstrate that injected mice had less macrophage infiltration in the interstitial space (identified by L1 staining). Gene expression analysis of M1 and M2 activation phase and recruitment genes was performed in both treated (n=6) and non-treated (n=6) mice after 5 days and 1 month of AFSC injection. Real time PCR analysis revealed significant downregulation in TNFα, CCL2, CXCL2, and M-CSF, (involved in the signaling pathway of M1 macrophages) in treated mice together with an increase in IL1-RII, expressed by M2 macrophages, at 5 days (D). Downregulation of CXCL2 and IL1-RI and an upregulation of IL1-RII were also present at 1 month in treated mice, which may indicate a balance toward tissue remodeling due to M2 phenotype macrophages (E).

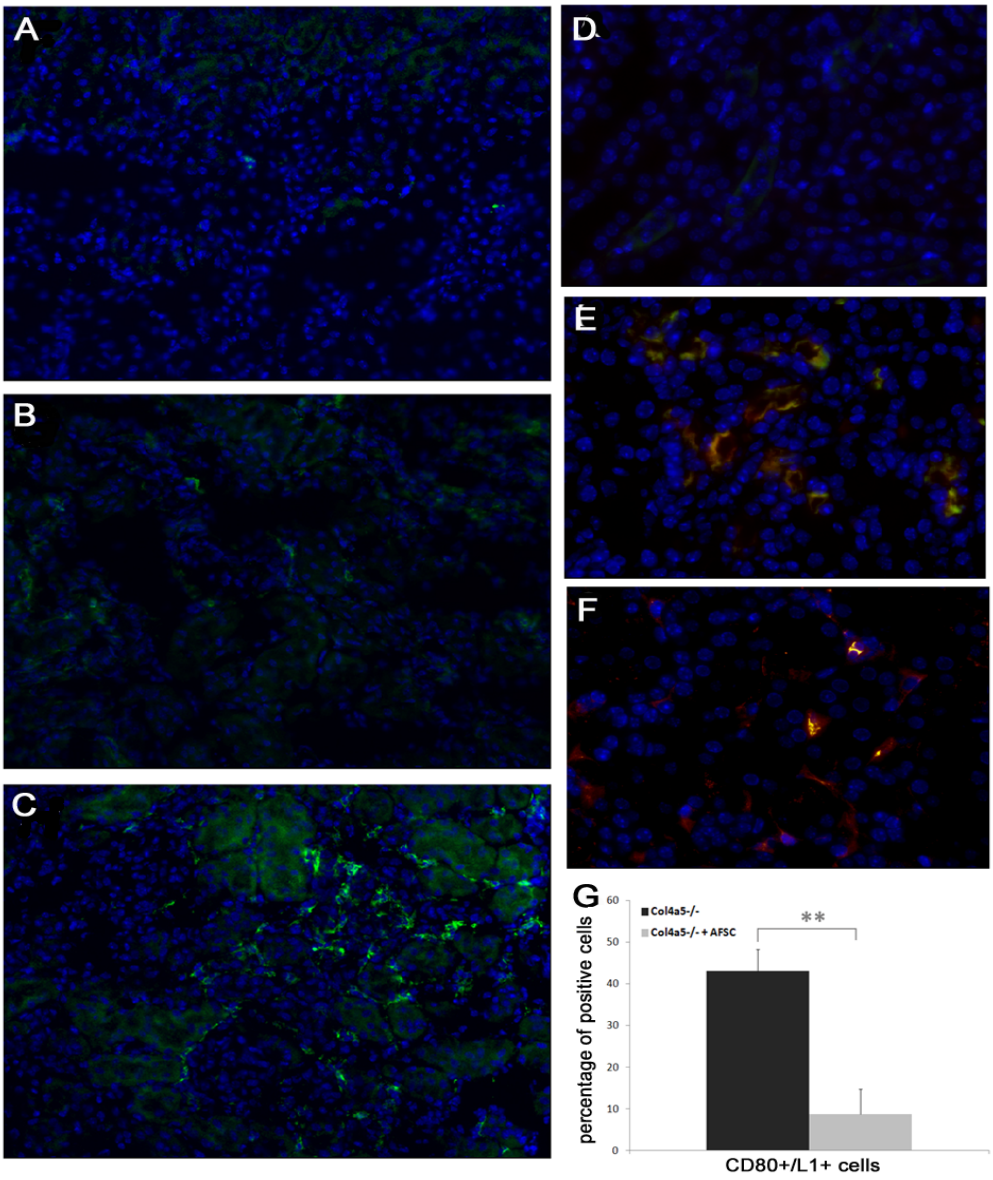

FIGURE 13. Immunohistochemistry and in vitro assays confirm the role of AFSC in macrophage activation. CD150 staining at 2.5 months confirmed the presence of M2-type macrophages in the interstitial space of injected mice (C, X20), whereas wild-type (A, X20) and untreated mice (B, X20) were mostly negative. Representative pictures of double immunostaining are shown for CD80 (green) and Macrophage/L1 Protein/Calprotectin Ab-1 (red) in WT (D, 40x), Col4a5$^{-/-}$ (E, 40X) and Col4a5$^{-/-}$ injected with AFSC (F, 40X) at 2.5 months post treatment. In non-treated mice increased number of macrophages is observed together with more positive double staining (arrow) indicating that non treated mice present more macrophage infiltration and activation of type 1 macrophages (M1) when compared with their treated siblings and WT. These data are confirmed in the graph (G) showing the percentage of double positive cells between injected (8.5%) and non-injected (30%) mice. In order to quantify the double positive cells (yellow) between the experimental groups, fraction of CD80/Macrophage/L1 Protein/Calprotectin Ab-1 cells was evaluated in 4 different interstitial areas per cross section per mouse (n=5 per experimental group) and statistics was performed as described in the Materials and Methods section. All values are presented as mean ± SEM (*P<0.05; **P<0.01). (WT, wild-type)

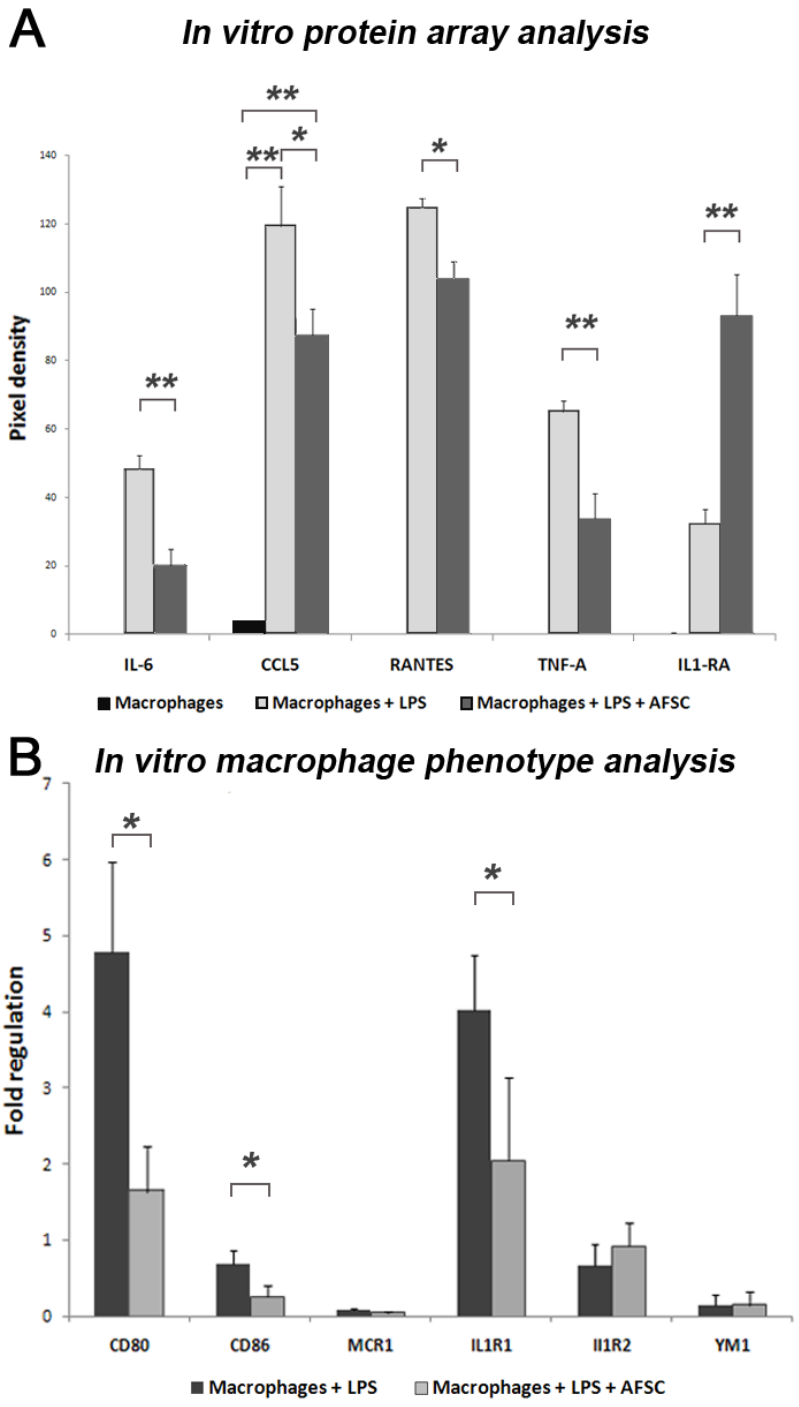

FIGURE 14. AFSC modulate macrophage activation. In vitro co-culture of activated macrophages and AFSC demonstrated that AFSC are able to decrease the expression of IL-6, CXCL2, RANTES and TNFα, important modulators of macrophage recruitment (A). Treatment of AFSC with lipopolysaccharide or analysis of AFSC with no stimulation produced no detectable signal for any of the above-mentioned markers (data not shown), suggesting that these cytokines are of macrophage origin. In addition CD80, CD86 and IL-RI were significantly downregulated, as shown by Real-Time PCR, which suggests that AFSC are able to induce an M1to M2 phenotype switch in macrophages (B).

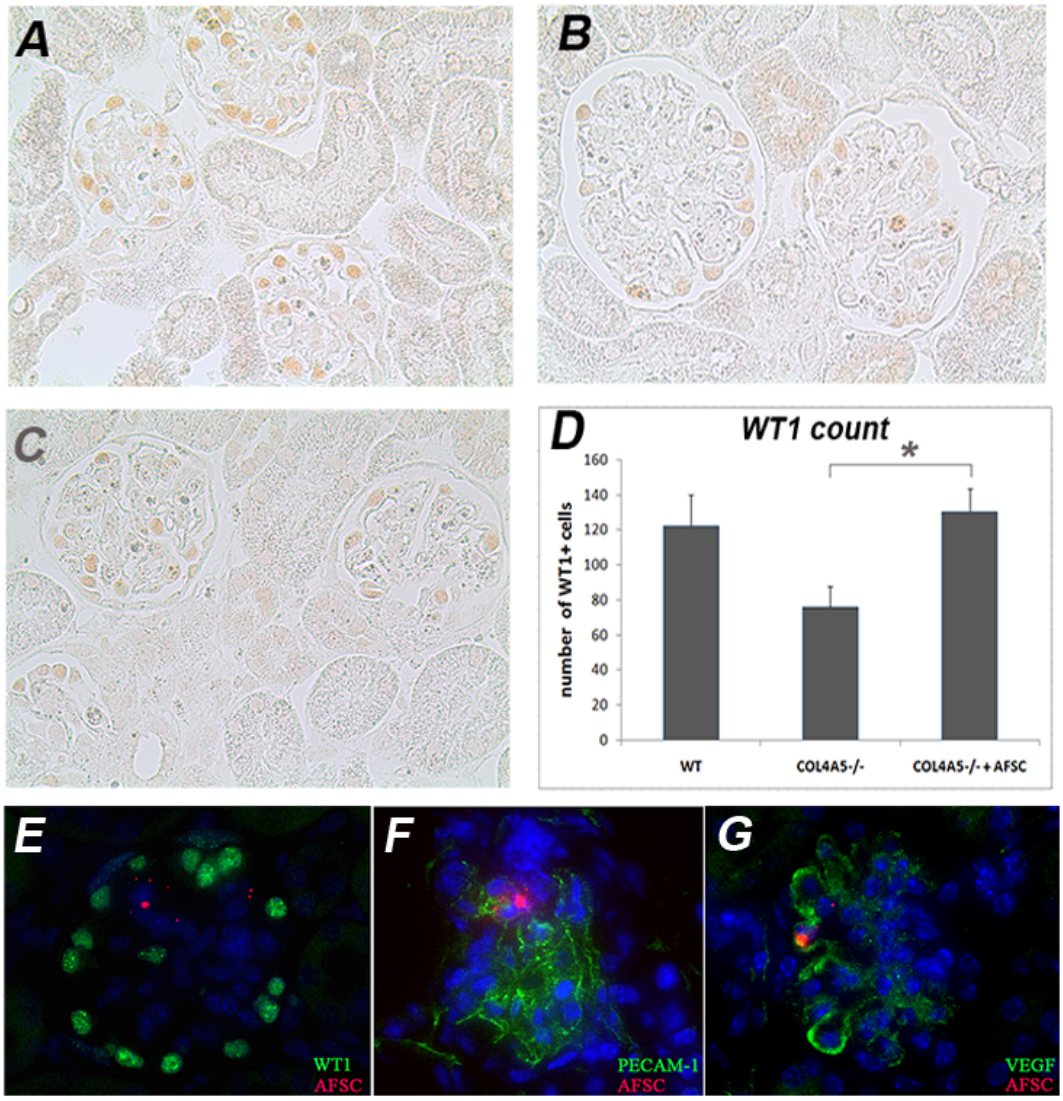

FIGURE 15. Injection of AFSC preserves podocyte number. Injection of AFSC preserved the number of podocytes in treated mice (A-D). Count of distribution of WT1 positive cells per 50 randomly selected glomeruli per mouse (n=10 mice per group) demonstrated that the number of WT1 positive cells is preserved in treated mice (D). Representative pictures show immunohistochemistry findings for WT1 in wild-type mice (A, X20) and in Col4a5$^{-/-}$ mice treated with AFSC and sacrificed at 2.5 months after injection (C, X20) versus non-injected Col4a5$^{-/-}$ sacrificed at 4 months after birth (B, X20). AFSC did not differentiate into podocyte-like cells after 2.5 months (E, X63), as shown by double staining of AFSC labeled with CM-DiI (red) and WT-1 (green). CM-DiI labeled AFSC (red) showed mild co-localization with PECAM-1 (green) (F,X63) and VEGF (green) (G, X63), indicating the possibility of AFSC differentiating into VEGF-producing–like cells.

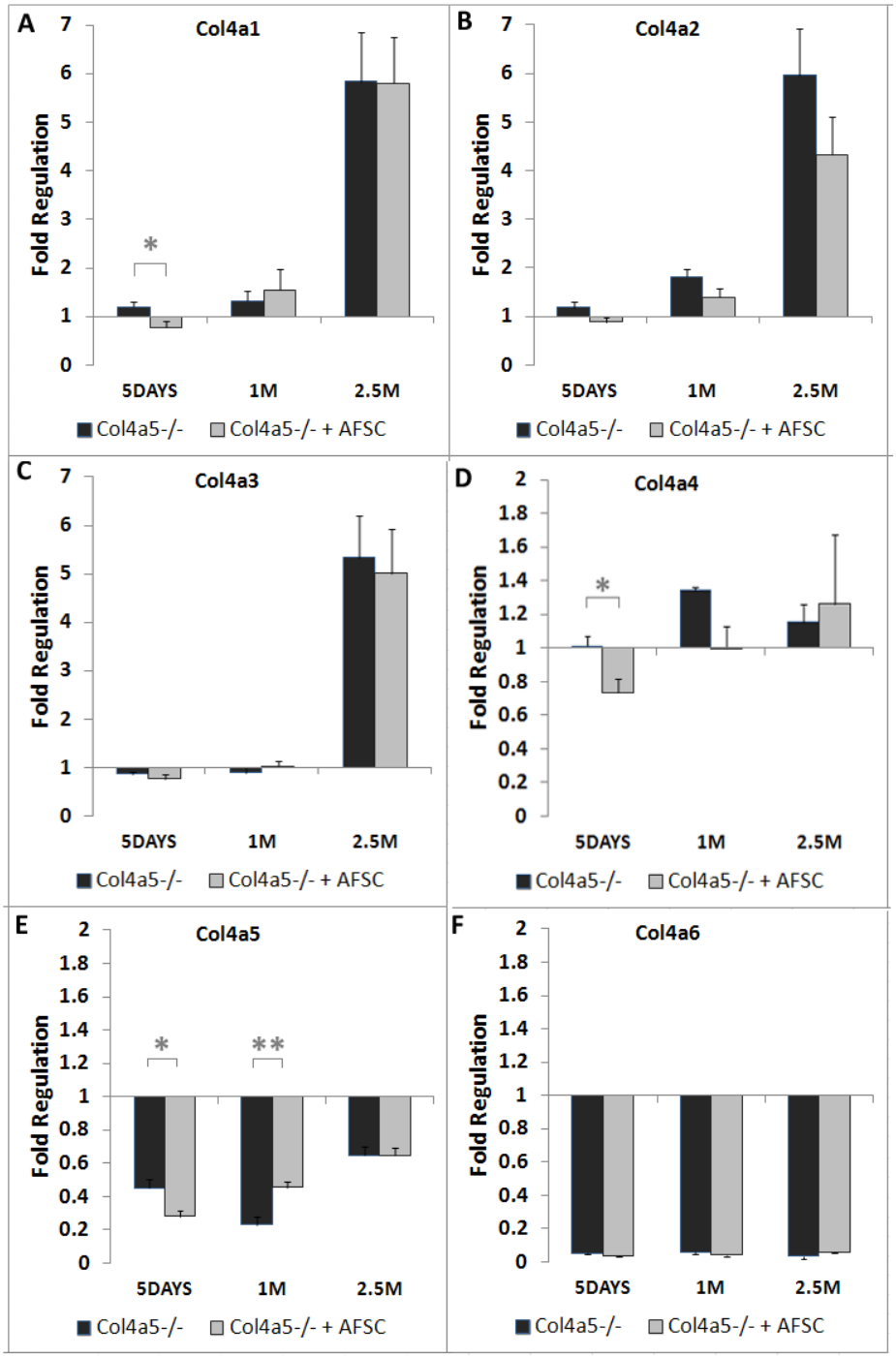

FIGURE 16. Real-Time PCR analysis of collagen type IV. Real Time PCR are shown for *collIVα1* (A), *collIVα2* (B), *collIVα3* (C), *collIVα4* (D), *collIVα5* (E) and *collIVα6* (F) at 5 days, 1 month and 2.5 months after injection in treated and non treated Col4a5$^{-/-}$. WT animals are used as reference. The levels of mRNA of *collIVα1* and *collIVα2* increase over time both in injected and non injected mice. At 2.5 months after injection, treated mice present decrease in level of *collIVα2* but the significance is below 95%. (A,B). Interestingly the levels of mRNA for *collIVα3* and *collIVα4* increase over time (C) both in treated and nontreated. The expressions of mRNA for *collIVα5* and *collIVα6* are downregulated at all time points in both treated and non-treated mice (E-F).

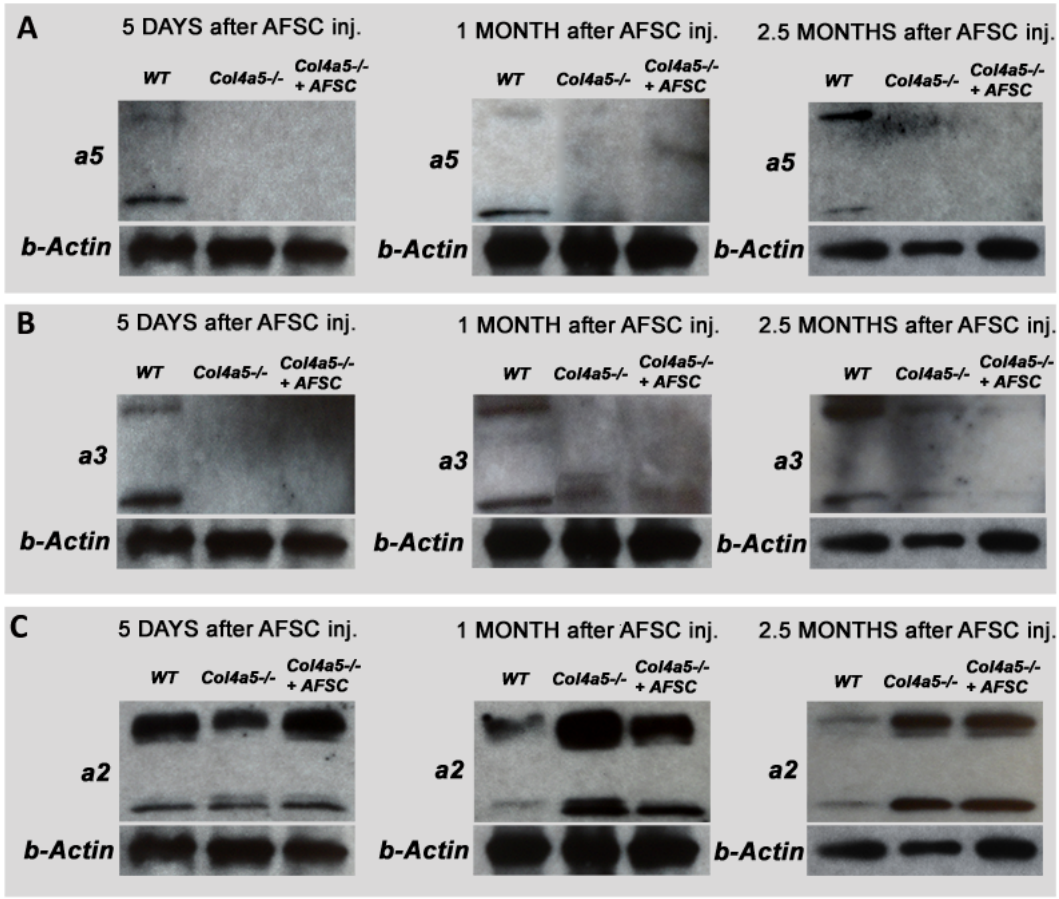

FIGURE 17. Western blot analysis of collagen type IV alpha chains. Representative Western Blotting of α5, α3 and α2 of collagen IV in all experimental groups at 5 days, 1 month and 2.5 months after injection. The expression of α5 chain is only detected in WT but never present in treated or non treated mice (A) for all the time points. Alpha3 expression is detected both in Alport and injected Alport mice at 1 month and 2.5 months after injection

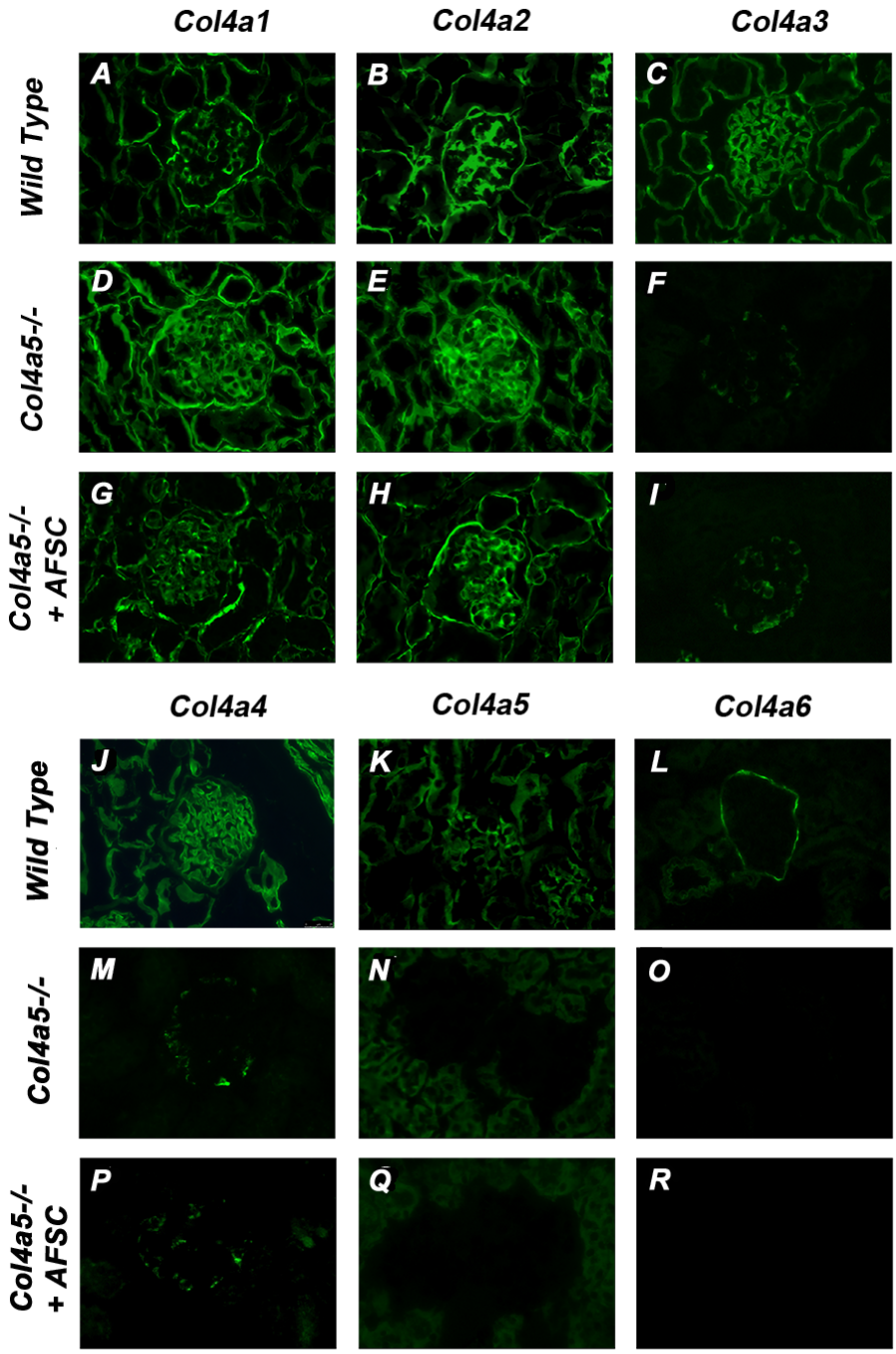

Figure 18. Immunostaining of all α-chains of type IV collagen. Immunostaining are shown for α chains 1-6 of Collagen Type IV in wild-type (A-C, and J-L 40X), Col4a5$^{-/-}$ (D-F, and M-O 40X) and Col4a5$^{-/-}$ injected with AFSC (G-I, and P-R 40X) at 2.5 months post treatment. No α5 chain is detected in the GBM of Col4a5$^{-/-}$ control mice (N), as well as in Col4a5$^{-/-}$ mice infused with AFSC (Q). Similar to the α5 chain, α6 chain was also absent in the GBM of Col4a5$^{-/-}$ control (O) and Col4a5$^{-/-}$ stem cell treated mice (R). We detected only minimal irregular expression of α3 and α4 chains in the GBM of Col4a5$^{-/-}$ control (F, M) and Col4a5$^{-/-}$ mice treated with AFSC (I, P). Enhanced expression of α1 and α2 chains was seen in the GBM of non treated mice (D,E) with apparent reduction in treated Col4a5$^{-/-}$ mice (G,H) in comparison to their littermate wild-type (A,B).

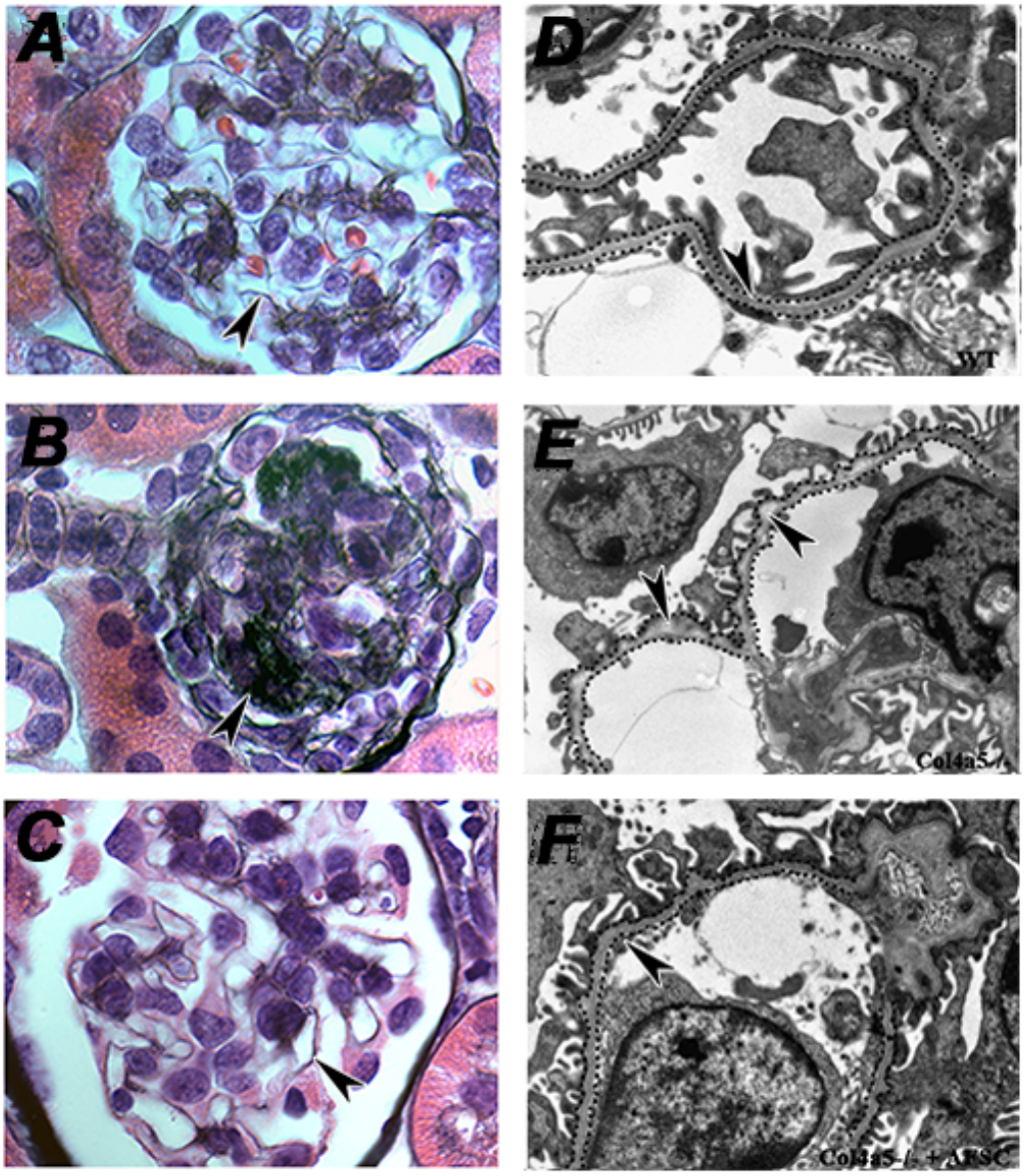

FIGURE 19. Structural analysis of the GBM. Mice that received AFSC infusion demonstrated a better morphology of the GBM (A-C). Representative pictures of Jones staining demonstrated that wild-type mice had a normal deposition of the GBM, shown by the black arrows (A, 100x), whereas the non-injected Col4a5$^{-/-}$ mice (B, 100x) had abundant matrix accumulation compared with their injected siblings (black arrow C, 100x). In addition, AFSC injection helped the preservation of GBM architecture (D-F). Representative electron transmission microscopy images showed severe thinning and splitting of GBM in Col4a5$^{-/-}$ mice (black arrow, E), when compared with their littermate wild-type (black arrow, D), whereas treated mice presented less thinning and splitting of the GBM at 2.5 months after injection (black arrow, F).

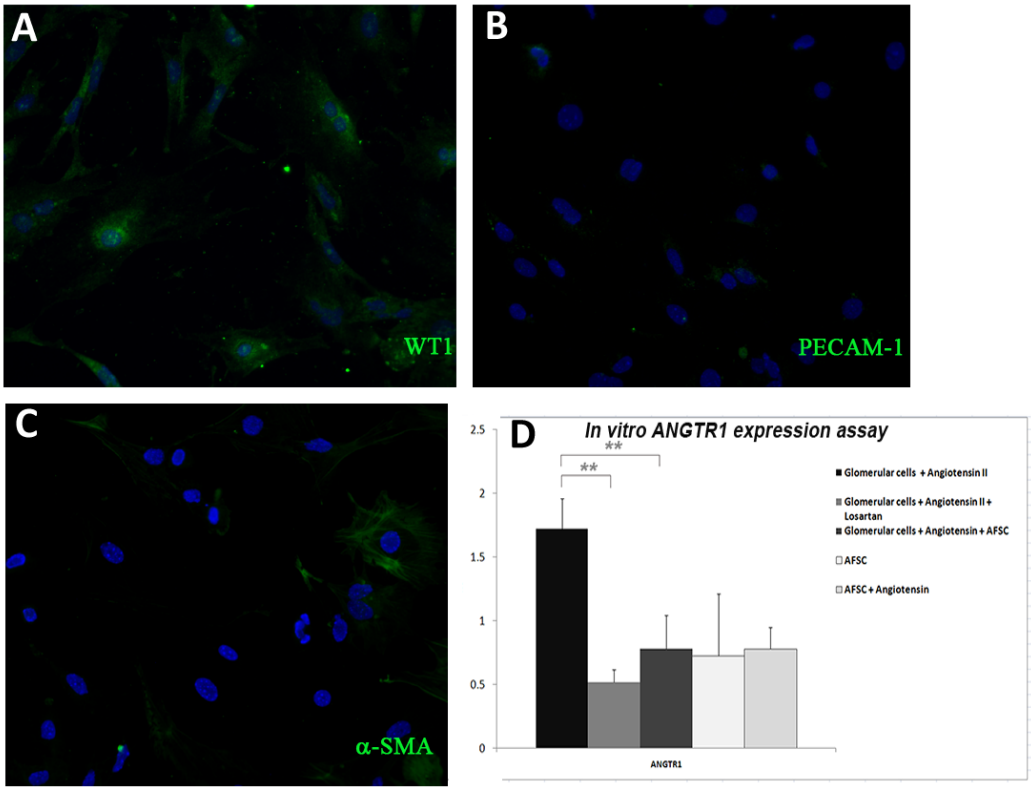

FIGURE 20. AFSC modulate angiotensin II signaling. Immunostaining are shown for WT1, PECAM-1 and α-SMA (A-C, 40x) of cultured cells from isolated glomeruli. Cultured cells resulted positive for WT-1 indicating that the majority of the cells were podocytes (A). They resulted negative for PECAM-1 showing no presence of endothelial cells (B) and few cells showed positivity for α-SMA confirming the limited presence of mesangial cells within the culture (C). AFSC block the expression of Ang II receptor 1 (ANGTR1). *In vitro* glomerular cells, stimulated with Ang II, showed increased ANGTR1 expression, while losartan (Ang II antagonist) blocked ANGTR1 expression (D). Similar to losartan AFSC successfully downregulate ANGTR1 thus, indicating their capability of acting as Ang II blocker. In addition AFSC exposed to Ang II did not present change in ANGTR1 expression level (D). (**$p < 0.01$).

REFERENCES

1. López-Hernández FJ, López-Novoa JM. Role of TGF-β in chronic kidney disease:an integration of tubular, glomerular and vascular effects. Cell Tissue Res. 2012 Jan;347(1):141-54.

2. Levey AS, Coresh J, Balk E, Kausz AT, Levin A, Steffes MW, Hogg RJ, Perrone RD, Lau J, Eknoyan G; National Kidney Foundation. National Kidney Foundation practice guidelines for chronic kidney disease: evaluation, classification, and stratification. Ann Intern Med. 2003 Jul 15;139(2):137-47.

3. Levey AS, Eckardt KU, Tsukamoto Y, Levin A, Coresh J, Rossert J, De Zeeuw D, Hostetter TH, Lameire N, Eknoyan G. Definition and classification of chronic kidney disease: a position statement from Kidney Disease: Improving Global Outcomes (KDIGO). Kidney Int. 2005 Jun;67(6):2089-100.

4. Coresh J, Selvin E, Stevens LA, Manzi J, Kusek JW, Eggers P, Van Lente F, Levey AS. Prevalence of chronic kidney disease in the United States. JAMA. 2007 Nov 7;298(17):2038-47.

5. Sharma SK, Zou H, Togtokh A, Ene-Iordache B, Carminati S, Remuzzi A, Wiebe N, Ayyalasomayajula B, Perico N, Remuzzi G, Tonelli M. Burden of CKD, proteinuria, and cardiovascular risk among Chinese, Mongolian, and Nepalese participants in the International Society of Nephrology screening programs. Am J Kidney Dis. 2010 Nov;56(5):915-27.

6. Zhang L, Zhang P, Wang F, Zuo L, Zhou Y, Shi Y, Li G, Jiao S, Liu Z, Liang W, Wang H. Prevalence and factors associated with CKD: a population study from Beijing. Am J Kidney Dis. 2008 Mar;51(3):373-84.

7. Cepoi V, Onofriescu M, Segall L, Covic A. The prevalence of chronic kidney disease in the general population in Romania: a study on 60,000 persons. Int Urol Nephrol. 2012 Feb;44(1):213-20.

8. Simões E Silva AC, Flynn JT. The renin-angiotensin-aldosterone system in 2011: role in hypertension and chronic kidney disease. Pediatr Nephrol. 2011 Sep 23.

9. *U.S. Renal Data System, USRDS. Annual Data Report: Atlas of Chronic Kidney Disease and End-Stage Renal Disease in the United States. Bethesda, MD: National Institutes of Health,*

National Institute of Diabetes and Digestive and Kidney Diseases, 2008

10. Bright, R (1827-1831). Reports of Medical Cases, Selected with a View of Illustrating the Symptoms and Cure of Diseases by a Reference to Morbid Anatomy, vol. I. London: Longmans

11. Cameron JS. Bright's disease today: the pathogenesis and treatment of glomerulonephritis--I. Br Med J. 1972 Oct 14;4(5832):87-90

12. Harris RC, Neilson EG. Toward a unified theory of renal progression. Annu Rev Med. 2006;57:365-80.

13. Segerer S, Kretzler M, Strutz F et al. Mechanisms of tissue injury and repair in renal diseases. In: Schrier R(ed). Diseases of the Kidney and Urinary Tract. Lippincott: Philadelphia, 2007

14. Ricardo SD, van Goor H, Eddy AA. Macrophage diversity in renal injury and repair. J Clin Invest. 2008 Nov;118(11):3522-30.

15. 21209251 - Wang Y, Harris DC. Macrophages in renal disease. J Am Soc Nephrol. 2011 Jan;22(1):21-7.

16. Gordon S. Alternative activation of macrophages. Nat Rev Immunol. 2003 Jan;3(1):23-35.

17. Mosser DM. The many faces of macrophage activation. J Leukoc Biol. 2003 Feb;73(2):209-12.

18. Wilson HM, Walbaum D, Rees AJ. Macrophages and the kidney. Curr Opin Nephrol Hypertens. 2004 May;13(3):285-90.

19. Wasilewska A, Taranta-Janusz K, Zoch-Zwierz W, Rybi-Szumińska A, Kołodziejczyk Z. Role of matrix metalloproteinases (MMP) and their tissue inhibitors (TIMP) in nephrology. Przegl Lek. 2009;66(9):485-90.

20. Cheng S, Pollock AS, Mahimkar R, Olson JL, Lovett DH. Matrix metalloproteinase 2 and basement membrane integrity: a unifying mechanism for progressive renal injury.FASEB J. 2006 Sep;20(11):1898-900.

21. Roberts AB, Anzano MA, Lamb LC, Smith JM, Sporn MB. New class of transforming growth factors potentiated by epidermal growth factor: isolation from non-neoplastic tissues.Proc Natl Acad Sci U S A. 1981 Sep;78(9):5339-43.

22. Massagué J. The transforming growth factor-beta family. Annu Rev Cell Biol. 1990;6:597-641.

23. Böttinger EP. TGF-beta in renal injury and disease. Semin Nephrol. 2007 May;27(3):309-20.

24. Mezzano SA, Ruiz-Ortega M, Egido J. Angiotensin II and renal fibrosis. Hypertension. 2001 Sep;38(3 Pt 2):635-8.

25. Johnston CI. Franz Volhard Lecture. Renin-angiotensin system: a dual tissue and hormonal system for cardiovascular control. J Hypertens Suppl. 1992 Dec;10(7):S13-26.

26. Wolf G, Mueller E, Stahl RA, Ziyadeh FN. Angiotensin II-induced hypertrophy of cultured murine proximal tubular cells is mediated by endogenous transforming growth factor-beta. J Clin Invest. 1993 Sep;92(3):1366-72.

27. Kagami S, Border WA, Miller DE, Noble NA. Angiotensin II stimulates extracellular matrix protein synthesis through induction of transforming growth factor-beta expression in rat glomerular mesangial cells. J Clin Invest. 1994 Jun;93(6):2431-7.

28. Nakamura S, Nakamura I, Ma L, Vaughan DE, Fogo AB. Plasminogen activator inhibitor-1 expression is regulated by the angiotensin type 1 receptor in vivo. Kidney Int. 2000 Jul;58(1):251-9.

29. Zoja C, Corna D, Gagliardini E, Conti S, Arnaboldi L, Benigni A, Remuzzi G. Adding a statin to a combination of ACE inhibitor and ARB normalizes proteinuria in experimental diabetes, which translates into full renoprotection. Am J Physiol Renal Physiol. 2010 Nov;299(5):F1203-11.

30. Jafar TH, Stark PC, Schmid CH, Landa M, Maschio G, de Jong PE, de Zeeuw D,Shahinfar S, Toto R, Levey AS; AIPRD Study Group. Progression of chronic kidney disease: the role of blood pressure control,proteinuria, and angiotensin-converting enzyme inhibition: a patient-levelmeta-analysis.Ann Intern Med. 2003 Aug 19;139(4):244-52.

31. Lewis EJ, Hunsicker LG, Bain RP, Rohde RD. The effect of angiotensin-converting-enzyme inhibition on diabetic nephropathy. The Collaborative Study Group.N Engl J Med. 1993 Nov 11;329(20):1456-62.

32. Brenner BM, Cooper ME, de Zeeuw D, Keane WF, Mitch WE, Parving HH, Remuzzi G, Snapinn SM, Zhang Z, Shahinfar S; RENAAL Study Investigators. Effects of losartan on renal and

cardiovascular outcomes in patients with type 2 diabetes and nephropathy.N Engl J Med. 2001 Sep 20;345(12):861-9.

33. Marre M, Chatellier G, Leblanc H, Guyene TT, Menard J, Passa P. Prevention of diabetic nephropathy with enalapril in normotensive diabetics with microalbuminuria. BMJ. 1988 Oct 29;297(6656):1092-5.

34. Ravid M, Lang R, Rachmani R, Lishner M. Long-term renoprotective effect of angiotensin-converting enzyme inhibition in non-insulin-dependent diabetes mellitus. A 7-year follow-up study.Arch Intern Med. 1996 Feb 12;156(3):286-9.

35. Ruggenenti P, Mosconi L, Sangalli F, Casiraghi F, Gambara V, Remuzzi G, Remuzzi A. Glomerular size-selective dysfunction in NIDDM is not ameliorated by ACE inhibition or by calcium channel blockade.Kidney Int. 1999 Mar;55(3):984-94.

36. Gross O, Licht C, Anders HJ, Hoppe B, Beck B, Tönshoff B, Höcker B, Wygoda S,Ehrich JH, Pape L, Konrad M, Rascher W, Dötsch J, Müller-Wiefel DE, Hoyer P; and Study Group Members of the Gesellschaft für Pädiatrische Nephrologie (GPN),Knebelmann B, Pirson Y, Grunfeld JP, Niaudet P, Cochat P, Heidet L, Lebbah S,Torra R, Friede T, Lange K, Müller GA, Weber M. Early angiotensin-converting enzyme inhibition in Alport syndrome delays renal failure and improves life expectancy.Kidney Int. 2011 Dec 14. doi: 10.1038/ki.2011.407.

37. Ding F, Humes HD. The bioartificial kidney and bioengineered membranes in acute kidney injury. Nephron Exp Nephrol. 2008;109(4):e118-22.

38. Aber GM, Morris LO, Housley E. Gluconeogenesis by the human kidney. Nature. 1966 Dec 31;212(5070):1589-90.

39. Wolfe RA, Ashby VB, Milford EL, Ojo AO, Ettenger RE, Agodoa LY, Held PJ, Port FK. Comparison of mortality in all patients on dialysis, patients on dialysis awaiting transplantation, and recipients of a first cadaveric transplant. N Engl J Med. 1999 Dec 2;341(23):1725-30.

40. Jais JP, Knebelmann B, Giatras I, De Marchi M, Rizzoni G, Renieri A, Weber M, Gross O, Netzer KO, Flinter F, Pirson Y, Verellen C, Wieslander J, Persson U, Tryggvason K, Martin P, Hertz JM, Schröder C, Sanak M, Krejcova S, Carvalho MF, Saus J, Antignac C, Smeets H, Gubler MC. X-linked Alport syndrome: natural history in 195 families and genotype- phenotype correlations in males. J Am Soc Nephrol. 2000 Apr;11(4):649-57.

41. Sadeghi M, Lahdou I, Daniel V, Schnitzler P, Fusch G, Schefold JC, Zeier M, Iancu M, Opelz G, Terness P. Strong association of phenylalanine and tryptophan metabolites with activated cytomegalovirus infection in kidney transplant recipients. Hum Immunol. 2011 Nov 18.

42. Kurnatowska I, Chrzanowski W, Kacprzyk F, Zamojska S, Kurnatowska A. [Prevalence of multifocal fungal infections in patients undergoing permanent immunosuppresion after renal transplantation]. Wiad Parazytol. 2002;48(4):419-24.

43. Vajdic CM, McDonald SP, McCredie MR, van Leeuwen MT, Stewart JH, Law M, Chapman JR, Webster AC, Kaldor JM, Grulich AE. Cancer incidence before and after kidney transplantation. JAMA. 2006 Dec 20;296(23):2823-31.

44. Sedrakyan S, Angelow S, De Filippo RE, Perin L. Stem cells as a therapeutic approach to chronic kidney diseases. Curr Urol Rep. 2012 Feb;13(1):47-54.

45. Brignier AC, Gewirtz AM. Embryonic and adult stem cell therapy. J Allergy Clin Immunol. 2010 Feb;125(2 Suppl 2):S336-44.

46. Li L, Black R, Ma Z, et al. Use of mouse hematopoietic stem and progenitor cells to treat acute kidney injury. Am J Physiol Renal Physiol. 2011 Sep 21.

47. Lee PT, Lin HH, Jiang ST, et al. Mouse kidney progenitor cells accelerate renal regeneration and prolong survival after ischemic injury. Stem Cells. 2010;28(3):573–84.

48. Morigi M, Benigni A, Remuzzi G, Imberti B. The regenerative potential of stem cells in acute renal failure. Cell Transplant. 2006;15 Suppl 1:S111–7.

49. Yokoo T, Kawamura T, Kobayashi E. Stem cells for kidney repair: useful tool for acute renal failure? Kidney Int. 2008;74(7):847–9.

50. Konstantinov IE. In search of Alexander A. Maximow: the man behind the unitarian theory of hematopoiesis. Perspect Biol Med. 2000 Winter;43(2):269-76.

51. Friedenstein AJ, Deriglasova UF, Kulagina NN, Panasuk AF, Rudakowa SF, Luriá EA, Ruadkow IA. Precursors for fibroblasts in different populations of hematopoietic cells as detected by the in vitro colony assay method. Exp Hematol. 1974;2(2):83-92.

52. Siminovitch L, Mcculloch EA, Till JE. The distribution of colony-forming cells among spleen colonies. J Cell Physiol. 1963 Dec;62:327-36.

53. Evans MJ, Kaufman MH. Establishment in culture of pluripotential cells from mouse embryos. Nature. 1981 Jul 9;292(5819):154-6.

54. Thomson JA, Itskovitz-Eldor J, Shapiro SS, Waknitz MA, Swiergiel JJ, Marshall VS, Jones JM. Embryonic stem cell lines derived from human blastocysts. Science. 1998 Nov 6;282(5391):1145-7. Erratum in: Science 1998 Dec 4;282(5395):1827.

55. Takahashi K, Yamanaka S. Induction of pluripotent stem cells from mouse embryonic and adult fibroblast cultures by defined factors. Cell. 2006 Aug 25;126(4):663-76.

56. Perin L, Sedrakyan S, Da Sacco S, De Filippo R. Characterization of human amniotic fluid stem cells and their pluripotential capability. Methods Cell Biol. 2008;86:85-99.

57. Gardner RL. Stem cells: potency, plasticity and public perception. J Anat. 2002 Mar;200(Pt 3):277-82.

58. Melcer S, Meshorer E. Chromatin plasticity in pluripotent cells. Essays Biochem. 2010 Sep 20;48(1):245-62.

59. Mitalipov S, Wolf D. Totipotency, pluripotency and nuclear reprogramming. Adv Biochem Eng Biotechnol. 2009;114:185-99.

60. Jiang Y, Jahagirdar BN, Reinhardt RL, Schwartz RE, Keene CD, Ortiz-Gonzalez XR, Reyes M, Lenvik T, Lund T, Blackstad M, Du J, Aldrich S, Lisberg A, Low WC, Largaespada DA, Verfaillie CM. Pluripotency of mesenchymal stem cells derived from adult marrow. Nature. 2002 Jul 4;418(6893):41-9.

61. Young HE, Black AC Jr. Adult stem cells. Anat Rec A Discov Mol Cell Evol Biol. 2004 Jan;276(1):75-102.

62. lport AC. Hereditary familial congenital haemorrhagic nephritis. Br Med J. 1927 Mar 19;1(3454):504-6.

63. Jais JP, Knebelmann B, Giatras I, De Marchi M, Rizzoni G, Renieri A, Weber M, Gross O, Netzer KO, Flinter F, Pirson Y, Dahan K, Wieslander J, Persson U, Tryggvason K, Martin P, Hertz JM, Schröder C, Sanak M, Carvalho MF, Saus J, Antignac C, Smeets H, Gubler MC. X-linked Alport syndrome: natural history and genotype-phenotype correlations in girls and women belonging to 195 families: a "European Community Alport

Syndrome Concerted Action" study. J Am Soc Nephrol. 2003 Oct;14(10):2603-10.

64. Gubler MC. Inherited diseases of the glomerular basement membrane. Nat Clin Pract Nephrol. 2008 Jan;4(1):24-37.

65. Peissel, B., et al., Comparative distribution of the alpha 1(IV), alpha 5(IV), and alpha 6(IV) collagen chains in normal human adult and fetal tissues and in kidneys from X-linked Alport syndrome patients. J Clin Invest, 1995. 96(4): p. 1948-57.

66. Zheng, K., et al., Canine X chromosome-linked hereditary nephritis: a genetic model for human X-linked hereditary nephritis resulting from a single base mutation in the gene encoding the alpha 5 chain of collagen type IV. Proc Natl Acad Sci U S A, 1994. 91(9): p. 3989-93.

67. Miner, J.H. and J.R. Sanes, Molecular and functional defects in kidneys of mice lacking collagen alpha 3(IV): implications for Alport syndrome. J Cell Biol, 1996. 135(5): p. 1403-13.

68. Cosgrove, D., et al., Collagen COL4A3 knockout: a mouse model for autosomal Alport syndrome. Genes Dev, 1996. 10(23): p. 2981-92.

69. Thorner, P.S., et al., Coordinate gene expression of the alpha3, alpha4, and alpha5 chains of collagen type IV. Evidence from a canine model of X-linked nephritis with a COL4A5 gene mutation. J Biol Chem, 1996. 271(23): p. 13821-8.

70. Kashtan, C.E. and Y. Kim, Distribution of the alpha 1 and alpha 2 chains of collagen IV and of collagens V and VI in Alport syndrome. Kidney Int, 1992. 42(1): p. 115-26.

71. Nakanishi, K., et al., Immunohistochemical study of alpha 1-5 chains of type IV collagen in hereditary nephritis. Kidney Int, 1994. 46(5): p. 1413-21.

72. Gubler, M.C., et al., Autosomal recessive Alport syndrome: immunohistochemical study of type IV collagen chain distribution. Kidney Int, 1995. 47(4): p. 1142-7.

73. Kashtan, C.E., Alport Syndrome and Thin Basement Membrane Nephropathy: Diseases Arising from Mutations in Type IV Collagen. Saudi J Kidney Dis Transpl, 2003. 14(3): p. 276-89.

74. Hahm, K., et al., Alphav beta6 integrin regulates renal fibrosis and inflammation in Alport mouse. Am J Pathol, 2007. 170(1): p. 110-25.

75. Haas M. Alport syndrome and thin glomerular basement membrane nephropathy: a practical approach to diagnosis. Arch Pathol Lab Med. 2009 Feb;133(2):224-32..

76. Gross O, Beirowski B, Koepke ML, Kuck J, Reiner M, Addicks K, Smyth N, Schulze-Lohoff E, Weber M. Preemptive ramipril therapy delays renal failure and reduces renal fibrosis in COL4A3-knockout mice with Alport syndrome. Kidney Int. 2003 Feb;63(2):438-46.

77. Abbate M, Remuzzi G. Renoprotection: clues from knockout models of rare diseases. Kidney Int. 2003 Feb;63(2):764-6.

78. Gross O, Kashtan CE. Treatment of Alport syndrome: beyond animal models. Kidney Int. 2009 Sep;76(6):599-603.

79. Cosgrove D, Meehan DT, Grunkemeyer JA, Kornak JM, Sayers R, Hunter WJ, Samuelson GC. Collagen COL4A3 knockout: a mouse model for autosomal Alport syndrome. Genes Dev. 1996 Dec 1;10(23):2981-92.

80. Miner JH, Sanes JR. Molecular and functional defects in kidneys of mice lacking collagen alpha 3(IV): implications for Alport syndrome. J Cell Biol. 1996 Dec;135(5):1403-13.

81. Rheault MN, Kren SM, Thielen BK, Mesa HA, Crosson JT, Thomas W, Sado Y, Kashtan CE, Segal Y. Mouse model of X-linked Alport syndrome. J Am Soc Nephrol. 2004 Jun;15(6):1466-74.

82. Kang JS, Wang XP, Miner JH, Morello R, Sado Y, Abrahamson DR, Borza DB. Loss of alpha3/alpha4(IV) collagen from the glomerular basement membrane induces a strain-dependent isoform switch to alpha5alpha6(IV) collagen associated with longer renal survival in Col4a3-/- Alport mice. J Am Soc Nephrol. 2006 Jul;17(7):1962-9.

83. Sugimoto H, Mundel TM, Sund M, Xie L, Cosgrove D, Kalluri R. Bone-marrow-derived stem cells repair basement membrane collagen defects and reverse genetic kidney disease. Proc Natl Acad Sci U S A. 2006 May 9;103(19):7321-6.

84. Bennett GG, Wolin KY, Viswanath K, Askew S, Puleo E, Emmons KM. Television viewing and pedometer-determined physical activity among multiethnic residents of low-income housing. Am J Public Health. 2006 Sep;96(9):1681-5.

85. Prodromidi EI, Poulsom R, Jeffery R, Roufosse CA, Pollard PJ, Pusey CD, Cook HT. Bone marrow-derived cells contribute to podocyte regeneration and amelioration of renal disease in a mouse model of Alport syndrome. Stem Cells. 2006 Nov;24(11):2448-55.

86. Katayama K, Kawano M, Naito I, Ishikawa H, Sado Y, Asakawa N, Murata T, Oosugi K, Kiyohara M, Ishikawa E, Ito M, Nomura S. Irradiation prolongs survival of Alport mice. J Am Soc Nephrol. 2008 Sep;19(9):1692-700.

87. LeBleu V, Sugimoto H, Mundel TM, Gerami-Naini B, Finan E, Miller CA, Gattone VH 2nd, Lu L, Shield CF 3rd, Folkman J, Kalluri R. Stem cell therapies benefit Alport syndrome. J Am Soc Nephrol. 2009 Nov;20(11):2359-70.

88. Ninichuk V, Gross O, Segerer S, Hoffmann R, Radomska E, Buchstaller A, Huss R, Akis N, Schlöndorff D, Anders HJ. Multipotent mesenchymal stem cells reduce interstitial fibrosis but do not delay progression of chronic kidney disease in collagen4A3-deficient mice. Kidney Int. 2006 Jul;70(1):121-9.

89. Perin L, Giuliani S, Jin D, Sedrakyan S, Carraro G, Habibian R, Warburton D, Atala A, De Filippo RE. Renal differentiation of amniotic fluid stem cells. Cell Prolif. 2007 Dec;40(6):936-48.

90. Lauronen J, Häyry P, Paavonen T. An image analysis-based method for quantification of chronic allograft damage index parameters. APMIS. 2006 Jun;114(6):440-8.

91. Li YM, Baviello G, Vlassara H, Mitsuhashi T. Glycation products in aged thioglycollate medium enhance the elicitation of peritoneal macrophages. J Immunol Methods. 1997 Feb 28;201(2):183-8.

92. da Silva Meirelles L, Chagastelles PC, Nardi NB. Mesenchymal stem cells reside in virtually all post-natal organs and tissues. J Cell Sci. 2006 Jun 1;119(Pt 11):2204-13.

93. Takemoto M, Asker N, Gerhardt H, Lundkvist A, Johansson BR, Saito Y, Betsholtz C. A new method for large scale isolation of kidney glomeruli from mice. Am J Pathol. 2002 Sep;161(3):799-805.

94. National Kidney Foundation. How your kidneys work. http://www.kidney.org/kidneydisease/howkidneyswrk.cfm

95. D'Amico G, Bazzi C. Pathophysiology of proteinuria. Kidney Int. 2003 Mar;63(3):809-25.

96. Kashtan CE, Kim Y. Distribution of the alpha 1 and alpha 2 chains of collagen IV and of collagens V and VI in Alport syndrome. Kidney Int. 1992 Jul;42(1):115-26.

97. Meehan DT, Delimont D, Cheung L, Zallocchi M, Sansom SC, Holzclaw JD, Rao V, Cosgrove D. Biomechanical strain causes maladaptive gene regulation, contributing to Alport glomerular disease. Kidney Int. 2009 Nov;76(9):968-76.

98. Andrews KL, Mudd JL, Li C, Miner JH. Quantitative trait loci influence renal disease progression in a mouse model of Alport syndrome. Am J Pathol. 2002 Feb;160(2):721-30

99. Gross O, Borza DB, Anders HJ, Licht C, Weber M, Segerer S, Torra R, Gubler MC, Heidet L, Harvey S, Cosgrove D, Lees G, Kashtan C, Gregory M, Savige J, Ding J, Thorner P, Abrahamson DR, Antignac C, Tryggvason K, Hudson B, Miner JH. Stem cell therapy for Alport syndrome: the hope beyond the hype. Nephrol Dial Transplant. 2009 Mar;24(3):731-4.

100. Abbate M, Zoja C, Remuzzi G. How does proteinuria cause progressive renal damage? J Am Soc Nephrol. 2006 Nov;17(11):2974-84.

101. Abbate M, Zoja C, Morigi M, Rottoli D, Angioletti S, Tomasoni S, Zanchi C, Longaretti L, Donadelli R, Remuzzi G. Transforming growth factor-beta1 is up-regulated by podocytes in response to excess intraglomerular passage of proteins: a central pathway in progressive glomerulosclerosis. Am J Pathol. 2002 Dec;161(6):2179-93.

102. Gorriz JL, Martinez-Castelao A. Proteinuria: detection and role in native renal disease progression. Transplant Rev (Orlando). 2012 Jan;26(1):3-13.

103. Perin L, Sedrakyan S, Giuliani S, Da Sacco S, Carraro G, Shiri L, Lemley KV, Rosol M, Wu S, Atala A, Warburton D, De Filippo RE. Protective effect of human amniotic fluid stem cells in an immunodeficient mouse model of acute tubular necrosis. PLoS One. 2010 Feb 24;5(2):e9357.

104. Herrera MB, Bussolati B, Bruno S, Morando L, Mauriello-Romanazzi G, Sanavio F, Stamenkovic I, Biancone L, Camussi G. Exogenous mesenchymal stem cells localize to the kidney by means of CD44 following acute tubular injury. Kidney Int. 2007 Aug;72(4):430-41.

105. Anders HJ, Ryu M. Renal microenvironments and macrophage phenotypes determine progression or resolution of renal inflammation and fibrosis. Kidney Int. 2011 Nov;80(9):915-25.

106. Vernon MA, Mylonas KJ, Hughes J. Macrophages and renal fibrosis. Semin Nephrol. 2010 May;30(3):302-17.

107. Sung SA, Jo SK, Cho WY, Won NH, Kim HK. Reduction of renal fibrosis as a result of liposome encapsulated clodronate induced macrophage depletion after unilateral ureteral obstruction in rats. Nephron Exp Nephrol. 2007;105(1):e1-9.

108. Kitamoto K, Machida Y, Uchida J, Izumi Y, Shiota M, Nakao T, Iwao H, Yukimura T, Nakatani T, Miura K. Effects of liposome clodronate on renal leukocyte populations and renal fibrosis in murine obstructive nephropathy. J Pharmacol Sci. 2009 Nov;111(3):285-92.

109. Ko GJ, Boo CS, Jo SK, Cho WY, Kim HK. Macrophages contribute to the development of renal fibrosis following ischaemia/reperfusion-induced acute kidney injury. Nephrol Dial Transplant. 2008 Mar;23(3):842-52. Epub 2007 Nov 5.

110. Cailhier JF, Partolina M, Vuthoori S, Wu S, Ko K, Watson S, Savill J, Hughes J, Lang RA. Conditional macrophage ablation demonstrates that resident macrophages initiate acute peritoneal inflammation. J Immunol. 2005 Feb 15;174(4):2336-42.

111. Wang W, Huang XR, Li AG, Liu F, Li JH, Truong LD, Wang XJ, Lan HY. Signaling mechanism of TGF-beta1 in prevention of renal inflammation: role of Smad7. J Am Soc Nephrol. 2005 May;16(5):1371-83.

112. Diamond JR, Pesek-Diamond I. Sublethal X-irradiation during acute puromycin nephrosis prevents late renal injury: role of macrophages. Am J Physiol. 1991 Jun;260(6 Pt 2):F779-86.

113. van Goor H, van der Horst ML, Fidler V, Grond J. Glomerular macrophage modulation affects mesangial expansion in the rat after renal ablation. Lab Invest. 1992 May;66(5):564-71.

114. Le Hir M, Hegyi I, Cueni-Loffing D, Loffing J, Kaissling B. Characterization of renal interstitial fibroblast-specific protein 1/S100A4-positive cells in healthy and inflamed rodent kidneys. Histochem Cell Biol. 2005 Jun;123(4-5):335-46.

115. Border WA. Transforming growth factor-beta and the pathogenesis of glomerular diseases. Curr Opin Nephrol Hypertens. 1994 Jan;3(1):54-8.

116. Li J, Campanale NV, Liang RJ, Deane JA, Bertram JF, Ricardo SD. Inhibition of p38 mitogen-activated protein kinase and transforming growth factor-beta1/Smad signaling pathways modulates the development of fibrosis in adriamycin-induced nephropathy. Am J Pathol. 2006 Nov;169(5):1527-40.

117. Liu Y. Cellular and molecular mechanisms of renal fibrosis. Nat Rev Nephrol. 2011 Oct 18;7(12):684-96.

118. Gouédard L, Chen YG, Thevenet L, Racine C, Borie S, Lamarre I, Josso N, Massague J, di Clemente N. Engagement of bone morphogenetic protein type IB receptor and Smad1 signaling by anti-Müllerian hormone and its type II receptor. J Biol Chem. 2000 Sep 8;275(36):27973-8

119. Clarke TR, Hoshiya Y, Yi SE, Liu X, Lyons KM, Donahoe PK. Müllerian inhibiting substance signaling uses a bone morphogenetic protein (BMP)-like pathway mediated by ALK2 and induces SMAD6 expression. Mol Endocrinol. 2001 Jun;15(6):946-59.

120. Benezra R, Davis RL, Lockshon D, Turner DL, Weintraub H. The protein Id: a negative regulator of helix-loop-helix DNA binding proteins. Cell. 1990 Apr 6;61(1):49-59.

121. Izumi N, Mizuguchi S, Inagaki Y, Saika S, Kawada N, Nakajima Y, Inoue K, Suehiro S, Friedman SL, Ikeda K. BMP-7 opposes TGF-beta1-mediated collagen induction in mouse pulmonary myofibroblasts through Id2. Am J Physiol Lung Cell Mol Physiol. 2006 Jan;290(1):L120-6.

122. Rodgers KD, Rao V, Meehan DT, Fager N, Gotwals P, Ryan ST, Koteliansky V, Nemori R, Cosgrove D. Monocytes may promote myofibroblast accumulation and apoptosis in Alport renal fibrosis. Kidney Int. 2003 Apr;63(4):1338-55.

123. Rao VH, Lees GE, Kashtan CE, Nemori R, Singh RK, Meehan DT, Rodgers K, Berridge BR, Bhattacharya G, Cosgrove D. Increased expression of MMP-2, MMP-9 (type IV collagenases/gelatinases), and MT1-MMP in canine X-linked Alport syndrome (XLAS). Kidney Int. 2003 May;63(5):1736-48.

124. Zeisberg M, Khurana M, Rao VH, Cosgrove D, Rougier JP, Werner MC, Shield CF 3rd, Werb Z, Kalluri R. Stage-specific action of matrix metalloproteinases influences progressive hereditary kidney disease. PLoS Med. 2006 Apr;3(4):e100.

125. Pistole TG, Britko JL. Bactericidal activity of amebocytes from the horseshoe crab, Limulus polyphemus. J Invertebr Pathol. 1978 May;31(3):376-82.

126. Hume DA, Ross IL, Himes SR, Sasmono RT, Wells CA, Ravasi T. The mononuclear phagocyte system revisited. J Leukoc Biol. 2002 Oct;72(4):621-7.

127. Rae F, Woods K, Sasmono T, Campanale N, Taylor D, Ovchinnikov DA, Grimmond SM,Hume DA, Ricardo SD, Little MH. Characterisation and trophic functions of murine embryonic macrophages based upon the use of a Csf1r-EGFP transgene reporter. Dev Biol. 2007 Aug 1;308(1):232-46.

128. Li L, Okusa MD. Macrophages, dendritic cells, and kidney ischemia-reperfusion injury. Semin Nephrol. 2010 May;30(3):268-77.

129. Tesch GH. Macrophages and diabetic nephropathy. Semin Nephrol. 2010 May;30(3):290-301.

130. Chadban SJ, Wu H, Hughes J. Macrophages and kidney transplantation. Semin Nephrol. 2010 May;30(3):278-89.

131. Williams TM, Little MH, Ricardo SD. Macrophages in renal development, injury, and repair. Semin Nephrol. 2010 May;30(3):255-67.

132. Martinez FO, Helming L, Gordon S. Alternative activation of macrophages: an immunologic functional perspective. Annu Rev Immunol. 2009;27:451-83.

133. Ninichuk V, Gross O, Reichel C, Khandoga A, Pawar RD, Ciubar R, Segerer S, Belemezova E, Radomska E, Luckow B, Perez de Lema G, Murphy PM, Gao JL, Henger A, Kretzler M, Horuk R, Weber M, Krombach F, Schlöndorff D, Anders HJ. Delayed chemokine receptor 1 blockade prolongs survival in collagen 4A3-deficient mice with Alport disease. J Am Soc Nephrol. 2005 Apr;16(4):977-85.

134. Cao Q, Zheng D, Wang YP, Harris DC. Macrophages and dendritic cells for treating kidney disease. Nephron Exp Nephrol. 2011;117(3):e47-52.

135. Gubler MC, Knebelmann B, Beziau A, Broyer M, Pirson Y, Haddoum F, Kleppel MM, Antignac C. Autosomal recessive Alport syndrome: immunohistochemical study of type IV collagen chain distribution. Kidney Int. 1995 Apr;47(4):1142-7.

136. Bonventre JV. Pathophysiology of acute kidney injury: roles of potential inhibitors of inflammation. Contrib Nephrol. 2007;156:39-46.

137. Hauser PV, De Fazio R, Bruno S, Sdei S, Grange C, Bussolati B, Benedetto C, Camussi G. Stem cells derived from human amniotic fluid contribute to acute kidney injury recovery. Am J Pathol. 2010 Oct;177(4):2011-21.

138. Villanueva S, Ewertz E, Carrión F, Tapia A, Vergara C, Céspedes C, Sáez PJ, Luz P, Irarrázabal C, Carreño JE, Figueroa F, Vio CP. Mesenchymal stem cell injection ameliorates chronic renal failure in a rat model. Clin Sci (Lond). 2011 Dec;121(11):489-99.

139. Eremina V, Jefferson JA, Kowalewska J, Hochster H, Haas M, Weisstuch J, Richardson C, Kopp JB, Kabir MG, Backx PH, Gerber HP, Ferrara N, Barisoni L, Alpers CE, Quaggin SE. VEGF inhibition and renal thrombotic microangiopathy. N Engl J Med. 2008 Mar 13;358(11):1129-36.

140. Eremina V, Sood M, Haigh J, Nagy A, Lajoie G, Ferrara N, Gerber HP, Kikkawa Y, Miner JH, Quaggin SE. Glomerular-specific alterations of VEGF-A expression lead to distinct congenital and acquired renal diseases. J Clin Invest. 2003 Mar;111(5):707-16.

141. Veron D, Reidy KJ, Bertuccio C, Teichman J, Villegas G, Jimenez J, Shen W, Kopp JB, Thomas DB, Tufro A. Overexpression of VEGF-A in podocytes of adult mice causes glomerular disease. Kidney Int. 2010 Jun;77(11):989-99.

142. Miner JH. Glomerular basement membrane composition and the filtration barrier. Pediatr Nephrol. 2011 Sep;26(9):1413-7. Epub 2011 Feb 15.

143. Steffes MW, Schmidt D, McCrery R, Basgen JM; International DiabeticNephropathy Study Group. Glomerular cell number in normal subjects and in type 1 diabetic patients. Kidney Int. 2001 Jun;59(6):2104-13.

144. Pagtalunan ME, Miller PL, Jumping-Eagle S, Nelson RG, Myers BD, Rennke HG, Coplon NS, Sun L, Meyer TW. Podocyte loss and progressive glomerular injury in type II diabetes. J Clin Invest. 1997 Jan 15;99(2):342-8.

145. Lemley KV, Lafayette RA, Safai M, Derby G, Blouch K, Squarer A, Myers BD. Podocytopenia and disease severity in IgA nephropathy. Kidney Int. 2002 Apr;61(4):1475-85.

146. Kim YH, Goyal M, Kurnit D, Wharram B, Wiggins J, Holzman L, Kershaw D, Wiggins R. Podocyte depletion and glomerulosclerosis have a direct relationship in the PAN-treated rat. Kidney Int. 2001 Sep;60(3):957-68.

147. Schiffer M, Bitzer M, Roberts IS, Kopp JB, ten Dijke P, Mundel P, Böttinger EP. Apoptosis in podocytes induced by TGF-beta and Smad7. J Clin Invest. 2001 Sep;108(6):807-16.

148. Cosgrove D, Rodgers K, Meehan D, Miller C, Bovard K, Gilroy A, Gardner H, Kotelianski V, Gotwals P, Amatucci A, Kalluri R. Integrin alpha1beta1 and transforming growth factor-beta1 play distinct roles in alport glomerular pathogenesis and serve as dual targets for metabolic therapy. Am J Pathol. 2000 Nov;157(5):1649-59.

149. Gross O, Girgert R, Beirowski B, Kretzler M, Kang HG, Kruegel J, Miosge N, Busse AC, Segerer S, Vogel WF, Müller GA, Weber M. Loss of collagen-receptor DDR1 delays renal fibrosis in hereditary type IV collagen disease. Matrix Biol. 2010 Jun;29(5):346-56.

150. Sharma M, Sharma R, Greene AS, McCarthy ET, Savin VJ. Documentation of angiotensin II receptors in glomerular epithelial cells. Am J Physiol. 1998 Mar;274(3 Pt 2):F623-7.

151. Hoffmann S, Podlich D, Hähnel B, Kriz W, Gretz N. Angiotensin II type 1 receptor overexpression in podocytes induces glomerulosclerosis in transgenic rats. J Am Soc Nephrol. 2004 Jun;15(6):1475-87.

152. Maschio G, Alberti D, Janin G, Locatelli F, Mann JF, Motolese M, Ponticelli C, Ritz E, Zucchelli P. Effect of the angiotensin-converting-enzyme inhibitor benazepril on the progression of chronic renal insufficiency. The Angiotensin-Converting-Enzyme Inhibition in Progressive Renal Insufficiency Study Group. N Engl J Med. 1996 Apr 11;334(15):939-45.

153. Randomised placebo-controlled trial of effect of ramipril on decline in glomerular filtration rate and risk of terminal renal failure in proteinuric, non-diabetic nephropathy. The GISEN Group (Gruppo Italiano di Studi Epidemiologici in Nefrologia). Lancet. 1997 Jun 28;349(9069):1857-63.

154. Jafar TH, Schmid CH, Landa M, Giatras I, Toto R, Remuzzi G, Maschio G, Brenner BM, Kamper A, Zucchelli P, Becker G, Himmelmann A, Bannister K, Landais P, Shahinfar S, de Jong PE, de Zeeuw D, Lau J, Levey AS. Angiotensin-converting enzyme inhibitors and progression of nondiabetic renal disease. A meta-analysis of patient-level data. Ann Intern Med. 2001 Jul

17;135(2):73-87. Erratum in: Ann Intern Med 2002 Aug 20;137(4):299.

155. de Zeeuw D, Remuzzi G, Parving HH, Keane WF, Zhang Z, Shahinfar S, Snapinn S, Cooper ME, Mitch WE, Brenner BM. Proteinuria, a target for renoprotection in patients with type 2 diabetic nephropathy: lessons from RENAAL. Kidney Int. 2004 Jun;65(6):2309-20.

156. Lewis EJ, Lewis JB. Treatment of diabetic nephropathy with angiotensin II receptor antagonist. Clin Exp Nephrol. 2003 Mar;7(1):1-8.

157. Andersen S, Tarnow L, Rossing P, Hansen BV, Parving HH. Renoprotective effects of angiotensin II receptor blockade in type 1 diabetic patients with diabetic nephropathy. Kidney Int. 2000 Feb;57(2):601-6.

158. Whaley-Connell A, Nistala R, Habibi J, Hayden MR, Schneider RI, Johnson MS, Tilmon R, Rehmer N, Ferrario CM, Sowers JR. Comparative effect of direct renin inhibition and AT1R blockade on glomerular filtration barrier injury in the transgenic Ren2 rat. Am J Physiol Renal Physiol. 2010 Mar;298(3):F655-61.

AKNOWLEDGMENTS

What is a scientist after all? It is a curious man looking through a keyhole, the keyhole of nature, trying to know what's going on.
Jacques Yves Cousteau

Science is fascinating and fun because it serves human curiosity and fuels our imagination, but most of all it is a road to a newer reality. I am privileged to have experienced this wonderful journey, and have done so with the help and encouragement of many great people.

I want to thank Dr. Laura Perin and Dr. Roger De Fillippo for giving me the opportunity to start this PhD work. I owe my deepest gratitude to Laura for her stupendous mentorship and support and encouragement and patience without which I would not have succeeded. Thank you Laura for doing every possible and even the impossible along every step during this journey to make my experience special and this study a success. You are a great mentor and friend.

I would like to acknowledge Stefano Da Sacco not only for his constant support throughout this work, but also for his readiness to help me learn some basic Italian. In this regard I am also grateful to Stefano Giuliani and not any less for training me to become a mouse surgeon. Thanks to Astgik for her assistance and companionship during long surgical procedures. Thanks to Liron for her support and the colorful stories that she has shared with many of us. I would like to thank Anna Milanesi for the great collaboration we had on the AFSC characterization project.

I would like to acknowledge Dr. Kevin Lemley for sharing his extensive expertise and making this study easier with his helpful ideas and suggestions. I also thank Sue Buckley for her important suggestions and tips to make my experiments work. I would like to also thank Gianni Carraro for his mentorship and support. I would like to acknowledge and thank Dr. David Warburton for his support and mentorship by sharing his extensive expertise in medicine and research.

I want to thank my distant friend in Italy Rosa Di Liddo who has provided an invaluable administrative support with my paperwork at the Univesity of Padova. Lastly, I would like to show my gratitude to Prof. Pier Paolo Parnigotto and Prof. Maria Teresa Conconi of Italy for being supportive and allowing me to conduct my research in Los Angeles.

Finally, I would like to thank my family for their outstanding support and encouragement. Thanks to my parents, my wife and my daughter for standing next to me all the time and helping me to pursue my PhD.